

5-2022

Efficacy Of Dual Cd19-Cd79B Car In B-Cell Malignancies

Xiaoyun Cheng

Follow this and additional works at: https://digitalcommons.library.tmc.edu/utgsbs_dissertations



Part of the [Medicine and Health Sciences Commons](#)

Recommended Citation

Cheng, Xiaoyun, "Efficacy Of Dual Cd19-Cd79B Car In B-Cell Malignancies" (2022). *Dissertations and Theses (Open Access)*. 1158.

https://digitalcommons.library.tmc.edu/utgsbs_dissertations/1158

This Thesis (MS) is brought to you for free and open access by the MD Anderson UTHealth Houston Graduate School at DigitalCommons@TMC. It has been accepted for inclusion in Dissertations and Theses (Open Access) by an authorized administrator of DigitalCommons@TMC. For more information, please contact digcommons@library.tmc.edu.

EFFICACY OF DUAL CD19-CD79b CAR IN B-CELL MALIGNANCIES

By

Xiaoyun Cheng, M.D.

APPROVED:

DocuSigned by:

Sattva Neelapu

C101A167CFA54C6

Sattva S Neelapu, M.D.
Advisory Professor

DocuSigned by:

Richard Davis

8E938F3A2312494...

Richard Eric Davis, M.D.

DocuSigned by:

Laura Bover

330B7390DD0B4DE...

Laura Bover, Ph.D.

DocuSigned by:

Greg Lizee

092237F763E9447...

Greg Lizee, Ph.D.

DocuSigned by:

Ryan Sun

B86AD1F9577343B...

Ryan Sun, Ph.D.

APPROVED:

Dean, The University of Texas
MD Anderson Cancer Center UTHealth Graduate School of Biomedical Sciences

EFFICACY OF DUAL CD19-CD79b CAR IN B-CELL MALIGNANCIES

A

THESIS

Presented to the Faculty of
The University of Texas
MD Anderson Cancer Center UTHealth
Graduate School of Biomedical Science
in Partial Fulfillment
of the Requirements
for the Degree of
MASTER OF SCIENCE

By

Xiaoyun Cheng, M.D.

Houston, Texas

May 2022

ACKNOWLEDGEMENTS

I would like to convey my deepest gratitude to my mentor, Dr. Sattva S Neelapu, for his mentorship throughout my master's thesis research. He was always there to offer his expertise and insight – helping me resolve any questions related to CAR-T research and providing guidance and support every step of the way, ultimately training me become a better researcher and critical thinker.

I also would like to express my sincere appreciation to my advisory committee: Drs. Eric Richard Davis, Laura Bover, Greg Lizee, and Ryan Sun for their support and guidance. They made sure that each committee meeting was full of valuable advice, thoughtful comments, and great encouragement.

Thank you to all the members of the Neelapu Lab – people who have not only supported me, but also helped me grow as a researcher. A special thanks to Drs. Jingwei Liu and Fuliang Chu, who provided vectors and aid.

Finally, thank you to my family. To my husband Guodong and my two daughters Jinghan and Jingzhuo, thank you for supporting me in my pursuit of a future as a scientist. To my parents, thank you for encouraging me to never stop learning and for showing me what it means to dedicate your life to improving the lives of others.

EFFICACY OF DUAL CD19-CD79b CAR IN B-CELL MALIGNANCIES

Xiaoyun Cheng, M.D.

Advisory Professor: Sattva S Neelapu, M.D.

Despite high clinical responses, about 30%-60% of patients with B-cell malignancies relapse following CD19-targeting chimeric antigen receptor (CAR) T cell therapy. CD19 loss is a major cause of relapse and resistance after CD19 CAR T therapy. Dual antigen targeting could overcome resistance due to antigen escape and improve outcomes after CAR T cell therapy.

We hypothesized that dual CD19-CD79b CAR T cells will be effective against B cell malignancies by targeting one or both antigens. I have engineered dual CAR targeting CD19 and CD79b antigens under the control of EF1 α promoter in a 3rd generation lentiviral vector. The dual CD19-CD79b CAR was composed of CD19 CAR with 4-1BB co-stimulatory domain and CD79b CAR with OX-40 linked by T2A self-cleavable peptide. High transduction efficiency of dual CD19-CD79b CAR was achieved and stable dual CAR expression was observed in both CD4⁺ and CD8⁺ T cell subsets. My method of generation of dual CAR T cells attained the optimal CD4⁺:CD8⁺ ratio of 1:1 on day 9 after transduction.

I demonstrated that both CD19 CAR and CD79b CAR are functional in the dual CAR construct by exhibiting degranulation, proliferation and robust cytotoxic activity against B cell lymphoma and leukemia cell lines expressing either CD19 or CD79b or both. The expression of two distinct CAR molecules in the same cell did not adversely affect T-cell differentiation during the CAR T generation as the phenotype and expression of various inhibitory receptors were similar to untransduced and CD19 CAR-transduced T cells. In summary, dual targeting of CD19 and CD79b could provide a feasible strategy to minimize antigen escape and improve

the efficacy of CAR T treatment for patients with relapsed or refractory B-cell non-Hodgkin lymphoma, hairy cell leukemia and chronic lymphocytic leukemia.

TABLE OF CONTENTS

Approvals	i
Title	ii
Acknowledgements	iii
Abstract.....	iv
Table of Contents.....	vi
List of Figures.....	xi
List of Tables.....	xii
List of Abbreviations	xiv
Chapter 1: Introduction.....	1
1. B-cell Malignancies.....	2
1.1 B-cell Malignancy Introduction	2
1.2 B-cell Malignancy Mechanism	2
1.2.1 B-cell Development.....	2
1.2.2 B-cell Activation	3
1.2.3 B-cell Mutations	3
1.3 Treatment for NHL and CLL.....	4
1.3.1 Conventional Treatment Methods	4
1.3.2 Immunotherapy	5
1.3.3 Limitation of Current Methods	6
2. Chimeric Antigen Receptor T cells.....	7

2.1 CAR T History.....	7
2.2 CAR T Mechanism.....	9
2.3 CAR Construct.....	10
2.3.1 CAR Ectodomain	11
2.3.2 Transmembrane Domain	12
2.3.3 CAR Endodomain	12
2.4 CAR Production.....	14
2.4.1 CAR Cloning.....	14
2.4.2 CAR Expression and Generation	16
3. CAR T Immunotherapy Targets.....	16
3.1 CD19 as an Ideal Target.....	16
3.2 CD19 CAR T Treatment	17
3.3 CD19 CAR T Limitations.....	17
3.4 Multiple Antigen Targeting	18
4. Hypothesis and Aims.....	22
4.1 Significance	22
4.2. Hypothesis.....	23
4.3 Aims	23
Chapter 2: Materials & Methods	24
1. Materials.....	25
1.1 Cell Lines and Culture Medium.....	25
1.2 Reagents.....	26
1.3 Reagents for Transfection and Transduction	26
1.4 Reagents for Cloning	27
1.5 Flow Cytometry Antibodies and Reagents	27

1.6 Plasmids.....	28
1.7 Primers.....	29
2. Methods for Molecular Biology	32
2.1 Restriction Enzyme Digestion.....	32
2.2 Gel Electrophoresis and Gel Extraction	32
2.3 Polymerase Chain Reaction	33
2.4 DNA Assembly	34
2.5 Transformation and DNA Extraction	34
2.6 DNA Sequencing	35
3. Methods for Cell Culture and Assays.....	35
3.1 Dual CD19-D79b CAR Expression in 293 T Cells.....	35
3.2 Flow Cytometry for Transient CAR Expression in 293 T Cells	36
3.3 Lentivirus Production	37
3.4 Lentivirus Concentration	38
3.5 PBMC Isolation.....	38
3.6 T Cell Isolation.....	39
3.7 T Cell Activation and Expansion	39
3.8 Lentiviral Transduction.....	39
3.9 Transduction Efficiency.....	40
3.10 CAR T Cell Degranulation.....	41
3.11 CAR T Cell Proliferation.....	42
3.12 CAR T Cell Cytotoxicity	43
3.13 Dual CD19-CD79b CAR T Cell Phenotype and Exhaustion Markers	43
Chapter 3: Results.....	46
1. Expression of CD19 CAR with CD28 hinge and transmembrane domain was lower....	47

than expression of CD79b CAR in dual CAR construct.....	47
2.Expression of CD19 CAR with CD28 H/TM and 4-1BB and OX40 was lower than	48
expression of CD79b CAR in dual CAR construct.	48
3. Expression of CD19 CAR was stable with CD8 α H/TM in a dual CAR construct.....	51
4.Transduction efficiency of dual CD19-CD79b CAR was improved in primary T-cells	54
when removing the tEGFR transduction marker, however, CAR expression	54
gradually decreased under the control of MSCV promoter.	54
5. The expression of CD19 CAR and CD79b CAR was stable after transduction under the control of promoter EF1 α	56
6. Generation of the dual CD19-CD79 CAR T Cells.	57
7. Dual CD19-CD79b CAR T cells degranulated in response to B-cell lymphoma and	60
leukemia cell lines in a CD19 or CD79b dependent manner.	60
8. Dual CD19-CD79b CAR T cells were cytotoxic to B-cell lymphoma and leukemia cell lines in a CD19 or CD79b dependent manner.	67
9. Dual CD19-CD79b CAR T cells proliferated in response to B-cell lymphoma and	72
leukemia cell lines in a CD19 or CD79b dependent manner.	72
10. CD19-CD79b CAR T cells produced effector cytokines in response to B-cell	75
lymphoma and leukemia cell lines in CD19 or CD79b dependent manner.....	75
11. The subset and phenotype of CD19-CD79b CAR T cells were similar to.....	78
untransduced T cells and CD19 CAR T cells.....	78
12. The expression of inhibitory receptors on CD19-CD79b CAR T cells was similar to ..	80

untransduced T cells and CD19 CAR T cells	80
Chapter 4: Discussions	83
Chapter 5. Conclusions and	91
Future Directions	91
Chapter 6. Bibliography	94
VITA.....	106

LIST OF FIGURES

Figure Number	Title	Page Number
1	CAR Construct and Generation.	10
2	Design of bicistronic CAR and tandem CAR	22
3	The expression of CD19 CAR, CD79b CAR and tEGFR	48
4	The expression of CD19 CAR, CD79b CAR and tEGFR	49
5	The expression of CD19 CAR, CD79b CAR and tEGFR	52
6	The transduction efficiency of dual CD19-CD79b CARs	55
7	The transduction efficiency of dual CD19-CD79b CARs	57
8	Generation of dual CD19-CD79b CAR T cells.	58
9	Tumor cell phenotypes and degranulation of dual CD19-CD79b CAR T cells	60
10	Dual CD19-CD79b CAR T cells were cytotoxic to CD19+CD79b+, CD19+CD79b-, and CD19-CD79b+ tumor cells	68
11	Dual CD19-CD79b CAR T cells proliferated in response to B-cell lymphoma and B-leukemia in CD19 or CD79b dependent manner	73
12	Dual CD19-CD79b CAR T cells released cytokines in response to tumor cells expressing either CD19 or CD79b and both	76
13	Phenotypic profile of untransduced T cells, CD19 CAR T, and CD19-CD79b CAR T cells	78
14	Low expression of PD-1 and CTLA-4 and high expression of TIM-3 were observed in both CD4+and CD8+ subsets	80

LIST OF TABLES

Table Number	Title	Page Number
1	Targeting dual antigens in clinical trials	21
2	Human cell lines and primary cells	25
3	Cell Culture Media	25
4	Reagents for CAR-T Cell Culture and CAR-T Assays	26
5	Reagents for transfection and transduction	26
6	Reagents for cloning	27
7	Flow Cytometry Antibodies and Reagents	27
8	Plasmids	29
9	Primers	29
10	gBlock	31
11	PCR reactions	33
12	Touchdown PCR protocol	33
13	DNA Assembly Reaction	34
14	Transfection components	36
15	Flow Panel for Checking CAR Expression	36
16	Lentivirus Production	37
17	Flow Panel for Checking Transduction Efficiency	41
18	Flow Panel for Degranulation	42
19	Flow Panel for Proliferation	43
20	Phenotype of CAR T Cells and Untransduced T cells	44

Table Number	Title	Page Number
21	Flow Panel for CAR T Cell and Untransduced T cell Phenotyping	44
22	Flow Panel for CAR T Cell and Untransduced T cell Exhaustion markers	44
23	Generation of vectors	47
24	Generation of vectors	49
25	Dual CAR expression 48 hours after transfection	50
26	Generation of vectors	51
27	Dual CAR expression 48 hours after transfection	53
28	Generation of Vectors by removing tEGFR	54
29	Generation of vectors	56

ABBREVIATION

Abbreviation	Explanation
ALL	Acute Lymphoblastic Leukemia
AML	Acute Myeloid Leukemia
APC	Allophycocyanin
APC	Antigen-Presenting Cell
BCR	B Cell Receptor
BTK	Bruton's tyrosine
CAR-T	Chimeric Antigen Receptor T
CEA	Carcinoembryonic Antigen
CHOP	Cyclophosphamide, hydroxydaunorubicin, Oncovin, prednisone
CLL	Chronic Lymphocyte Leukemia
CR	Complete Response
Cri	Complete Response with incomplete hematological recovery
CTLA-4	Cytotoxic T-Lymphocyte Associated Protein 4
DLBCL	Diffuse Large B-cell Lymphoma
DMEM	Dulbecco's Modified Eagle Medium
E. coli	Escherichia coli
EBV	Epstein-Barr Virus
EGFR	Epidermal Growth Factor Receptor
FBS	Fetal Bovine Serum
FITC	Fluorescein Isothiocyanate
GD2	Disialoganglioside
HDAC	Histone Deacetylase
HER2	Human Epidermal Growth Factor Receptor 2

ICOS	Inducible T- cell CoStimulator
ITAM	Immune receptor Tyrosine based Activation Motif
LAG3	Lymphocyte Activation Gene-3
LTR	Long Terminal Repeat
MCL	Mantle Cell Lymphoma
MHC	Major Histocompatibility Complex
MM	Multiple Myeloma
NHL	Non-Hodgkin's Lymphoma
ORR	Overall Response Rate
PBMC	Peripheral Blood Mononuclear Cell
PBS	Phosphate Buffered Saline
PD-1	Programmed Cell Death-1
PE	Phycoerythrin
PI3K	Phosphatidylinositol 3-kinase
PR	Partial Response
RPMI 1640	Roswell Park Memorial Institute 1640 Medium
scFv	Single Chain Variable Fragment
SCR	Stringent Complete Response
TAA	Tumor Associated Antigen
TAE	Tris Acetate EDTA Buffer
T _{CM}	Central Memory T cells
TCR	T Cell Receptor
TD	Transduction
T _{EM}	Effector Memory T cells
T _{EMRA}	Terminally Differentiated Effector Memory T cells

TIGIT	T-cell Immunoreceptor with Immunoglobulin and ITIM domain
TIM-3	T-cell Immunoglobulin and mucin domain-3
T _N	Naïve T cells
T _{SCM}	T memory stem cells
TRUCKs	T-cell Redirected for Universal Cytokine-mediated Killing
UTD	Untransduced T cells
VGPR	Very Good Partial Response
V _H	Heavy chain Variable domain
V _L	Light chain Variable domain

Chapter 1: Introduction

1. B-cell Malignancies

1.1 B-cell Malignancy Introduction

In the US, lymphoid neoplasms have become the fourth most common type of cancer. Lymphoid neoplasms encompass a large and heterogenous group of B-cell and T-cell lymphomas and leukemias, with the most prominent subgroups being Non-Hodgkin lymphoma (NHL) and leukemia, as the 7th and 9th most common cancer for males, and 6th and 10th for females in the US respectively (1, 2). Within NHLs, about 85% are B-cell lymphomas, including diffuse large B-cell lymphoma, follicular lymphoma, and mantle cell lymphoma. Chronic lymphocyte leukemia (CLL) accounts for a third of all leukemias in adult and is the most common leukemia in the western hemisphere (3). Given their significant numbers and biological features which allow for similar targeting mechanisms, B-cell lymphoma and CLL will be the focus of this project.

1.2 B-cell Malignancy Mechanism

The development, maturation, and activation of B-cells is a multi-step, complex process that traverses multiple organs. Genomic errors and abnormalities can lead to neoplasms, ultimately resulting in B-cell malignancies.

1.2.1 B-cell Development

B-cells start out in the bone marrow as lymphoid progenitors. B-cell receptor (BCR) production is initiated by V(D)J gene recombination of first heavy and then light chains. Before differentiating into an immature B-cell, the cell goes through a quality control step. Apoptosis occurs if recombination-activating gene (RAG) enzymes fail to produce a structurally sound heavy chain. CD21 and CD22 are expressed in an immature B-cell in addition to membrane

bound IgM. If the cell has both productive BCR and not self-reactive, maturation will continue in a secondary lymph organ, such as the spleen (4).

1.2.2 B-cell Activation

In a naïve, mature B-cell, two signals are required for activation. The first signal involves antigen presentation from an antigen-presenting cell (APC), triggering upregulation of CD80/86 (which provides the second signal for T-cell activation) and CD40. Additionally, the antigen and its corresponding BCR are endocytosed to be processed and presented on the B-cell's major histocompatibility complex (MHC) II. As T-cells are activated through antigen presentation on B cells and interaction of CD28 on T cells with the upregulated CD80/86 on B cells, they express CD40L which binds to CD40 on B cells. This CD40-CD40L interaction provides signal two, at which point the activated B-cell forms a germinal center. In the germinal center, the B-cell undergoes two important processes: class-switching and somatic hypermutation. Finally activated B-cells can become either memory B-cells or plasma cells (4).

1.2.3 B-cell Mutations

It is possible to use immunophenotypic and molecular markers to classify B-cell lymphomas. Most B-cell lymphomas arise from germinal center or post-germinal center B cells. Neoplasms usually arise due to three main factors: chromosomal translocation, gene mutations, and viruses. Epstein-Barr virus (EBV) is a well-known cause of Burkitt's lymphomas, as well as post-transplant primary effusion lymphomas. Genetic mutations in important tumor-suppressing genes such as TP53 and ATM can also lead to various examples of B-cell malignancies, including CLL and diffuse large B-cell lymphoma. Finally, chromosomal translocations are common in B-cell malignancies. Chromosomal translocations can be in the Ig locus or the non-Ig locus. In the non-Ig locus, translocations often occur in the

germinal center during class-switching or somatic hypermutation. In the Ig locus, translocations can be due to faulty V(D)J recombination during early B-cell development, or breakpoints introduced during class-switching or somatic hypermutation. These three types of translocations often involve exchange between Ig genes and proto-oncogenes, resulting in constitutive expression of oncogenes (5).

1.3 Treatment for NHL and CLL

1.3.1 Conventional Treatment Methods

Historically, the standard of care for NHL and CLL was chemotherapy, which is usually given intravenously or orally as one or multiple drugs. These drugs can be categorized by their different mechanisms into alkylating agents, corticosteroids, platinum drugs, purine analogs, anti-metabolites, and anthracyclines. One of the most common combinations is CHOP, which is comprised of the drugs **c**yclophosphamide, **d**oxorubicin (also known as **h**ydroxydaunorubicin), **v**incristine (**O**ncovin), and **p**rednisone. Another common combination is CVP (**c**yclophosphamide, **v**incristine, and **p**rednisone). Currently, the first line treatment for many NHLs continues to be chemotherapy, often in combination with radiation therapy or immunotherapy. The dosing of the drugs and number of cycles given are dependent on the specific subtype and stage of disease (6).

Radiation therapy utilizes a beam of radiation (photons, protons, or electrons) to eliminate disease. In the case of certain early-stage NHLs, it can be used as the primary form of treatment. It can also be used in stem cell transplantation for systemic eradication of lymphoma cells. Radiation therapy, in addition to chemotherapy, is most often recommended for bulky disease, but recent research has shown it can also improve overall survival and progression-free survival even in those with non-bulky disease for large B-cell lymphoma (6).

There has been significant innovation in targeted drug therapy in recent years. This encompasses proteasome inhibitors, histone deacetylase (HDAC) inhibitors, Bruton's tyrosine kinase (BTK) inhibitors, Phosphatidylinositol 3-kinase (PI3K) inhibitors, EZH2 inhibitors, and nuclear export inhibitors. Due to unique mechanisms that are different from that of traditional chemotherapy drugs, targeted drug therapy can be effective in patients who show lack of response to conventional chemotherapy. (7)

High dose chemotherapy has become possible and more common with stem cell transplants. The biggest barrier to using higher dosage of chemotherapy drugs, despite potential greater efficacy, are the side effects. The bone marrow, where new blood cells originate, is highly susceptible to immense damage with high doses of chemotherapy. However, with stem cell transplants, fresh stems cells can be infused, negating this issue (8).

1.3.2 Immunotherapy

Complete remission and patient survival have been greatly improved when immunotherapy is combined with traditional cancer treatments. Immunotherapy seeks to ameliorate the effects of tumor escape mechanisms. Tumor cells prevent T cells from recognizing tumor specific antigens (TSA) and tumor associated antigens (TAA) presented by tumor cells and killing them by releasing perforin, granzyme, and cytokines (IFN- γ and TNF- α). Firstly, cancer cells can decrease or lose expression of all MHC I molecules. The recognition of antigen peptides presented by the MHC I of tumor cells is crucial for evoking a CD8+ T cell response. Secondly, tumor cells that do not express costimulatory CD80 and CD86 and therefore can induce anergy in T cells by failing to engage CD28. Thirdly, cytotoxic T cells lose the capacity to proliferate and evoke anti-tumor activity if they become "exhausted" due to persistent stimulation and are inhibited by immune checkpoints (PD-1, LAG3, CTLA-4,

TIM3 and TIGIT). Finally, self-antigens expressed by most tumors have low or no immunogenicity, restraining T-cells from recognition due to low-affinity TCRs (9).

Monoclonal antibodies, a type of immunotherapy, have been the answer to these instances of reduced T-cell immune responses. Monoclonal antibodies are man-made analogs to target specific proteins expressed in different B-cell malignancies, bypassing the need for antigen presentation by tumor cells. Some of the most used monoclonal antibodies target different surface proteins on B lymphocytes, such as CD20, CD19, CD52, CD30, and CD79b. Combined with chemotherapy, anti-CD20 monoclonal antibody, rituximab, has been used to treat B-cell NHL. Antibody-drug conjugates are also used, in which a chemotherapy drug is attached to a monoclonal antibody that targets a surface antigen. Anti-CD79b antibody drug conjugate, polatuzumab vediton, has been approved to treat relapsed or refractory (R/R) large B-cell lymphoma (DLBCL). Another use of monoclonal antibodies is in inhibiting T-cell immune checkpoints such as CTLA-4 and PD-1, allowing for a stronger immune response to cancer cells. Anti-CTLA-4 and anti-PD-1 antibodies can restore tumor-infiltrating lymphocyte (TIL) CD8+ anti-tumor activity, with improved patient survival in cancer treatments for melanoma, non-small cell lung cancer (NSCLC), renal cell carcinoma (RCC), among others (10).

1.3.3 Limitation of Current Methods

Although chemoimmunotherapy may be curative in certain B-cell NHLs, most patients eventually relapse. Patients with B-cell malignancies who relapse after chemoimmunotherapy or have resistant tumors have a very poor prognosis. The novel chimeric antigen receptor T (CAR T) cell therapy approach provides a promising treatment option for patients with relapsed or refractory B-cell malignancies and has been shown to induce prolonged remission and long-term survival even in patients who have chemorefractory disease.

2. Chimeric Antigen Receptor T cells

2.1 CAR T History

In 1987, Dr. Zelig Eshhar from the Weizmann Institute of Science revolutionized the use of CAR T cells. The chimeric antigen receptors (CAR) were able to recognize specific antigens expressed on cancer cell surfaces and activate T cells to attack tumor cells with an MHC-independent mechanism. CARs contained sequences that expressed single-chain variable fragments (scFv) from a monoclonal antibody's heavy chain (HC) and light chain (LC). The scFv was fused to the γ chain of the immunoglobulin Fc or to the ζ chain of CD3. This was the first-generation model of the CAR T cells. While ground-breaking in concept, the first-generation model failed to achieve expected clinical activity due to limited expansion and poor persistence without a co-stimulatory domain (11).

With further research and investment in CAR T, Dr. Finney and his colleagues were able to introduce co-stimulatory domains (CD28) to the previous CAR construct, greatly improving CAR T killing efficacy by enhancing CAR T proliferation, cytokine production, and persistence (12).

Pre-clinical trials of 2nd generation CD19-CAR T with co-stimulatory domains CD28 and 4-1BB have achieved great success in treatment for patients with relapsed and refractory B-cell malignancies. The clinical trial was conducted at Children's Hospital of Philadelphia using CD19-targeting CTL019 T cells with 4-1BB costimulatory domain for the treatment of relapsed and refractory ALL. With a study group of 30 children and adults, the results were very promising – with a complete response (CR) rate of 90%, 6-month event-free survival rate of 67%, and overall survival of 78% (13, 14). Other clinical trials were conducted at the National Cancer Institute (NCI) and at Memorial Sloan Kettering Cancer Center (MSKCC) by using CD28 co-stimulatory domains. These studies were able to achieve 67% CR and 88% CR, respectively (15, 16).

Two important CD19 CAR T products have recently been approved to treat patients with B-cell malignancies. On August 30th, 2017, the FDA approved the first CD19 CAR T cell immunotherapy live drug, tisagenlecleucel (Kymriah; 4-1BB co-stimulatory domain), to be used for treating patients under 25 years of age with relapsed or refractory acute lymphoblastic leukemia (ALL) (17). On May 1st, 2018, Kymriah was approved by the FDA for treating patients with relapsed or refractory large B-cell lymphoma, based on results from the Novartis pivotal JULIET trial (18).

On October 18th, 2017, based on the ZUMA-1 trial, axicabtagene ciloleucel (Yescarta; CD28 co-stimulatory domain) was approved by the FDA for treating patients with relapsed or refractory large B-cell lymphoma including DLBCL, high-grade B-cell lymphoma, primary mediastinal large B-cell lymphoma, and DLBCL arising from follicular lymphoma (19). On March 5th, 2021, axicabtagene ciloleucel was approved by the FDA also for treating patients with relapsed or refractory follicular lymphoma based on the results of Kite's ZUMA-5 studies (20).

On July 24th, 2020, brexucabtagene autoleucel (Tecartus) was approved by FDA for treating patients with relapsed or refractory mantle cell lymphoma (MCL). On October 1st, 2021, based on the result of ZUMA-3 trial, brexucabtagene autoleucel was approved by FDA for treating adult patients with relapsed or refractory B-cell precursor acute lymphoblastic leukemia (ALL) (21).

On February 5th, 2021, Lisocabtagene maraleucel (Breyanzi) was approved by FDA to treat adult patients with relapsed or refractory large B-cell lymphoma including DLBCL, high-grade B-cell lymphoma, primary mediastinal large B-cell lymphoma, and follicular lymphoma grade 3B (22).

On March 27th, 2021, idecabtagene vicleucel (Abecma)-the first CAR T cell therapy targeting B-cell maturation antigen (BCMA) was approved by FDA for treating patients with relapsed or refractory multiple myeloma (23).

On February 28th, 2022 , Ciltacabtagene autoleucl (Carvykti) was approved by FDA for treating adult patients with refractory/relapsed multiple myeloma after four or more other lines of therapy (24).

2.2 CAR T Mechanism

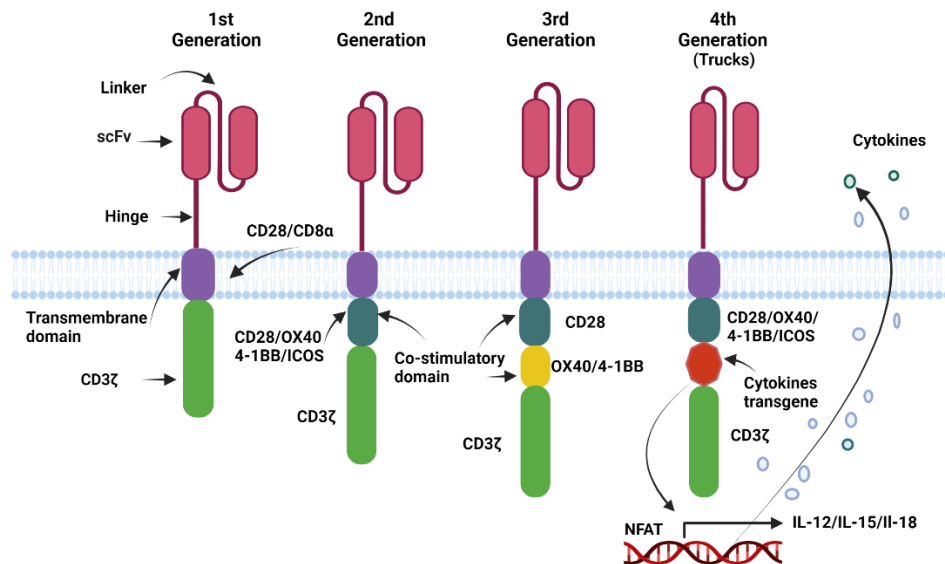
CAR T cells are engineered to express chimeric antigen receptors that allow for activation and recognition of tumor-specific antigens, while bypassing the standard two-signal activation pathway. Normal T cells are activated with two signals from APCs. The first signal comes from the interaction of CD4/CD8 T-cell receptors (TCR) with their corresponding MHCs, forming immunological synapses. This recruits tyrosine kinase Lck to phosphorylate the Immune-receptor-Tyrosine-based-Activation-Motif (ITAM) regions of TCR cytoplasmic domains. These events activate ZAP-70, a Syk family tyrosine kinase that provides the capability for triggering downstream signaling pathways and elicits the first signal. In the second signal, CD80/86 (B7-1/7-2) on the APC bind to CD28 on the T-cell, leading to PI3K activation, which in turn activates numerous transcription factors and production of IL-2, fulfilling the second signal (25, 26).

On the other hand, CAR T cells have a far more streamlined process that leads to full activation of the T-cell. In the first generation of CAR-T cells, the CAR was modified with an ectodomain consisting of a scFv linked to an endodomain of CD3 ζ , which could induce activation through ZAP70 with a single tumor antigen. The use of a scFv recognition domain allows for MHC-independent recognition and ligand binding. Later generations have included adding a co-stimulatory endodomain such as CD28, 4-1BB, ICOS, or OX40, which allowed for stronger phosphorylation and greater downstream signaling. Compared with unmodified T cells, CAR T cells have a greater advantage in attacking tumor cells by circumventing tumor cell escape mechanisms (25, 26).

Activated CAR T cells will undergo either of two pathways, similar to normal T cells. Activated CD4+ T cells will receive a third signal based on the cytokine from the APC. This induces different transcription factors that will allow it to produce more cytokines to recruit other immune cells for a stronger systemic host immune response. Activated CD8+ T cells will initiate killing of the tumor cell through two primary mechanisms: lysis and apoptosis. To lyse the tumor cell, the CD8+ T cells will release perforin and granzymes. The CD8+ T cells can also upregulate FasL on its surface, which can induce tumor cell apoptosis via Fas (26).

2.3 CAR Construct

The basic CAR construct consists of an ectodomain, transmembrane domain, and endodomain.



Created with BioRender

Figure 1. CAR Construct and Generation. CARs consist of an extracellular (scFv & hinge), transmembrane and intracellular domain (CD3 ζ /Co-stimulatory domain). The first-generation CARs only contain CD3 ζ intracellular signal domain. The second-generation CARs were engineered with co-stimulatory domain such as CD28, OX40, 4-1BB and ICOS. The third-generation CARs were incorporated with two co-stimulatory domain such as CD28-OX40/4-1BB. The fourth-generation CARs were engineered to secrete proinflammatory cytokines such as IL-12, IL-15 and IL18 to enhance effector T cell function.

2.3.1 CAR Ectodomain

The ectodomain opens into the extracellular space and includes antigen recognition domain and hinge.

The **signal peptide** is responsible for directing the protein to the endoplasmic reticulum, where it is then cleaved, while the CAR is processed and transported to the membrane as a membrane protein.

The **antigen recognition domain** consists of a single chain variable fragment (scFv) made up of the variable parts of the heavy and light chain of a tumor-selective monoclonal antibody and are connected with a peptide linker. The use of scFv for CARs in the place of a full-length monoclonal has several advantages.

Firstly, the small size of scFv allows antigen-specific target localization and faster serum clearance compared with full length antibodies. Secondly, the scFv reduces nonspecific binding associated with the Fc receptor. The antibody Fc region can interact with Fc receptors expressed on other immune cells including natural kill (NK) cells, monocytes, macrophages and dendritic cells (DC). IgG antibodies also can initiate the classical pathway of complement activation through binding of the Fc region. These aspects of full-length antibody interactions can all reduce overall target specificity (27).

The scFv generation is critical for CAR construction because the properties of the scFv can impact CAR T efficacy and safety. Most scFvs are generated by hybridoma approach, which involves immunization of mice, B cell isolation, high affinity antibody screening, and heavy and light chain generation through PCR-mediated amplification from cDNA (hybridoma RNA) (27).

The variable portions of heavy (V_H) and light chain (V_L) are linked by the glycine-rich peptide (Gly₄ser)₃. The linker is important as it allows for independent folding of the heavy and light chains.

The **hinge** is designed to connect the scFv to the transmembrane domain. It determines the distance between the cell membrane and target antigen and the flexibility of the scFv. Currently, the hinge sequence is mainly derived from the hinges of CD8 α , CD28, and IgG constant domains. The hinge domain strongly affects the efficacy of the CAR-T cell in many ways. Increased flexibility of the hinge can allow targeting of epitopes that normally suffer from steric hindrance. Distance is also an important factor, as longer hinges can lead to poor synapse formation and decreased signaling and lytic capability (28).

2.3.2 Transmembrane Domain

The transmembrane domain serves as the communication pathway between the ligand-binding ectodomain and the signal-transducing endodomain. The variation in transmembrane domain sequence strongly affects CAR membrane expression stability. In the past, CD3 ζ , CD4, CD8, and CD28 molecules have all been used. Currently, CD28/CD8 α are used most frequently (27).

2.3.3 CAR Endodomain

The cytoplasmic portion of the CAR has undergone the most drastic adaptations with increasing research and can be classified into four different generations. All generations have in common a CD3 ζ intracellular signaling domain.

The first-generation CAR was a basic construct with only one intracellular signaling domain – either CD3 ζ or the γ chain of an Fc receptor. The second-generation CAR added a co-stimulatory activation domain such as CD28, 4-1BB, ICOS, or OX40. The third-generation CAR added two or more co-stimulatory domains. Finally, the fourth generation endodomain modified the second generation endodomain with the addition of cytokines such as IL-7, IL-12, IL-15, IL-18, and IL-23 to the base of the stimulatory domains. It is also known as T-cell redirected for universal cytokine-mediated killing (TRUCKs). Modification with these cytokines is meant to enhance T cell activation and the innate immune cell response in killing tumor cells (27, 29, 30)

A few factors have affected the success and intensity of intracellular signaling *in vitro* and *in vivo*: (1) type and number of co-stimulatory domains; (2) order of co-stimulatory domains; and (3) number of ITAMs.

After the efficacy of the first-generation CAR T construct was deemed too weak with only CD3 ζ , more domains were added in future generations. It has been proven that having at least one more co-stimulatory domain greatly increases persistence and anti-tumor potency as it mirrors the two-signal activation pathway of normal TCRs; however, adding more does not yield the same result. While early studies showed that third-generation CARs increased phosphorylation, it has still been outperformed by second-generation CARs in tumor-killing activity in many studies. The specific co-stimulatory domain selected also makes an immense difference. Two common co-stimulatory domains are CD28 and 4–1BB. The former has stronger and faster signaling, but it comes at the price of greater tonic signaling, which leads to early exhaustion. The latter has weaker and slower signaling but has greater persistence and can reduce tonic signaling and early exhaustion (25, 31).

Another consideration is the ordering of the domain molecules. When CD28 is the membrane-proximal molecule as opposed to CD3 ζ , IL-2 is produced at higher levels, which encourages greater proliferation and longer sustained activity. It has been hypothesized that

this might be due to the proximity of CD28 or other co-stimulatory domains to tyrosine kinases which cluster near the membrane (27).

Finally, the number of ITAMs plays a role in intracellular signaling. TCRs typically have ten ITAMs, while a conventional CAR has only three. However, homodimeric CARs have two CD3 ζ domains, allowing for six ITAMs. This has been shown to allow for higher IL-2 levels and greater T-cell proliferation compared to monomeric CARs (27).

2.4 CAR Production

2.4.1 CAR Cloning

Once the various parts of the CAR have been optimized, the sequences of all the components need to be assembled into a retroviral plasmid. The most commonly used vectors are lentiviral and gammaretroviral vectors. The retroviral vector is transfected into vector-producing cell lines to generate a replication-deficient virus that can integrate into mammalian cells. A supernatant of the virus can then be collected for T-cell infection.

Essential to the process are plasmids containing vital sequences for virus assembly and a plasmid for the CAR gene sequence. These plasmids have faulty long terminal repeat (LTR) promoters, which renders the virus incapable of replicating in host cells while maintaining tropism. Three essential components for virus assembly are *env*, *gag*, and *pol* genes. The *env* gene encodes for the viral envelope protein that can determine infectivity. The *gag* gene encodes for a variety of essential structural proteins. And the *pol* gene encodes for reverse transcriptase, which produces dsDNA from genomic RNA, and integrase, which integrates the newly constructed dsDNA into the host genome. The second-generation packing system for lentivirus has a *tat* gene sequence, which also assists in viral replication. On the other hand, the third-generation system has a modification of the 5' LTR and eliminates the need for *tat* (32).

The selection of the retrovirus vector is a very significant aspect of cloning CARs in T cells. Not only does it strongly affect the expression efficacy, but it also poses a tremendous safety concern. One of these apprehensions is the ability of the pseudotyped virus to become replication-competent once transduced into primary T cells. However, the likelihood of this event has become greatly decreased with new and improved transduction techniques and modification of vector LTR promotion sequences, such as deleting the U3 sequences in the 3' LTR (32).

Traditionally, lentiviruses and gammaretroviruses have both been very effective in T-cell modification. However, lentiviral vectors exhibit certain advantages over gammaretroviral vectors. Lentiviral vectors are effective even in nondividing cells, giving it the capability to target a greater variety of cells, such as muscle and brain cells. Additionally, there are less incidences of promoter regions in the T cell genome (32) .

Two new transposon-based systems have been introduced for CAR cloning and expression: *sleeping beauty (SB)* and *PiggyBac*. The SB system utilizes (1) a plasmid encoding transposase and (2) a transposon-based vector contained within inverted repeat/direct repeat (IR/DR) sequences to clone a CAR expression cassette. The transposon can be integrated precisely into the genome at TA/TA sites through recognition of IR/DR sequences by the transposase. The modified T cells are then activated with artificial APCs. The *Piggybac* system utilizes (1) a *Super Piggybac* transposase and (2) a *Piggybac* vector contained within inverted terminal repeat (ITR) sequences. In a similar mechanism to SB, the Super Piggybac transposase recognizes ITR sequences in the vector to integrate at TTAA sites in the host genome (32).

These new systems have shown greater stability and control for safer and higher efficacy CAR expression. The *Piggybac* system allows for strict and simple control of CAR expression through its transposon, which can remove the chimeric genomic information by itself (32).

2.4.2 CAR Expression and Generation

Once the viral particles are transduced into the T cells, they are able to introduce the CAR genomic information into the T cell genome through conventional retroviral processes. From the chimeric RNA transcripts, reverse transcriptase produces dsDNA, which is then integrated into the host genome. Once integrated, the CAR will be expressed in the host cell and the T-cell undergoes expansion with the new genomic additions.

The T cells are collected from the patient through leukapheresis. The blood is separated for leukocyte harvesting and T cell enrichment using counterflow centrifugation elutriation. Then T cells are modified to generate chimeric antigen receptor on the surface of the cells. After expansion of CAR T cells, CAR T cells will be frozen and sent to hospital for treatment (33).

3. CAR T Immunotherapy Targets

To date, FDA approved six CAR T products including Kymriah (CD19 CAR T), Yescarta (CD19 CAR T), Breyanzi (CD19 CAR T), Abecma (BCMA CAR T) and Tecartus (CD19 CAR T). Presently, there are more than 500 CAR-T clinical trials being conducted worldwide (34). Most CAR T clinical trials are in B-cell malignancies; however, a number of CAR T studies are also focusing on multiple myeloma. Although it is difficult to find an ideal target antigen for solid tumor, CAR T targeting tumor's associated antigen (TAA) such as HER2, CEA, EGFR, GD2, mesothelin, MUC1 and PSMA have been studied in both laboratory research and clinical trials (35).

3.1 CD19 as an Ideal Target

CD19 is a type 1 transmembrane glycoprotein and belongs to a member of the immunoglobulin superfamily. CD19, along with CD21 form a B-cell co-receptor complex,

which plays an important role in B-cell activation and antibody production. CD19 is a B cell lineage marker and is expressed on the surface of all B-cells from early pro-B cell to mature B-cell, except for plasma cells. Secondly, CD19 is expressed on most B-cell malignancies including 80% of ALLs, 88% of B-cell lymphomas and 100% of B-cell leukemias. Finally, CD19 is not expressed on hematopoietic stem cells and other normal essential tissue, which helps to prevent toxic side effects. These conditions all make CD19 an ideal target for CAR T immunotherapy (14).

3.2 CD19 CAR T Treatment

Treating patients with relapsed or refractory B-ALL and DLBCL using CD19 CAR T has yielded extraordinary clinical results, with a high CR between 90% and 60%. This has led the FDA to approve the two CAR T products axicabtagene ciloleucel (Yescarta) and tisagenlecleucel (Kymriah) for use in treating patients with relapsed or refractory B cell malignancies including B-ALL, DLBCL and Follicular lymphoma.

3.3 CD19 CAR T Limitations

Despite the great clinical results from CD19-targeted CAR T for treating relapsed or refractory B cells malignancies, about 30-60% patients eventually relapse following treatment. Relapsed patients fall into two categories: CD19 positive relapse and CD19 negative relapse (36).

CD19 positive relapses are due to poor CD19 CAR T persistence, dysfunctional T cells or due to tumor intrinsic resistance mechanisms. Poor CD19 CAR T persistence is associated with the selection of the CAR costimulatory domain. Based on the results of published studies and clinical trials, CAR T cells with a 4-1BB co-stimulatory domain has better persistence than CD28. For CAR T treatment using CD19-CD28 ζ , the median and longest time for persistence was 3 months and 7 months, respectively. For CAR-T using CD19-4-1BB ζ , 68% of patients

had evidence of persistence for 6 months and the longest time was 20 months. The median CD19 positive relapse rate for CD19-4-1BB ζ and CD19-CD28 ζ CAR-T treatments were 16.7% and 22.7%, respectively. Increased tumor burden is correlated with greater CAR T clearance from the circulation, CAR T inactivation, and CAR internalization, which all contribute to lower CAR T tumor-killing efficiency. Another rare situation that has occurred is epitope masking, or when a CD19 CAR is accidentally transduced into a leukemia cell. This allows the CD19 CAR to self-bind to CD19 in the tumor cell, which shields it from CAR T cells(36, 37).

Among relapsed patients, CD19 negative relapse comprise 10-20%. CD19 negative relapse is caused by CD19 antigen loss. Mutations in CD19 can contribute to CD19 antigen loss due to CD19 gene deletion or frameshift. Alternative splicing of exons 2, 5 and 6 can also cause CD19 loss. Alternative splicing of exon 2 affects the extracellular epitope expression of CD19. Alternative splicing of exons 5 and 6 cause a deficiency in the transmembrane domain of CD19, which leads to loss of CD19 expression. Additionally, due to immune pressure, previously undetectable CD19 negative clones are selected and become the dominant clones. CD19 antigen loss is also caused by cell lineage switching. Lineage switch occurs when a patient relapses with a genetically related but phenotypically different malignancy. Some studies reported patients with mixed lineage leukemia (MLL) rearranged B-ALL relapsed with CD19 negative AML after CD19 CAR T treatment (38).

3.4 Multiple Antigen Targeting

Since downregulation or antigen loss has been observed in relapsed patients treated with CAR-T therapy targeting a single antigen such as CD19 CAR or CD22 CAR, a potential strategy to improve efficacy is to target more than one antigen. Pan B-cell antigens such as CD20, CD22, and CD79b are also expressed on B-cell malignancies and can be used for dual

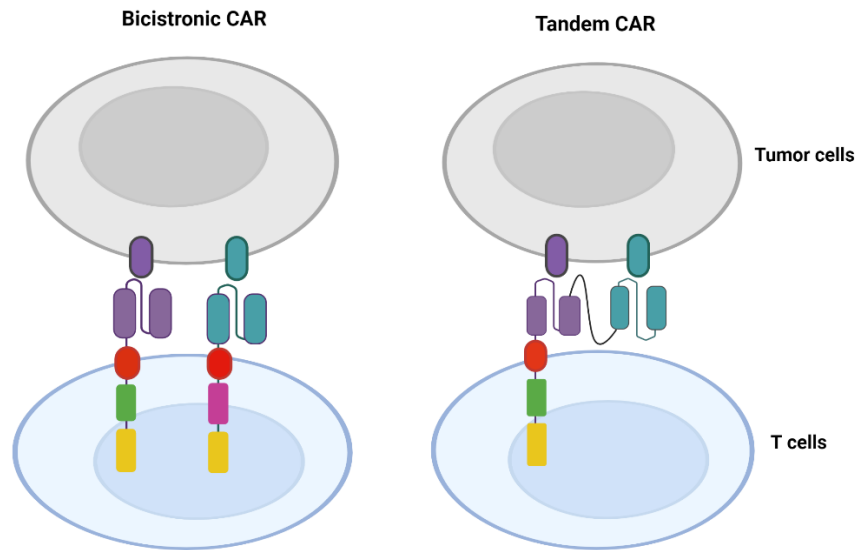
targeting. Currently, 4 methods, co-administration, co-transduction, tandem CAR, and bicistronic CAR, have been used for targeting two antigens. In co-administration, two mono CAR T cells such as CD19 CAR and CD22 CAR are infused to patients simultaneously or sequentially. Co-transduction transduces T cells with two different vectors encoding distinctive CARs. After co-transduction, four T cell groups are expected: untransduced T cells, one single CAR T (such as CD19 CAR-T), another single CAR-T (such as CD22 CAR-T), and T cells simultaneously expressing CD19 CAR and CD22 CAR. Co-administration and co-transduction are more expensive to manufacture because of heterogeneous and inconsistent products. In tandem CAR, two different antigen binding scFvs are connected to a single CAR endodomain with the same hinge. While this method homogeneously targets both receptors, the orientation of the two receptors in proximity can result in steric hindrance. Finally, bicistronic CAR T expresses two different CARs in the same T-cell and are transduced with a single vector. This allows for almost equal expression of the two different CARs in the cell, which enhances CAR-T and tumor engagement, increasing tumor potency (37, 39).

Currently, a number of clinical trials are focusing on dual targeting to minimize antigen escape observed after single CAR T therapy (Table 1) (35). Two phase 1 trials of CAR T targeting CD19 and CD22 have demonstrated the manufacturing feasibility of dual CAR T cells and safety profile such as no dose-limiting toxicities. A bispecific CD19-22.BB.z CAR has achieved 100% ORR and 86%CR in patients with B-ALL and 62% ORR and 29% CR in patients with LBCL. However, in relapsed patients CD19 loss or low CD19 expression was observed but CD22 loss or low density was not. Additionally, the final CAR product was dominated by CD4+ CD19-CD22 CAR T cells with higher expression of PD-1 and CD39. The authors concluded that future work will focus on modifying CAR T manufacturing to achieve optimal ratio of CD4:CD8 and optimizing CD22 CAR to improve bispecific CAR efficacy (40). A bicistronic CAR product, CD19-OX40/CD22-4-1BB, was tested in AUTO3 trial in patients with relapsed or refractory B-ALL and has resulted in one-year overall survival of 60% and

event-free survival of 32%, which appear to be inferior compared to historical data with CD19 CAR alone. Patients relapsed with CD19 negative, or dim CD22 or loss of both CD19 and CD22. Limited CAR T cell persistence was observed on this study. The authors are therefore pursuing strategies to improve dual CAR T cell persistence and optimize CD22 CAR efficacy to recognize tumor cells with low antigen density in the future (41).

Table 1. Targeting dual antigen in clinical trials

Year	Clinical Trial register	Target	CAR Generation; Methods	Disease	Clinical outcome
2018	NCT03233854	CD19&CD22	2G: 4-1BB; Bispecific	B-ALL; DLBCL	33% CR
2019	NCT03289455 (Amelia)	CD19&CD22	2x 2G: OX40(CD19) 4-1BB (CD22) (AUTO3); Bicistronic	B-ALL; (pediatric/ young adults)	100% CR/Cri
2020	NCT03019055	CD19&CD20	2G: 4-1BB; Bispecific CAR	B-NHL; B-CLL	82% ORR; 64% CR
2020	NCT03287817 (Alexander)	CD19&CD22	2x 2G: OX40(CD19) 4-1BB (CD22) (AUTO3); Bicistronic	DLBCL	dose >50x 106: 64% ORR; 55% CR
2020	NCT03185494	CD19&CD22	2G: 4-1BB; Bispecific CAR	B-ALL	100% CR
2020	ChiCTR-OIB-17013670	CD19&CD22	2G: 41BB; Sequential CAR T-cell infusions	B-ALL (pediatric)	100% CR
2020	NCT03097770	CD19&CD22	2G: 4-1BB; Bispecific CAR	B-NHL	79% ORR; 71% CR
2020	ChiCTR-OPN-16008526	CD19&CD22	3G: CD28 & 41BB; sequential CAR T-cell infusions	B-ALL; B-NHL	B-ALL: 96%CR; B-NHL: 55% CR
2020	NCT03207178	CD19&CD20	2G: 41BB; co-infusion of CAR T-cells	DLBCL	81% ORR; 52.4% CR
2018	NCT03455972	CD19&BCMA	3G: CD28 + OX40; Sequential CAR T-cell infusions	MM	100% CR
2019	ChiCTR-OIC-17011272	CD19BCMA	Both 2G: 41BB and infused on the same day	MM	95% ORR; 57% CR
2019	ChiCTR1800018143	BCMA& CD38	2G: 41BB; Bispecific CAR	MM	85% ORR; 50% SCR; 12.5%/VGPR; 25% PR
2019	NCT03196414	CD19&BCMA	3G: CD28 + OX40 Sequential infusions	MM	92.6% ORR; 40.7% CR
2019	NCT03287804	BCMA&TAC1	3G: CD28 + OX40 dual antigen targeted CAR (AUTO2)	MM	43% ORR 28% PR



Created with BioRender

Figure 2. Construct of bicistronic CAR and tandem CAR

Bicistronic CARs are engineered to express two different CARs on the same cell to target two different antigens. Tandem CARs are modified to express two distinct scFvs in tandem in a single receptor to target two different antigens.

4. Hypothesis and Aims

4.1 Significance

CD19 antigen loss is a major cause of relapse and resistance after CD19 CAR T therapy. CD79b is not altered in the relapsed patients with or without CD19 loss. In addition, CD79b is pan-B cell marker broadly expressed in 95% of B-cell lymphoma cells as well as

chronic lymphocytic leukemia (CLL) and hairy cell leukemia. Dual targeting CD19 and CD79b could be a strategy to overcome immune escape and improve efficacy of CAR T therapy in patients with B-cell non-Hodgkin lymphoma and CLL and hairy cell leukemia.

4.2. Hypothesis

We hypothesize that dual CD19-CD79b CAR-T cells will be effective against B cell malignancies by targeting one or both antigens.

4.3 Aims

Aim 1: To generate bicistronic constructs expressing distinct CD19 CAR and CD79b CAR from a single vector.

CD19 CAR (murine anti-CD19 FMC63 clone) and CD79b CAR (murine anti-CD79b 28B clone) linked by 2A self-cleavable peptide will be cloned into a third-generation lentiviral backbone under the control of murine stem cells virus (MSCV) or human EF1 α promoter.

Aim 2: To determine dual CAR expression in 293 T-cells.

293 T-cells will be transfected by a lentiviral vector consisting of dual CARs using lipofectamine 3000. Cells will be harvested after 48 hours and the expression of CD19 CAR and CD79b CAR will be determined by flow cytometry.

Aim 3: To assess the expression and function of dual CARs in normal donor T-cells.

The expression of CD19 CAR and CD79b CAR will be determined by flow cytometry by staining CD19 protein-conjugated FITC and CD79b protein-conjugated PE. The function of dual CD19-CD79b CAR-T will be evaluated through degranulation, cytotoxicity, cytokine production, and proliferation assays.

Chapter 2: Materials & Methods

1. Materials

1.1 Cell Lines and Culture Medium

HEK-293 T cells, Daudi, SUDHL6, NALM6, K562 were obtained from the ATCC. PDX203-5D4 and PDX300-5E6 are patient-derived xenografts provided by Dr. Michael Green's Laboratory at UT MD Anderson Cancer Center. Daudi CD19KO was generated using CRISPR/Cas9 to knock out CD19 and was provided by Dr. Sattva Neelapu's Laboratory (MDACC). SUDHL6 CD19KO also used the CRISPR/Cas9 system and was provided by Dr. Eric Davis's laboratory. 293 T cells were cultured with completed DMEM. Tumor cells lines, untransduced and CAR-T cells, were cultured with completed RPMI 1640 (Table 2). The cell culture media are described in Table 3.

Table 2. Human cell lines and primary cells

Cell Lines	Providers	Description	Culture Medium
HEK-293T	ATCC CRL-3216	Modified human embryonic kidney 293 cells containing SV40 T-antigen	DMEM
Daudi	ATCC CCL-213	Burkitt's Lymphoma	RPMI 1640
SUDHL6	ATCC CRL-2959	Large B-cell Lymphoma	RPMI 1640
NALM6	ATCC CCL-243	Acute Lymphoblastic Leukemia	RPMI 1640
K-562	ATCC CCL-243	Chronic Myelogenous Leukemia	RPMI 1640
PDX203-5D4	MDACC	High Grade B-cell Lymphoma	RPMI 1640
PDX300-5E6	MDACC	High Grade B-cell Lymphoma	RPMI 1640
Daudi CD19KO	MDACC	Burkitt's Lymphoma, CD19 Knock-out	RPMI 1640
SUDHL6 CD19KO	MDACC	Large B-cell Lymphoma, CD19 Knock-out	RPMI 1640

Table 3. Cell Culture Media

Medium	Composition
DMEM High glucose GlutaMAX supplement Cat No. 10569044	DMEM + 10% FBS (v/v) + 1% Penicillin-Streptomycin(100U/mL)
RPMI 1640 GlutaMAX supplement Cat No. 61870127	RPMI 1640 + 10%FBS (v/v) + HEPES Buffer (25mM) + 1% Sodium Pyruvate (1mM, v/v)) + 1% Penicillin-Streptomycin(100U/mL) + β -mercaptoethanol (55 μ M) + 0.2% Normocin (100 μ g/mL) + 1% MEM Non-Essential Amino Acid Solution(v/v)

1.2 Reagents

T-cells were enriched using Pan T-cell isolation kit. T cells were activated with ImmnoCult Human CD3/CD28/CD2 and cultured in the presence of IL-2. Protein Transport Inhibitor was used in the assay of CAR-T degranulation (Table 4).

Table 4. Reagents for CAR-T Cell Culture and CAR-T Assays

Items	Supplier & Catalog Number
IL-2, Human	Genscript; Z00368-1
ImmunoCult™ Human CD3/CD28/CD2 T Cell Activator	StemCell Technologies; 10990
Pan T-Cell Isolation Kit, human	Miltenyi Biotec; 130-096-535
Protein Transport Inhibitor Solution 0.7mL	BD Biosciences; 554724
Histopaque(R)-1077	Sigma Aldrich; 10771-500ML
LS Columns	Miltenyi Biotec; 130-042-401
autoMACS Running Buffer	Miltenyi Biotec; 130-091-221

1.3 Reagents for Transfection and Transduction

Reagents for transfection and transduction are describe as below in Table 5.

Table 5. Reagents for transfection and transduction

Items	Supplier & Catalog Number
Lipofectamine 3000 Transfection Reagent	Life Technologies; L3000015
Opti-MEM I Reduced Serum Medium	Life Technologies; 31985062
Lenti-X™ Concentrator	Takara Bio USA; 631231
Lenti-X™ GoStix™ Plus	Takara Bio USA; 631281

RetroNectin® Recombinant Human Fibronectin Fragment	Takara Bio USA; T100B
3rd Generation Packaging System Mix	Applied Biological Materials; LV053
Millipore™ Steriflip™ Sterile Disposable Vacuum Filter Units	Millipore; SE1M003M00

1.4 Reagents for Cloning

Restriction enzyme, reagents, and kits for cloning were purchased from New England Biolabs (NEB) and QIAGEN (Table 6)

Table 6. Reagents for cloning

Items	Supplier & Catalog Number
BamH1	NEB; R0136L
MluI	NEB; R0198L
AgeI-HF	NEB; R3552L
PacI	NEB; R0547L
SpeI-HF	NEB; R3133L
BstEII-HF	NEB; R3162S
AvrII	NEB; R0174L
XbaI	NEB; R0145S
CutSmart Buffer(10X)	NEB; B7204S
Q5 Hot Start 2X high fidelity Master Mix buffer	NEB; M0494S
Monarch DNA Gel Extraction Kit	NEB; T1020S
NEBuilder HiFi DNA Assembly Master Mix	NEB; E2621
NEB Stable Competent E. coli (High Efficiency)	NEB; C3040H
QIAprep Spin Miniprep Kit (250)	QIAGEN; 27106
12663 HiSpeed Plasmid Maxi Kit (25)	QIAGEN; 12663

1.5 Flow Cytometry Antibodies and Reagents

Flow antibodies and reagents for flow cytometry were obtained from BD Biosciences, Biolegend, Life Technologies, R&D systems, AcroBiosystems, and Creative Biomart. CD79b-conjugated APC was kindly provided by Dr. Fuliang Chu (Table 7).

Table 7. Flow Cytometry Antibodies and Reagents

Items	Supplier & Catalog Number
Alexa Fluor® 700 anti-human CD3 [Clone: SK7]	BioLegend; 344822
PerCP/Cyanine5.5 anti-human CD4 [Clone: A161A1]	BioLegend; 357414
PE/Dazzle™ 594 anti-human CD8 [Clone: SK1]	BioLegend; 344744
PE/Dazzle™ 594 anti-human CD62L [Clone: DREG-56]	BioLegend; 304842
PE/Cyanine7 anti-human CD45RA	BioLegend; 304126
Brilliant Violet 605™ anti-human TIGIT (VSTM3) [Clone: A15153G]	BioLegend; 372711
Brilliant Violet 421™ anti-human CD366 (Tim-3) [Clone: F38-2E2]	BioLegend; 345007
Brilliant Violet 785™ anti-human CD152 (CTLA-4) [Clone: BNI3]	BioLegend; 369624
APC anti-human CD279 (PD-1) [Clone: EH12.2H7]	BioLegend; 329908
PE/Cyanine7 anti-human CD223 (LAG-3) [Clone: 11C3C65]	BioLegend; 369310
APC anti-human CD79b (Igβ) [Clone: CB3-1]	BioLegend; 341406
Hu CD8 BV605 SK1	BD Biosciences; 564116
Hu CD107a APC H4A3	BD Biosciences; 641581
PE anti-human CD19 [Clone: 4G7]	BioLegend; 392505
FITC-Labeled Human CD19 (20-291) Protein Fc Tag	AcroBiosystems; CD9HF251
Recombinant Human CD79B protein Fc-tagged, R-PE labeled	Creative Biomart; CD79B-239HP
CD79b-Conjugated with APC	MDACC
LIVE/DEAD Fixable Aqua Dead Cell Stain Kit for 405 nm excitation	Life Technologies; L34966
CountBright Absolute Counting Beads for flow cytometry	Life Technologies; C36950
CellTrace Far Red Cell Proliferation Kit for flow cytometry	Life Technologies; C34564
CellTrace Violet Cell Proliferation Kit for flow cytometry	Life Technologies; C34557
Human EGFR (Cetuximab) Alexa Fluor® 647-conjugated Antibody	R&D Systems; FAB9577R-100
Brilliant Stain Buffer 100Tst	BD Biosciences; 563794

1.6 Plasmids

The vectors J7m, J5a, J3v and R3r were kindly provided by Dr. Jingwei Liu (Dr. Neelapu Lab). T26 CD79b CAR and 28B C79b CAR were kindly provided by Dr. Fuliang Chu (Dr. Neelapu Lab). psPAX2 was purchased from Addgene (Table 8).

Table 8. Plasmids

Vectors	Description
J7m	Three-generation lentiviral expression vector encoding CD19 CAR with short CD28 H/TM and CD28 co-stimulation under the control of a MSCV promoter
J5a	three-generation lentiviral expression vector encoding CD19 CAR with CD8 α H/TM and OX40 co-stimulation under the control of a MSC promoter
J3v	three-generation lentiviral expression vector encoding CD19 CAR with CD28 H/TM and CD28 co-stimulation under the control of a MSC promoter
T26-CD79b CAR	three-generation lentiviral expression vector encoding CD19 CAR with CD α 8 H/TM and 4-1BB co-stimulation under the control of a MSC promoter
28B-CD79b CAR	three-generation lentiviral expression vector encoding CD19 CAR with CD α 8 H/TM and OX40 co-stimulation under the control of a MSC promoter
psPAX2	2nd generation lentiviral packaging plasmid; Addgene; Plasmid#12260
R3r	envelop expression vector expressing RD114

1.7 Primers

Customized primers and g-block fragments were synthesized by Integrated DNA Technologies (IDT) (Table 9 and Table 10).

Table 9. Primers

Primers	Sequence (5'-3')
F-CD79b-X1A	CACCTCGGGGGTCTTTTCATACGCGTGCCACCATGGCCCTGCCTGTGACAGC
R-CD79b-X1A	CCGCTTCCACGAGGTGGAAGTGCTTGCA
F-CD19-X1A	CTTCCACCTCGTGGAAGCGGCCACAACTT
R-CD19-A1A	GCTCTCCTGCAGCTTACCTCGGATCCTC
F-CD79b-X1B	CACCTCGGGGGTCTTTTCATGGATCCGCCACCATGGCCCTGCCTGTG
R-CD79b-X1B	TGCAGAGACAGTGACCAGAGTCCCTTG
F-CD8 H/TM-X1B	CTCTGGTCACTGTCTCTGCAACCACAACCCCTGCACCAAG
R-CD8 H/TM-X1B	AGGTCCTGGATTGCTTTCAACATCAC

F-CD19-X1B	GTTGAAAGCAATCCAGGACCTATGCTGCTGCTCGTGACCTC
R-CD19-X1B	GCCCCCTCCCTCTCCAGAACCGGTCCGTGGAGGCAGGGCCTGC
R-CD8 H/TM-X1C	CCTTCCCTCTCCAGAACCGGTTCTAGGTGGCAGTGCCTGCA
F- CD19-X1D	CACCTCGGGGGTCTTTTCATGGATCCGCCACCATGCTGCTGCTCGT G
R- CD19-X1D	GCCCCCTCCCTCTCCAGAACCGGTCCGTGGAGGCAGGGCCTGC
R-CD79b-X1E	CAGCAGCATAGGGCCGGGGTTCTCCTCCAC
F-CD19-X1E	ACCCCGGCCCTATGCTGCTGCTCGTGACCTC
R-CD19-X1E	CTTCCCTCTCCAGAACCGGTCCGTGGAGGCAGGGCCTGCA
F-CD19-X1F	CCACCTCGGGGGTCTTTTCATGGATCCGCCACCATGCTGCTGCTCG TGACC
R-CD19-X1F	AGGGCCATAGGTCCTGGATTGCTTTCAA
F-CD79b-X1F	AATCCAGGACCTATGGCCCTGCCTGTGACAGC
R-CD79b-X1F	CCCTTCCCTCTCCAGAACCGGTACGAGGTGGAAGTGCTTGCA
F-CD19-X1G	CACCTCGGGGGTCTTTTCATGGATCCGCCACCATGCTGCTGCTCGT GACCTC
R-CD19-X1G	AGGGCCATAGGTCCTGGATTGCTTTCAA
F-CD79b-X1G	AATCCAGGACCTATGGCCCTGCCTGTGACAGC
R-CD79b-X1G	CCCTTCCCTCTCCAGAACCGGTTCTAGGTGGCAGTGCCTGCA
F-CD19-X1H	CACCTCGGGGGTCTTTTCATGGATCCGCCACCATGGCCCTGCCAGT GACCGC
R-CD19-X1H	AGGGCCATAGGTCCTGGATTGCTTTCAA
F-CD79b-X1H	AATCCAGGACCTATGGCCCTGCCTGTGACAGC
R-CD79b-X1H	CCCCTTCCCTCTCCAGAACCGGTTCTAGGTGGCAGTGCCTGCA
F-CD19-X1I	AATCCAGGACCTATGGCCCTGCCAGTGACCGC
R-CD19-X1I	CCAGAACCCCGTGGTGGCAGCGCCTGCA
F-E2A- X1I	CTGCCACCACGGGGTTCTGGCCAGTGTACCAA
R-E2A -X1I	AGGGCCATAGGTCCTGGATTGCTTTCAA
R-CD79b-X1I	CCTTCCCTCTCCAGAACCGGTTCTAGGTGGCAGTGCCTGC
R-CD79b-X1J	AGCAGCATAGGGCCGGGGTTCTCCTCCA
F-CD19-X1J	AACCCCGGCCCTATGCTGCTGCTCGTGACCTC
R-CD19-X1J	TCGCGCCTCACCCAAAAGATGATGAAGG
F-CD19-X1K	CACCTCGGGGGTCTTTTCATGGATCCGCCACCATGCTGCTGCTCGT GACCTC
R-CD19-X1K	CCGCTTCCCCGTGGTGGCAGCGCCTGCA
F- P2A- X1K	CTGCCACCACGGGGAAGCGGCGCCACAACTT
R- P-2A-X1K	AGGGCCATAGGGCCGGGGTTCTCCTCCA
R-CD19-X1L	CCCCTTCCCTCTCCAGAACCGGTCCGTGGTGGCAGCGCCTGCA
R-CD79b CAR&CD19-X1N	GTCGTGGTGCTAGACACTGTCACAGAGG
R-CD19b-X1P	CCGCTTCCCCGTGGTGGCAGCGCCTGCA
F-P2A-X1P	CTGCCACCACGGGGAAGCGGCGCCACAACTT
R-P2A-X1P	AGGGCCATAGGGCCGGGGTTCTCCTCCA
F-CD79b-X1P	AACCCCGGCCCTATGGCCCTGCCTGTGACAGC
R-CD79b-X1P	CCCCTTCCCTCTCCAGAACCGGTTCTAGGTGGCAGTGCCTGCA
R-CD79b CAR&CD19-X1T	TTGCTCCTCACCCAGCAATACAATGTAA
F-CD79b-X1U	AACCCCGGCCCTATGGCCCTGCCTGTGACAGC

R-CD19 CAR- CD79b-X1W	CCTCGTTTGCAGTAAAGGGTGATAACCA
F-4-1BB-X1W	ACCCTTTACTGCAAACGAGGTAGAAAAAACT
R-CD79b-CD19 CAR-X2A	CGATAAGCTTGATATCGGTCACCTTACCGTGGTGGCAGCGCCTGC A
R-CD19b-CD79b CAR-X2B	CGATAAGCTTGATATCGGTCACCTTATCTAGGTGGCAGTGCCTGC A
F-CD79b-X2E	AGTTTTTTTCTTCCATTTATCCTAGGATCCATGGCCCTGCCTGTGA CAGC
R-CD79b-X2E	TTCACCCTGATCTTGGCCAGGGTGGAGT
F-CD19-X2E	CTGGCCAAGATCAGGGTGAAGTTTTCTCGCAG
R-CD79b-X2G- MutCD3	CCGCTTCCACGAGGTGGAAGTGCTTGCA
F-CD19-X2G	CTTCCACCTCGTGGAAGCGGCCACAACTT
F-CD19-CAR-X2K	AGTTTTTTTCTTCCATTTATCCTAGGATCCATGCTGCTGCTCGTGA CCTC
R-CD19-CAR-X2K	CCAGAACCCCGTGGTGGCAGCGCCTGCA
F-T2A-X2K	CTGCCACCACGGGGTTCTGGAGAGGGAAGGGG
R-T2A-X2K	AGGGCCATTGGGCCAGGATTCTCCTCCA
F-CD79b CAR-X2K	AATCCTGGCCCAATGGCCCTGCCTGTGACAGC
R-CD79b-CAR-X2K	GATAAGCTTGATATCGGTCACCTTATCTAGGTGGCAGTGCCTGCA

Table 10. gBlock

gblock	Sequence 5'-3'
4-1BB-CD3 ζ condon-1	TTCATCATCTTTTGGGTGAAACGAGGTAGAAAAAACTTCTTTATATATTCAAACAACC ATTTATGAGACCACTACAACTACTCAAGAGGAAGATGGATGTAGTTGTCGATTTCCA GAAGAAGAAGAAGGAGGATGTGAACTGAGGGTAAAATTTAGTAGATCCGCCGACGC CCCGGCTTACCAGCAGGGTCAGAATCAACTCTATAACGAGCTGAACCTCGGGCGCA GAGAAGAGTACGACGTCTTGGATAAGCGGAGAGGGCGAGACCCTGAAATGGGGGG AAAACCGCGACGGAAGAATCCTCAAGAGGGACTCTACAACGAGTTGCAGAAGGACA AAATGGCGGAAGCGTACAGTGAGATAGGAATGAAAGGAGAACGCAGACGCGGTAAG GGCCATGACGGGCTCTACCAGGGCCTGTCAACAGCTACAAAAGATACATACGACGC CCTTCATATGCAGGCGCTGCCACCACGGaccGGTTCTGGAGAGGGAAGGGGC
OX40-CD3 ζ condon-1	TTCATCATCTTTTGGGTGAGGCGCGACCAGCGGCTGCCACCTGATGCACACAAGCC ACCAGGAGGAGGCTCTTTCCGGACCCCAATCCAGGAGGAGCAGGCAGACGCACAC AGCACACTGGCCAAGATCAGGGTAAAATTTAGTAGATCCGCCGACGCCCGGCTTA CCAGCAGGGTCAGAATCAACTCTATAACGAGCTGAACCTCGGGCGCAGAGAAGAGT ACGACGTCTTGGATAAGCGGAGAGGGCGAGACCCTGAAATGGGGGGAAAACCGCG ACGGAAGAATCCTCAAGAGGGACTCTACAACGAGTTGCAGAAGGACAAAATGGCGG AAGCGTACAGTGAGATAGGAATGAAAGGAGAACGCAGACGCGGTAAGGGCCATGAC GGGCTCTACCAGGGCCTGTCAACAGCTACAAAAGATACATACGACGCCCTTCATATG CAGGCGCTGCCACCACGGaccGGTTCTGGAGAGGGAAGGGGC

CD8 H/TM- Codon-2-4-1BB-CD3ζ Codon-1

ACCACGACACCGGCTCCAAGACCACCCACTCCCGCGCCCACAATCGCTTCCCAACC
ATTGAGCCTTAGGCCTGAGGCGTGCCGACCGGCAGCGGGTGGAGCTGTACACACTA
GGGGGCTCGACTTTGCGTGTGACATTTATATCTGGGCGCCATTGGCCGGTACTTGTG
GTGTATTGCTCCTCTCCCTTGTATTACATTGTATTGCTGGGTGAAACGAGGTAGAAA
AAAACCTTCTTTATATATTCAAACAACCATTTATGAGACCAGTACAACTACTCAAGAGG
AAGATGGATGTAGTTGTTCGATTTCCAGAAGAAGAAGAAGGAGGATGTGAACTGAGGG
TAAAATTTAGTAGATCCGCCGACGCCCCGGCTTACCAGCAGGGTCAGAATCAACTCT
ATAACGAGCTGAACCTCGGGCGCAGAGAAGAGTACGACGTCTTGGATAAGCGGAGA
GGGCGAGACCCTGAAATGGGGGGAAAACCGCGACGGAAGAATCCTCAAGAGGGAC
TCTACAACGAGTTGCAGAAGGACAAAATGGCGGAAGCGTACAGTGAGATAGGAATG
AAAGGAGAACGCAGACGCGGTAAGGGCCATGACGGGCTCTACCAGGGCCTGTCAA
CAGCTACAAAAGATACATACGACGCCCTTCATATGCAGGCGCTGCCACCACGG

CD28CO-CD3zeta-Codon-1- P2A

ACATTGTATTGCTGGGTGAGGAGCAAGCGGAGCAGGCTGCTGCACAGCGACTACAT
GAACATGACCCCCCGGAGACCCGGCCCTACAAGAAAGCACTATCAGCCTTACGCAC
CACCAAGGGACTTCGCAGCCTATAGAAGCAGGGTAAAATTTAGTAGATCCGCCGACG
CCCCGGCTTACCAGCAGGGTCAGAATCAACTCTATAACGAGCTGAACCTCGGGCGC
AGAGAAGAGTACGACGTCTTGGATAAGCGGAGAGGGCGAGACCCTGAAATGGGGG
GAAAACCGCGACGGAAGAATCCTCAAGAGGGACTCTACAACGAGTTGCAGAAGGAC
AAAATGGCGGAAGCGTACAGTGAGATAGGAATGAAAGGAGAACGCAGACGCGGTAA
GGCCATGACGGGCTCTACCAGGGCCTGTCAACAGCTACAAAAGATACATACGACG
CCCTTCATATGCAGGCGCTGCCACCACGGGGAAAGCGGCGCCACAACTTCTCTTTG
CTTAAACAGGCCGGAGATGTGGAGGAGAACCCCGGCCCTATGGCCCTGCCTGT

2. Methods for Molecular Biology

2.1 Restriction Enzyme Digestion.

In the total reaction volume of 50µl, 1µg vector was digested with 20 units of restriction enzymes in the cut smart buffer (1x) at 37°C for 2 hours.

2.2 Gel Electrophoresis and Gel Extraction

Dependent on DNA size, 0.8% to 2% agarose gel was used for this study. The agarose gel was made by heating the mixture of agarose and 1X TAE buffer (gram of agarose/milliliters of TAE buffer), with the addition of DNA stain-Gel red at the end. After adding loading dye to

digested DNA samples, the gel was run for 30-50 minutes at 90 V to separate the DNA fragments.

The DNA fragments were quickly cut by using UV Transilluminator to avoid DNA damage.

Excised DAN fragments were extracted by following the protocol for Monarch DNA Gel Extraction kit.

2.3 Polymerase Chain Reaction

Polymerase chain reaction (PCR) was used to amplify DNA sequences. In this study, Q5 high fidelity DNA polymerase was used for amplifying DNA fragments due to highest fidelity amplification and ultra-low error rates. Touchdown PCR was performed for increasing specificity and sensitivity for DNA amplification. The below PCR reaction (Table 11) and Touch Down PCR protocol (Table 12) were used in this study.

Table 11. PCR reactions

Component	Volume	Final Concentration
Q5 Hot Start 2X High Fidelity Master Mix Buffer	25µl	1x
Forward primer (12.5µM)	2µl	0.5µM
Reverse primer (12.5µM)	2µl	0.5µM
Template DNA	1µl	100 ng
ddH2O	20µl	
	50µl	

Table 12. Touchdown PCR protocol

Step	Temperature	Time	Cycles
Denature	94°C		
Phase 1	Annealing temp decreases 1°C per cycle		10
Denature	98°C	10 s	
Anneal	72°C	30 s	
Extension	72°C	1 min 30 s	
Phase 2			27
Denature	98°C	10 s	
Anneal	68°C	30 s	

Extension	72°C	1 min 30 s
Final Extension	72°C	7 min
Cooling	4°C	∞

2.4 DNA Assembly

NEBuilder HiFi DNA Assembly Master Mix, which allows the assembly of four fragments at the same time, was used for this study to increase efficiency and accuracy. The primers were designed to generate DNA fragments with 20-24bp overlap for DNA assembly. Single-strand 3' overhangs created by the exonuclease facilitate annealing at the overlap region. The gaps within each annealed fragment and nicks in the assembled DNA were fixed by DNA polymerase and DNA ligase, respectively.

The mass of insert DNA fragments were calculated using NEBcalculator. The ratio of insert DNA to vector is 3:1. HiFi DNA Assembly protocol is described in the below table (Table 13). Prepared samples were incubated in a thermocycler at 50°C for 60 minutes.

Table 13. DNA Assembly Reaction

Component	Volume	3-4 Fragment Assembly
NEBuilder HiFi DNA Assembly Master Mix	10µl	
Insert DNA 1	1µl	0.015-0.1pmol
Insert DNA 2	1µl	0.015-0.1pmol
Vector	1µl	0.015-0.1pmol
ddH ₂ O	7µl	
	20µl	

2.5 Transformation and DNA Extraction

NEB Stable Competent *E. coli* was used for transformation due to its high efficiency. By following the protocol, 2µl of chilled Assembly product was added to a tube of thawed NEB stable Competent *E. coli* Cell. DNA was mixed carefully by flicking the tube 4-5 times. After incubating on ice for 30 minutes, the mixture was heat shocked at 42°C for 30 seconds and

incubated on ice for 5 minutes. After adding 950µl of room temperature NEB 10-beta/Stable Outgrowth Medium into the mixture, the tube was shaken horizontally at 250rpm at 30°C for 60 minutes. 50-100µl of cells were then spread onto a warm Ampicillin plate. The plates were incubated at 30°C overnight or 24 hours. Four or six colonies were picked up for DNA extraction using the QIAprep Spin Miniprep Kit.

2.6 DNA Sequencing

Plasmid DNA was digested with specific restriction enzyme and correct colonies were picked based on the bands from the DNA gel. DNA sequencing was performed by the Sequencing and Microarray Facility of MDACC using customized sequencing primers.

3. Methods for Cell Culture and Assays

3.1 Dual CD19-D79b CAR Expression in 293 T Cells.

To determine of CD19 CAR and CD79b CAR expression, 293 T cells were used for checking transient expression of CARs. The method is described below.

Day 0:

4.5 x10⁵ cells were plated in a 6-well plate with 2mL of Completed DMEM Medium

Day 1:

At 70-85% confluency, 293T cells were transfected with different vectors. 2µg of vector encoding CARs and P3000 was added to a tube labeled DNA (D) with 150µl Opti-MEM. Lipofectamine 3000 was added to a tube labeled Lipofectamine (L) with 150µl Opti-MEM (Table 14). The DNA and Lipofectamine tubes were then mixed and incubated for 10 minutes at room temperature. The transfection mix was gently added to the 293 cells to avoid dislodging the cells.

Table 14. Transfection components

Tubes	Component	Amount
DNA	Plasmid DNA	2µg
	P3000	6µl
Lipofectamine	Lipofectamine 3000	9µl

Day 3:

293 T cells were collected to check for CD19 CAR and CD79b CAR expression by flow cytometry.

3.2 Flow Cytometry for Transient CAR Expression in 293 T Cells

After transfection for 48 hours, 293 T cells were gently washed by prewarmed PBS and 200µl of 0.25% Trypsin-EDTA (0.25%) were added into each well to incubate at 37°C for 1 minute. The cells were collected and washed by adding completed DMEM. After aspirating supernatant, transfected 293 T-cells were resuspended with 2mL of 1% FBS in PBS (Flow cytometry staining buffer). 5 x10⁵ cells were centrifuged and resuspended with 50µl of staining buffer in 1.1mL tube for staining.

2µl of CD19 protein conjugated FITC, 0.3µl of CD79protein conjugated PE, 2µl of anti-EGFR-AF647 (epidermal growth factor receptor) and 0.5µl of live-dead Amcyan were added to the cell suspension. After mixing with a gentle pulse vortex, the cells were incubated at 2-8°C or on ice for 30 minutes (Table14).

Table 15. Flow Panel for Checking CAR Expression

Fluorochrome	Markers	Volume
FITC	CD19 Protein	2µl
PE	CD79b Protein	0.3µl
AF647	Anti-EGFR	2µl
Amcyan	Live-dead	0.5µl

The cells were washed twice by adding 500µl of staining buffer. The centrifugation was performed at 1500 rpm at 4°C for 5 minutes. The stained cells were resuspended with 350µl of staining buffer for acquiring data by flow cytometry.

3.3 Lentivirus Production

In this study, 2nd generation packing systems were used for lentivirus generation, which included lentiviral transfer plasmid (3rd generation lentiviral CD19-CD79b CAR), packaging plasmid (psPAX2 encoding the Gag, Pol, Rev and Tat genes) and envelope plasmid (R3r encoding RD114 protein). The protocol is described below.

Day 0:

4.8 x10⁶ cells were plated inside T75 flask with 10mL of completed DMEM Medium.

Day 1:

At 70-85% confluency, 293T cells were transfected with a mixture of 3rd generation lentiviral transfer plasmids (CD19-CD79b CAR), packaging plasmid (psPAX2) and envelope plasmid (R3r). Two tubes were labeled DNA (D) and Lipofectamine (L) respectively, each containing 850µl Opti-MEM. 17µg of transfer plasmid, packing plasmid, envelope plasmid and 34µl of P3000 were added to the D tube. Lipofectamine 3000 was added to the L tube (Table 16).

Table 16. Lentivirus Production

Tubes	Component	Amount
DNA	Plasmid DNA	7.02µg
	psPAX2	6.12µg
	R3r	3.86µg
	P3000	34µl
Lipofectamine	Lipofectamine 3000	51µl

The DNA and Lipofectamine tubes were mixed and incubated for 10 minutes at room temperature. The transfection mix was gently added to the 293 T-cells to avoid dislodging the cells.

Day 2:

After incubation for 18 to 24 hours, the medium containing lentivirus was carefully collected into 50mL tubes and stored at 4°C. 10mL of the prewarmed fresh completed DMEM was added without detaching the cells.

Day 3:

After incubating for 36 to 48 hours, the medium containing lentivirus was harvested. The medium from both day 2 and day 3 were then combined.

3.4 Lentivirus Concentration

The lentivirus supernatant was first filtered through an 0.45µm filter after the lentivirus medium was centrifuged at 500 x g for 10 minutes. The Lenti-X-Concentrator was added to clarified lentivirus supernatant with a volume ratio of 1:3. The mixture was incubated at 4°C for 30 minutes to overnight after gentle inversion. The off-white pellet of concentrated lentivirus was visible after centrifuging the cooled mixture at 1,500 x g for 45 minutes at 4°C. The pellet was resuspended with Opti-MEM and stored at -80°C. Lenti-X GoStix Plus can be used to test the lentiviral titer or confirm the successful lentivirus production.

3.5 PBMC Isolation

Histopaque(R)-1077 (Ficoll-Paque) was used for isolating peripheral blood mononuclear cells from a normal donor's buffy coats. The buffy coat was first diluted with pre-warmed PBS at a volume ratio of 1:1 (25mL buffy coat +25mL PBS). Then 25mL of diluted buffy coat was slowly added to 15mL of prewarmed Histopaque (around 20°C) in 50mL tubes. The tubes with two layers of diluted buffy coat and Histopaque were centrifuged at 2000 rpm for 20 minutes at 20°C with the brake off. After centrifugation, four layers were visible. From the top to bottom: plasma layer, PBMCs layer, Ficoll-Paque layer, and erythrocytes and granulocytes layer. The white mononuclear layer between the layers of plasma and Histopaque were carefully

harvested by removing the upper layer of plasma. Finally, the PBMC was washed twice with 50mL PBS at 1400 rpm for 10 minutes at 20°C to remove Ficol-Paque and platelets. PBMC was frozen with 90% FBS+10% DMSO and stored in a liquid nitrogen tank after keeping for 24 hours in -80C freezer.

3.6 T Cell Isolation

Untouched human T cells were isolated from PBMCs by using the Pan T Cell Isolation Kit to deplete non-T cells including B-cells, NK cells, monocytes, platelets, dendritic cells, granulocytes, and stem cells. By following the protocol of Pan T cell Isolation kit, 50µl of Pan T Cell Biotin-Antibodies Cocktail was added to 50×10^6 PBMCs in the 200µl buffer. The mixture was incubated for 5 minutes in the refrigerator. After adding 150µl buffer into the mixture, 100µl Pan T-Cell Microbeads Cocktail was added. After mixing well, the mixture of PMBCs, Biotin-antibodies Cocktail and Microbeads Cocktail was incubated for 10 minutes in the refrigerator.

The LS column was placed in the magnetic field of a MACS separator. After balancing the column by rinsing with 3mL of buffer, the cell mixture was applied onto the column. Unlabeled T cells passed through the column. Magnetically labeled non-T cells bound in the column. After washing the column with 3 mL of buffer, untouched T cells were in the collecting tubes.

3.7 T Cell Activation and Expansion

The enriched T cells were activated and expanded using ImmunoCult human CD2/CD3/CD28 Cell Activator which contains soluble tetrameric antibody complexes that bind CD3, CD28 and CD2. T-cell Activator was added with 25µl/mL to T Cells in the presence of IL-2 (200IU/mL) at a concentration of 1×10^6 /mL.

3.8 Lentiviral Transduction

T cells were transduced with lentivirus containing CAR constructs after T cells were activated for 66-72 hours. The transduction protocol is described below.

Day 0: Isolation T cells from PBMC.

T cells were activated by ImmunoCult human CD2/CD3/CD28 Cell Activator with 25µl/mL at a concentration of 1×10^6 /mL and cultured in the presence of IL-2 (200IU/mL).

Day 2: Preparation of RetroNectin-coated plates.

The working RetroNectin solution was prepared by diluting 25µl of RetroNectin with 500µl PBS. 525µl of RetroNectin solution at a concentration of 47.6µg/mL was placed into a non-treated 12-well plate for a density of 6.6µg/cm². The RetroNectin-coated plate was incubated at 4°C overnight.

Day 3: Lentiviral Transduction

The RetroNectin-coated plate was blocked with 1 mL of 2% Bovine serum albumin (BSA) in PBS at room temperature for 30 minutes after removing the RetroNectin solution. The plate was washed with 1 mL of PBS after removing the BSA solution. The plate is ready to use after removing PBS. The centrifuge was pre-heated to 32°C.

1×10^6 activated T-cells were centrifuged at 1200 rpm for 5 minutes and resuspended in 250µl of Opti-MEM medium. The 250µl of lentivirus was mixed with 1×10^6 activated T cells and added into the RetroNectin-coated plate. Inoculated T cells were spun at 1000 x g at 32°C for 2 hours with a reduced breaking speed (deceleration=3). 1000 µl of prewarmed complete RPMI with IL-2 (culture concentration at 200IU/mL) was gently added into the T cells.

3.9 Transduction Efficiency

After transduction for 4 days, cells were stained with CD19 protein conjugated FITC, CD79b protein conjugated PE or APC, and live-dead Amcyan. The protocol of staining cell surface CARs for Flow cytometry is describe below.

1. 2×10^5 cells were centrifuged and resuspended with 500 μ l of 1% FBS in PBS (flow cytometry staining buffer) in a 1mL tube. After washing with staining buffer, the cells were resuspended in 50 μ l staining buffer.
2. The cell suspension was added with 2 μ l of CD19 protein conjugated FITC, 0.3 μ l of CD79b protein-conjugated PE or APC, and 0.5 μ l of live-dead Amcyan. After mixing with a gentle pulse vortex, the cells were incubated at 2-8°C or on ice for 30 minutes.
3. The cells were washed twice by adding 500 μ l of staining buffer. The centrifuge was performed at 1500 rpm at 4°C for 5 minutes. The stained cells were resuspended with 350 μ l of staining buffer for acquiring data via flow cytometry.

Table 17. Flow Panel for Checking Transduction Efficiency

Fluorochrome	Markers	Volume
FITC	CD19 Protein	2 μ l
PE	CD79b Protein	0.3 μ l
Amcyan	Live-dead	0.5 μ l

3.10 CAR T Cell Degranulation

The detection of CAR T and untransduced T cell degranulation was measured by CD107a expression on the surface of cells. The protocol for detection of CAR T and T cells degranulation is described below.

1. CAR T cells and untransduced T cells were resuspended with completed RPMI after washing twice. Based on the transduction efficiency, 1×10^5 to 2×10^5 effector cells were used for this assay. B-cell leukemia and B-cell lymphoma cell lines were used as target cells. Target cells were labelled with CellTrace Violet. Effector cells were co-cultured with

target cells at a ratio of 1:2 (E: T) or 1:1 in 600µl complete RPMI of 5 mL polystyrene tube in the presence of 3µl of anti-CD107a APC and 0.42µl of monensin (BD Golgistop protein transport inhibitor).

2. The cells mixture was incubated in the incubator at 37°C and 5% CO₂ for 5 or 6 hours.
3. After co-culture for 5 or 6 hours, cells were centrifuged and washed with Flow Cytometry staining buffer. The cells were resuspended with 50µl staining buffer. The antibodies and protein conjugated dye were added to the cell suspension. The flow panel is described in Table 17.

Table 18. Flow Panel for Degranulation

Fluorochrome	Markers	Volume
FITC	CD19 Protein	2µl
PE	CD79b Protein	0.3µl
PE-CF594	Anti-CD8	2µl
PerCP-Cy5.5	Anti-CD4	2µl
AF700	Anti-CD3	2µl
APC	Anti-107a	2µl
Pacific Blue	Tumor cells	
Amcyan	Live-dead	0.5µl

3.11 CAR T Cell Proliferation

CAR T cell proliferation was tested using CellTRace Far Red Cell Proliferation Kit. CellTrace Far Red stock solution was prepared by adding 20µl of DMSO. Effector cells (CAR T cells and untransduced T cells) were washed with PBS after removing the medium by centrifuge. The cell concentration was approximately 2-3 x10⁶ cells/mL. 1 µl of stock solution was added to each mL of cell suspension in PBS for a final working solution. The cells were incubated for 20 minutes in the incubator at 37°C protected from light.

Five times of complete RPMI were added to the cells. The cells were incubated for 5 minutes in the incubator at 37°C to remove any free dye remaining in the solution. The cells were centrifuged and resuspended with fresh pre-warmed complete RPMI. Effector cells labelled

with CellTrace Far Red were co-cultured with target cells labelled with CellTrace Violet at a ratio of 1:1 for 1 day, 2 days, and 4 days.

At each time point, the cells were collected and stained with the below protein-conjugated dye and antibodies.

Table 19. Flow Panel for Proliferation

Fluorochrome	Markers	Volume
FITC	CD19 Protein	2µl
PE	CD79b Protein	0.3µl
PE-CF594	Anti-CD8	2µl
PerCP-Cy5.5	Anti-CD4	2µl
APC-CellTrace Far Red	Effector cells	
Pacific Blue Trace Violet	Tumor cells	
Amcyan	Live-dead	0.5µl

3.12 CAR T Cell Cytotoxicity

Target cells (B-cell leukemia and B-cell lymphoma cell lines) were labelled with CellTrace Violet. Effector cells (CAR-T cells and untransduced T-cells) were co-cultured with targeted cells at a ratio of 1:2, 1:1, and 2:1 (E: T) for 1 day, 2 days, and 4 days. The cells were stained with Live-dead Amcyan. The live tumor cells were analyzed by flow cytometry by adding CountBright Absolute Counting Beads. CAR T cell cytotoxicity was determined by the percentage of specific survival of tumor cells and specific lysis, which were calculated according to the below formula.

$$\text{The Percentage of Specific Lysis} = 1 - \left[\frac{\text{live target cells with CAR T cells}}{\text{live target cells with untransduced T cells}} \right]$$

3.13 Dual CD19-CD79b CAR T Cell Phenotype and Exhaustion Markers

Dual CD19-CD79b CAR T cell phenotype included Naïve T cells, central memory T cells (T_{CM}), effector memory T cells (T_{EM}) and terminally differentiated effector memory T cells (T_{EMRA}). 1×10^6 cells were stained with flow antibodies and the phenotype was analyzed by flow cytometry. The summary of CAR T and untransduced T cells and flow panel are described below.

Table 20. Phenotype of CAR T Cells and Untransduced T cells

Phenotype	Description
Naïve Cells	CD62L+CD45RA+
Central Memory T cells	CD62L+CD45RA-
Effector Memory T cells	CD62L-CD45RA-
Terminally Differentiated Effector Memory T cells	CD62L-CD45RA+

Table 21. Flow Panel for CAR T Cells and Untransduced T cells Phenotype

Fluorochrome	Markers	Volume
FITC	CD19 Protein	2 μ l
PE	CD79b Protein	0.3 μ l
PE-CF594	Anti-CD62L	2 μ l
PE-CY7	Anti-CD45RA	2 μ l
PerCP-Cy5.5	Anti-CD4	2 μ l
AF700	Anti-CD3	2 μ l
APC	Anti-CD8	2 μ l
Amcyan	Live-dead	1 μ l

The exhaustion markers of dual CD19-CD79b CAR were determined by flow cytometry. 1×10^6 cells were stained with brilliant staining buffer and washed with 1%FBS/PBS staining buffer. The flow panel is described in Table 21 and Table 22.

Table 22. Flow Panel for CAR T Cell and Untransduced T cell Exhaustion Markers

Fluorochrome	Markers	Volume
FITC	CD19 Protein	2 μ l
PE	CD79b Protein	0.3 μ l
PE-CF594	Anti-CD62L	2 μ l
PE-CY7	Anti-CD45RA	2 μ l
PerCP-Cy5.5	Anti-CD4	2 μ l
AF700	Anti-CD3	2 μ l
APC	Anti-CD8	2 μ l
BV421	Anti-PD-1	2 μ l

BV605	Anti-TIM-3	2µl
BV786	Anti-CTLA-4	2µl
Amcyan	Live-dead	1µl

Chapter 3: Results

1. Expression of CD19 CAR with CD28 hinge and transmembrane domain was lower than expression of CD79b CAR in dual CAR construct.

The first dual CD19-CD79b CAR -pX1A (Table 23) was generated using a third-generation lentiviral vector under the control of promoter MSCV. CD19 CAR comprised of an anti-CD19 scFv (murine anti-human FMC63 clone), short CD28 hinge and transmembrane domain, CD28 co-stimulation and CD3 zeta signaling domain. CD79b CAR contained anti-CD79b scFv (murine anti-human T26 clone), CD8 α hinge and transmembrane domain, 4-1BB co-stimulation and CD3 zeta signaling domain. CD19 CAR was linked with CD79b CAR by self-cleaving peptide E2A/P2A. The truncated epidermal growth factor receptor (tEGFR) protein was used as a reporter gene to assess transduction efficiency. 293 T cells were used for testing the expression of the dual CAR construct. Cells were collected after 48 hours post-transfection. CD19 CAR and CD79b CAR expression was assessed by flow cytometry. CD19 CAR of X1B, X1E, X1F and X1G used regular CD28 hinge and transmembrane. CD79b CAR of X1B and X1G used OX40 co-stimulation, and CD79b CAR of X1E and X1F used 4-1BB co-stimulation. CD19CAR and CD79b CAR were alternatively located after MSCV promoter. Based on the flow data, CD79b CAR can express stably when placed either after the promoter or after a 2A self-cleaving peptide. However, CD19 CAR expression was low when compared with CD79b CAR expression. In addition, tEGFR expression was stable in mono- CAR or dual CD19-CD79b CAR (Figure 3) (Table 25)

Table 23. Generation of vectors.

Vectors:	Description
pX1A	MSCV-CD79b-CD8 α H/TM-4-1BB ζ -P2A-CD19-CD28 H/TM (short) -CD28 ζ -T2A-tEFFR
pX1B	MSCV-CD79b-CD8 α H/TM-OX40 ζ -E2A-CD19-CD28 H/TM-CD28 ζ -T2A-tEFFR
pX1C	MSCV-CD79b-CD8 α H/TM-OX40 ζ -tEFFR
pX1D	MSCV- CD19-CD28 H/TM-CD28 ζ -T2A-tEFFR
pX1E	

MSCV-CD79b-CD8 α H/TM-4-1BB ζ -P2A-CD19-CD28 H/TM-CD28 ζ -T2A-tEgFR
pX1F
MSCV-CD19-CD28H/TM-CD28 ζ -P2A-CD79b-CD8 α H/TM-4-1BB ζ -T2A-tEgFR
pX1G
MSCV-CD19-CD28H/TM-CD28 ζ -E2A-CD79b-CD8 α H/TM-OX40 ζ -T2A-tEgFR

Figure 3.

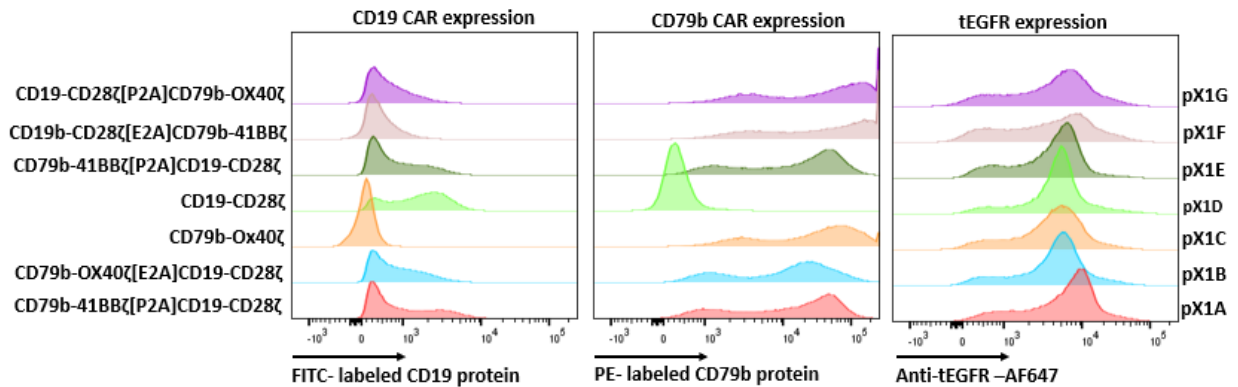


Figure 3: The expression of CD19 CAR, CD79b CAR and tEGFR.

The expression of CD19 CAR and CD79b CAR were determined by flow cytometry using CD19 protein conjugated FITC and CD79b protein conjugated PE stains. The expression of tEGFR was assessed by flow cytometry using an anti-tEGFR AF647 stain.

2.Expression of CD19 CAR with CD28 H/TM and 4-1BB and OX40 was lower than expression of CD79b CAR in dual CAR construct.

CD28 co-stimulation was replaced with 4-1BB and OX40 for CD19 CAR in the dual CD19-CD79b CAR construct. pX1H, pX1I, pX1J and pX1K were generated for this purpose. pX1L and pX1M are CD19 CAR with co-stimulation of 4-1BB and OX40, respectively (Table 24). CD19 CAR and CD 79b CAR expression were tested 48 hours after transfection by using

293 T-cells through flow cytometry. Based on the flow data, expression of CD19 CAR with either 4-1BB or OX40 was lower than the expression of CD79b CAR (Figure 4) (Table 25)

Table 24. Generation of vectors

Vectors: Description
pX1H MSCV-CD79b-CD8 α H/TM-OX40 ζ -E2A-CD19-CD28 H/TM-4-1BB ζ -T2A-tEFFR
pX1I MSCV-CD19-CD28H/TM-4-1BB ζ -E2A-CD79b-CD8 α H/TM-OX40 ζ -T2A-tEFFR
pX1J MSCV-CD79b-CD8 α H/TM-4-1BB ζ -P2A-CD19-CD28 H/TM-4-OX40 ζ -T2A-tEFFR
pX1K MSCV-CD19-CD28H/TM-OX40 ζ -P2A-CD79b-CD8 H/TM--4-1BB ζ -T2A-tEFFR
pX1L MSCV-CD19-CD28H/TM- -4-1BB ζ -T2A-tEFFR
pX1M MSCV-CD19-CD28H/TM-OX40 ζ -T2A-tEFFR

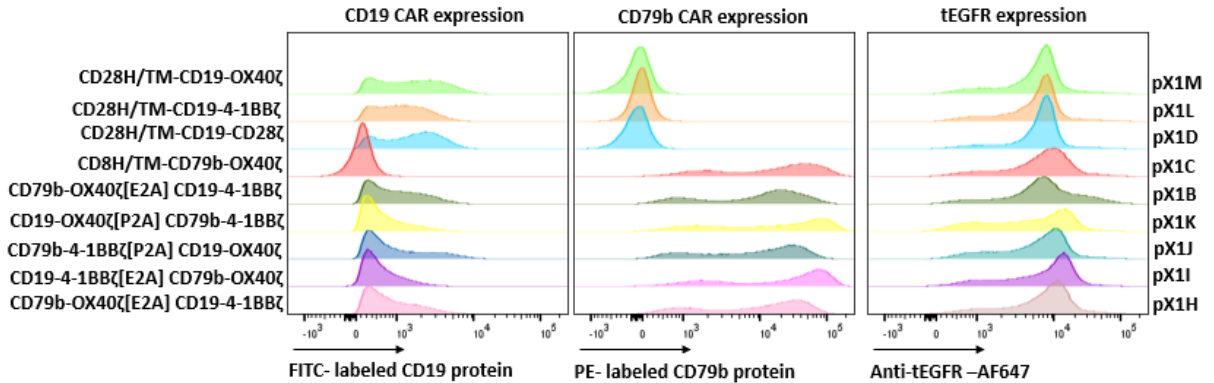


Figure 4: The expression of CD19 CAR, CD79b CAR and tEGFR.

The expression of CD19 CAR and CD79b CAR were determined by flow cytometry using CD19 protein conjugated FITC and CD79b protein conjugated PE stains. The expression of tEGFR was assessed by flow cytometry using an anti-tEGFR AF647 stain.

Table 25. Dual CAR expression 48 hours after transfection.

Dual CAR Name	Promoter	First CAR Design	2A Self-cleaving peptide	Second CAR Design	Dual CAR Expression	CD19 CAR Expression	CD79b CAR Expression
pXA1	MSCV	CD79b CAR [anti-CD79b-CD8αH/TM-4-1BBζ]	P2A	CD19 CAR [anti-CD19-CD28 H/TM (short)-CD28ζ]	45.80%	46.12%	70.60%
pXB1	MSCV	CD79b CAR [anti-CD79b-CD8αH/TM-OX40ζ]	E2A	CD19 CAR [anti-CD19-CD28 H/TM -CD28ζ]	46.60%	46.99%	71.80%
pXE1	MSCV	CD79b CAR [anti-CD79b-CD8αH/TM-4-1BBζ]	P2A	CD19 CAR [anti-CD19-CD28 H/TM -CD28ζ]	41.70%	41.89%	72.00%
pXF1	MSCV	CD19 CAR [anti-CD19-CD28 H/TM -CD28ζ]	P2A	CD79b CAR [anti-CD79b-CD8αH/TM-4-1BBζ]	24.70%	24.93%	68.70%
pXG1	MSCV	CD19 CAR [anti-CD19-CD28 H/TM -CD28ζ]	E2A	CD79b CAR [anti-CD79b-CD8αH/TM-OX40ζ]	34.10%	34.39%	65.80%
pXH1	MSCV	CD79b CAR [anti-CD79b-CD8αH/TM-OX40ζ]	E2A	CD19 CAR [anti-CD19-CD28 H/TM -4-1BBζ]	36.10%	36.10%	70.20%
pXI1	MSCV	CD19 CAR [anti-CD19-CD28 H/TM -4-1BBζ]	E2A	CD79b CAR [anti-CD79b-CD8αH/TM-OX40ζ]	25.70%	25.98%	66.80%
pXJ1	MSCV	CD79b CAR [anti-CD79b-CD8αH/TM-4-1BBζ]	P2A	CD19 CAR [anti-CD19-CD28 H/TM -OX40ζ]	39.60%	39.92%	68.50%
pXK1	MSCV	CD19 CAR [anti-CD19-CD28 H/TM -OX40ζ]	P2A	CD79b CAR [anti-CD79b-CD8αH/TM-4-1BBζ]	27.80%	27.98%	65.90%

3. Expression of CD19 CAR was stable with CD8 α H/TM in a dual CAR construct.

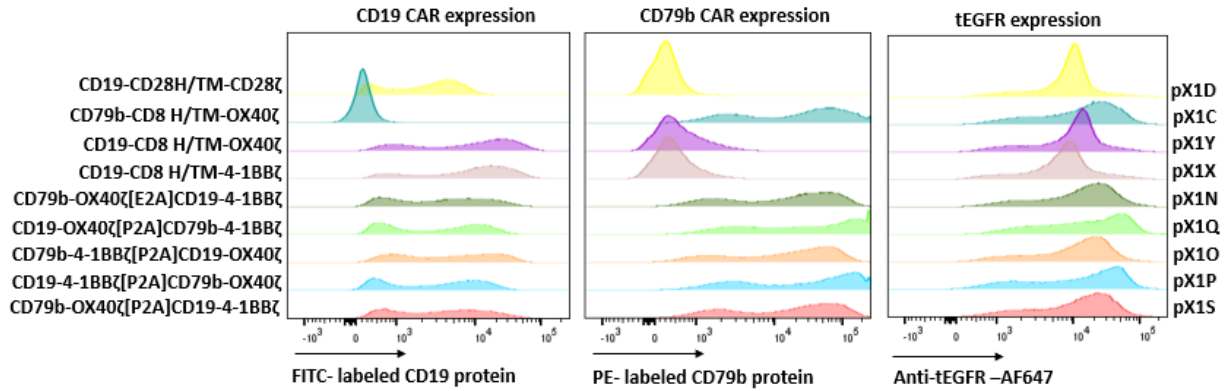
CD28 hinge and transmembrane of CD19 CAR was replaced with CD8 α in CD19-CD79b CAR. CD19 CAR's co-stimulation used 4-1BB, OX40 and CD28 (Table 26). 293 T cells were transfected with CD79b CAR (pX1Z) and dual CD19-CD79b (pX1T, pX1U, pX1V, and pX1W).

The expression of CD19 CAR and CD79b CAR of transfected 293 T cells were determined by flow cytometry. (Figure 5A and 5B). Based on the flow data, CD8 α H/TM improved the expression of CD19 CAR (Table 27)

Table 26. Generation of vectors

Vectors: Description
pX1N MSCV-CD79b-CD8 α H/TM-OX40 ζ -E2A-CD19-CD8 α H/TM-4-1BB ζ -T2A-tEFFR
pX1O MSCV-CD79b-CD8 α H/TM-4-1BB ζ -P2A-CD19-CD8 α H/TM-4-OX40 ζ -T2A-tEFFR
pX1P MSCV-CD19-CD8 α H/TM-4-1BB ζ -P2A-CD79b-CD8 α H/TM-OX40 ζ -T2A-tEFFR
pX1Q MSCV-CD19-CD8 α H/TM-OX40 ζ -P2A-CD79b-CD8 H/TM--4-1BB ζ -T2A-tEFFR
pX1S MSCV-CD79b-CD8 α H/TM-OX40 ζ -P2A-CD19-CD8 α H/TM-4-1BB ζ -T2A-tEFFR
pX1T MSCV-CD79b-CD8 α H/TM-OX40 ζ -P2A-CD19-CD8 α H/TM-CD28 ζ -T2A-tEFFR
pX1U MSCV-CD19-CD8 α H/TM-CD28 ζ -P2A-CD79b-CD8 α H/TM-OX40 ζ -T2A-tEFFR
pX1V MSCV-CD79b-CD8 α H/TM-4-1BB ζ -P2A-CD19-CD8 α H/TM-4-CD28 ζ -T2A-tEFFR
pX1W MSCV-CD19-CD8 α H/TM-CD28 ζ -P2A-CD79b-CD8 H/TM--4-1BB ζ -T2A-tEFFR
pX1X MSCV-CD19-CD8 α H/TM-4-1BB ζ -T2A-tEFFR
pX1Y MSCV-CD19-CD8 α H/TM-OX40 ζ -T2A-tEFFR
pX1Z MSCV-CD79b-CD8 α H/TM-4-1BB ζ -T2A-tEFFR

A:



B:

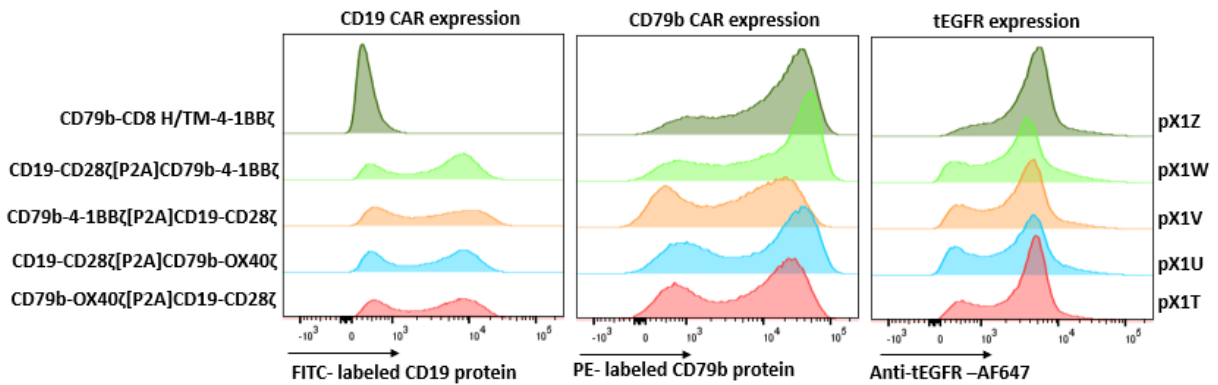


Figure 5 A and B: The expression of CD19 CAR, CD79b CAR and tEGFR.

The expression of CD19 CAR and CD79b CAR were determined by flow cytometry using CD19 protein conjugated FITC and CD79b protein conjugated PE stains. The expression of tEGFR was assessed by flow cytometry using an anti-tEGFR AF647 stain.

Table 27. Dual CAR expression 48 hours after transfection.

Dual CAR Name	Promoter	First CAR Design	2A Self-cleaving peptide	Second CAR Design	Dual CAR Expression	CD19 CAR Expression	CD79b CAR Expression
pXN1	MSCV	CD79b CAR [anti-CD79b-CD8 α H/TM-OX40 ζ]	E2A	CD19 CAR [anti-CD19-CD8 α H/TM-4-1BB ζ]	65.10%	67.18%	67.16%
pXO1	MSCV	CD79b CAR [anti-CD79b-CD8 α H/TM-4-1BB ζ]	P2A	CD19 CAR [anti-CD19-CD8 α H/TM -OX40 ζ]	67.30%	72.01%	69.05%
pXP1	MSCV	CD19 CAR [anti-CD19-CD8 α H/TM-4-1BB ζ]	P2A	CD79b CAR [anti-CD79b-CD8 α H/TM-OX40 ζ]	62.50%	63.95%	64.52%
pXQ1	MSCV	CD19 CAR [anti-CD19-CD8 α H/TM -OX40 ζ]	P2A	CD79b CAR [anti-CD79b-CD8 α H/TM-4-1BB ζ]	59.70%	61.88%	61.22%
pXS1	MSCV	CD79b CAR [anti-CD79b-CD8 α H/TM-OX40 ζ]	P2A	CD19 CAR [anti-CD19-CD8 α H/TM-4-1BB ζ]	66.40%	68.60%	68.44%
pXT1	MSCV	CD79b CAR [anti-CD79b-CD8 α H/TM-OX40 ζ]	P2A	CD19 CAR [anti-CD19-CD8 α H/TM -CD28 ζ]	64.10%	66.31%	65.50%
pXU1	MSCV	CD19 CAR [anti-CD19-CD8 α H/TM -CD28 ζ]	P2A	CD79b CAR [anti-CD79b-CD8 α H/TM-OX40 ζ]	62.70%	63.80%	65.21%
pXV1	MSCV	CD79b CAR [anti-CD79b-CD8 α H/TM-4-1BB ζ]	P2A	CD19 CAR [anti-CD19-CD8 α H/TM -CD28 ζ]	60.30%	62.48%	63.08%
pXW1	MSCV	CD19 CAR [anti-CD19-CD8 α H/TM -CD28 ζ]	P2A	CD79b CAR [anti-CD79b-CD8 α H/TM-4-1BB ζ]	71.00%	72.46%	73.34%

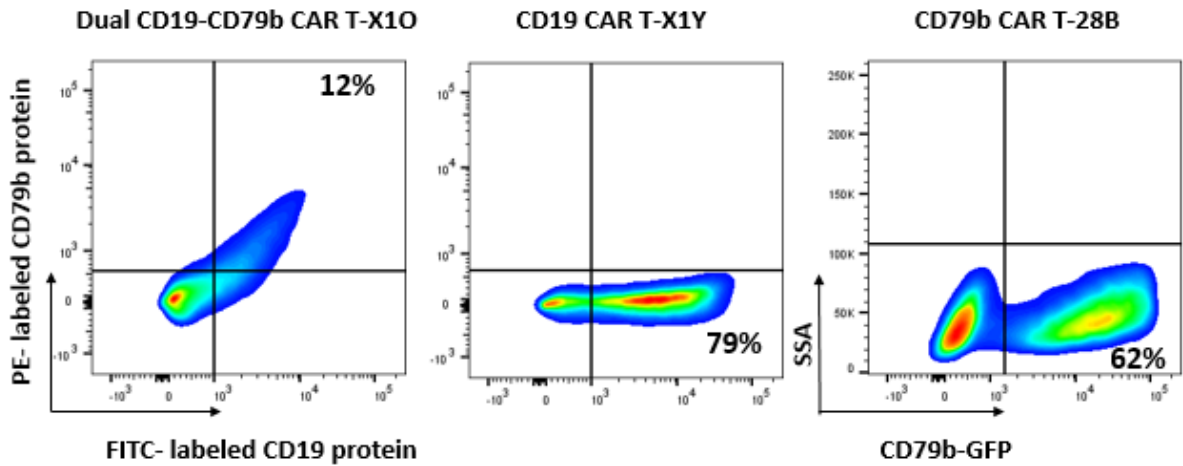
4. Transduction efficiency of dual CD19-CD79b CAR was improved in primary T-cells when removing the tEGFR transduction marker, however, CAR expression gradually decreased under the control of MSCV promoter.

Primary T cells were transduced lentivirally with dual CD19-CD79b CAR (pX10), CD19 CAR (X1Y) and CD79b CAR (28B). The transduction efficiency of dual CD19-CD79b was low (12%) compared with CD19 CAR and CD79b CAR (Figure 6A). To increase transduction efficiency, four new dual CD19-CD79b CARs were generated by removing tEGFR (Table 28). CAR expression gradually decreased on day 8 after transduction under the control of promoter of MSCV (Figure 6B).

Table 28. Generation of Vectors by removing tEGFR

Vectors: Description
pX2A MSCV-CD79b-CD8 α H/TM-OX40 ζ -P2A-CD19-CD8 α H/TM-4-1BB ζ
pX2B MSCV-CD19-CD8 α H/TM-4-1BB ζ -P2A-CD79b-CD8 α H/TM-OX40 ζ
pX2C MSCV-CD79b-CD8 α H/TM-4-1BB ζ -P2A-CD19-CD8 α H/TM-4-OX40 ζ
pX2D MSCV-CD19-CD8 α H/TM-OX40 ζ -P2A-CD79b-CD8 H/TM--4-1BB ζ

A.



B.

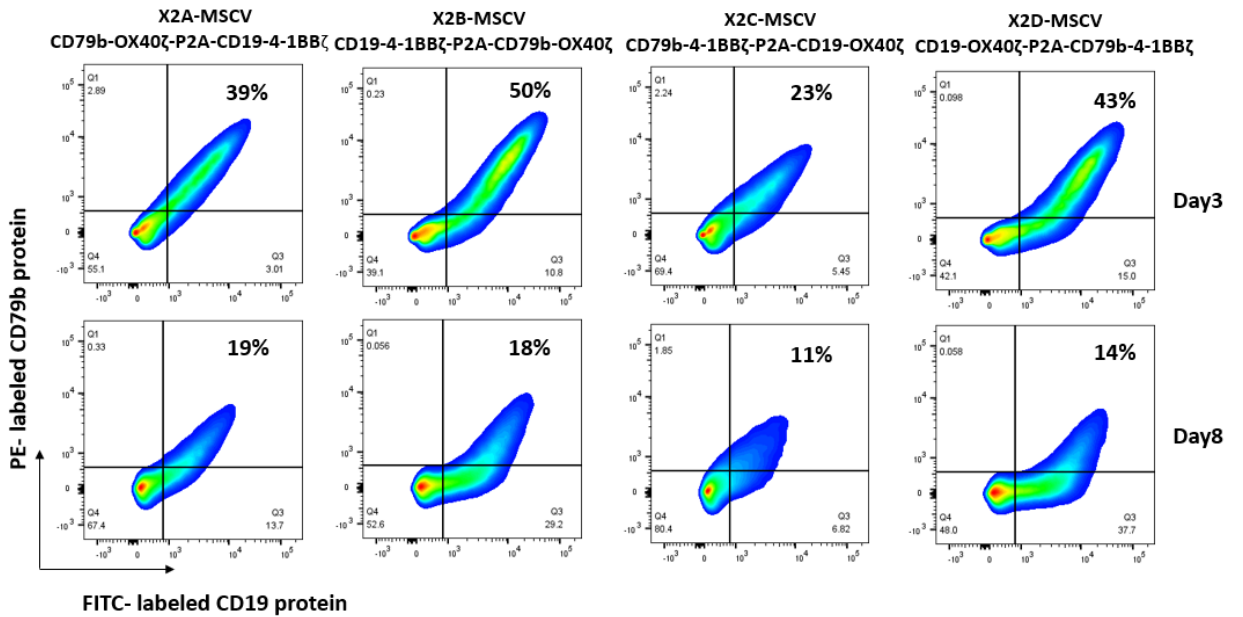


Figure 6: The transduction efficiency of dual CD19-CD79b CARs.

A: The expression of CD19 CAR and CD79b CAR were assessed on day 3 after transduction by flow cytometry using CD19 protein conjugated FITC and CD79b protein conjugated PE stains. **B:** The expression of CD19 CAR and CD79b CAR were evaluated on day 3 and day 8 after transduction by using the same staining and flow analysis.

5. The expression of CD19 CAR and CD79b CAR was stable after transduction under the control of promoter EF1 α .

Next, the MSCV promoter was replaced with EF1 α and 4-1BB co-stimulatory domain was replaced with OX-40 in CD79b CAR and four different dual CD19-CD79 CAR constructs were designed (Table 29). After transduction of primary T cells, the expression of CD19 CAR and CD79b CAR were tested on day 3, day 7 and day 10 (Figure 7). Under the control of EF1 α promoter, the expression of CD19 CAR and CD79 CAR were stable in the culture.

Table 29. Generation of vectors

Vectors: Description
pX2E EF1 α -CD79b-CD8 α H/TM-OX40 ζ -P2A-CD19-CD8 α H/TM-4-1BB ζ
pX2F EF1 α -CD79b-CD8 α H/TM-OX40 ζ -P2A-CD19-CD8 α H/TM-OX40 ζ
pX2K EF1 α -CD19-CD8 α H/TM-4-1BB ζ -T2A-CD79b-CD8 α H/TM-OX40 ζ
pX2L EF1 α -CD19-CD8 α H/TM-OX40 ζ -T2A-CD79b-CD8 α H/TM-OX40 ζ
pX2Q EF1 α -CD19-CD8 α H/TM-4-1BB ζ
pX2U EF1 α -CD79b-CD8 α H/TM-OX40 ζ

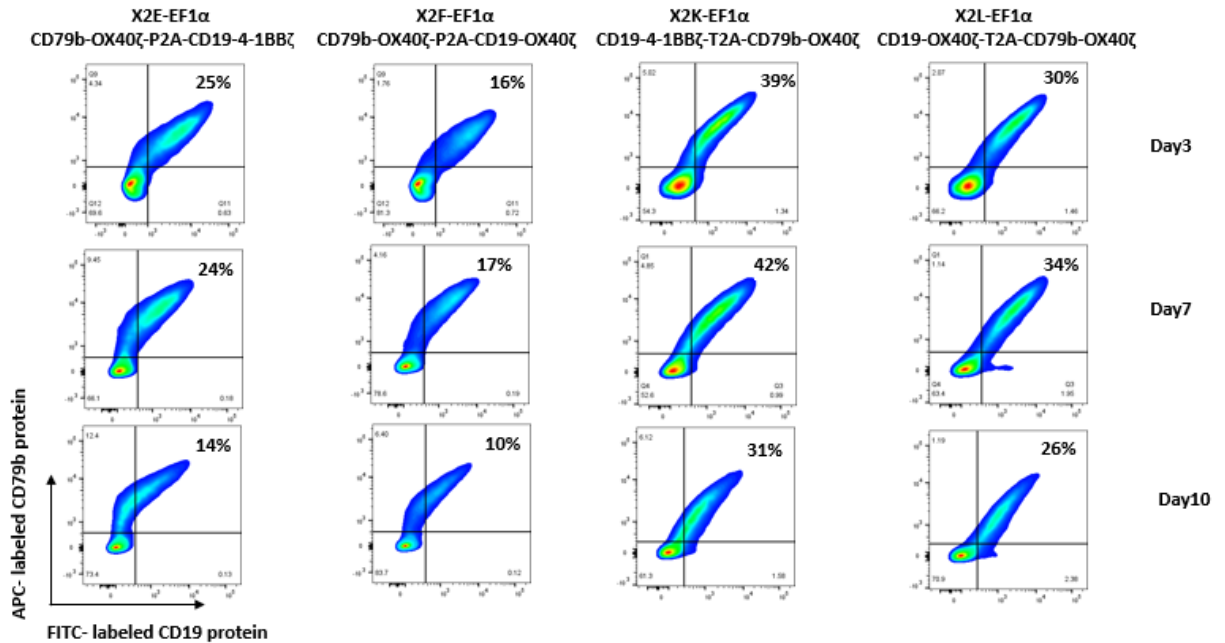


Figure 7: The transduction efficiency of dual CD19-CD79b CARs.

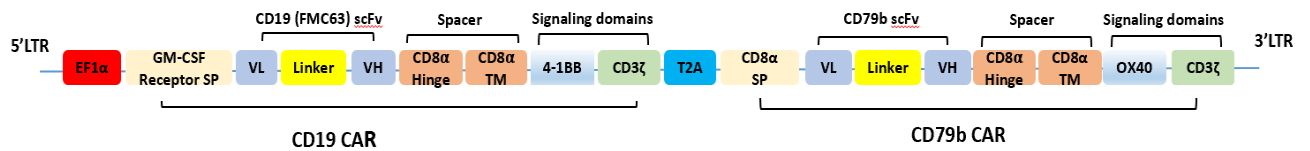
The expression of CD19 CAR and CD79b CAR were assessed on day 3, day7 and day 10 after transduction via flow cytometry using CD19 protein conjugated FITC and CD79b protein conjugated PE stains.

6. Generation of the dual CD19-CD79 CAR T Cells.

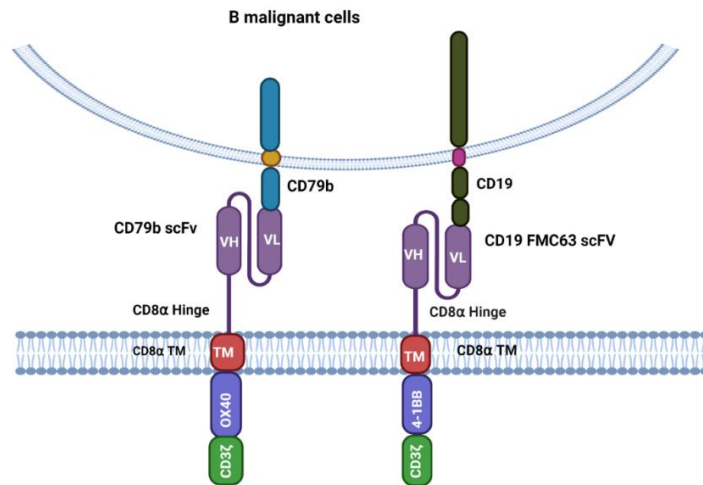
Based on transduction efficiency and stability of CAR expression, the X2K dual CD19-CD79b CAR construct was chosen as optimal (Figure 8A). Dual CD19-CD79b CAR was composed of a 2nd generation CD19 CAR directly after the promoter EF1α and CD79b CAR linked with CD19 CAR by a self-cleaving peptide T2A. CD19 CAR comprised of anti-CD19 scFv (murine anti-human FMC63 clone), CD8α hinge and transmembrane domain, 4-1BB co-stimulatory domain and CD3ζ signaling domain. CD79b CAR consisted of anti-CD79b (murine anti-human 28B clone), CD8α hinge and transmembrane domain, OX40 co-stimulatory domain and CD3ζ signaling domain (Figure 6A). The bicistronic CD19 and CD79b CAR

construct allowed simultaneous expression of both CARs on the surface of primary T-cells for targeting B-cell leukemia and B-cell Lymphoma cells (Figure 8B). The expression of CD19 CAR and CD79b CAR on day 4 and day 9 after transduction of primary T cells was determined by flow cytometry with CD19 protein conjugated with FITC and CD79b protein conjugated with APC stains, respectively. The expression of CD19 CAR and CD79b CAR was equally distributed in the CD4+ and CD8+ subset (Figure 8C). The ratio of CD4 to CD8 in the expression of dual CD19-CD79b CAR was around 2:1 on day4 and 1:1 on day9 (Figure 8D).

A



B



Created with BioRender

C

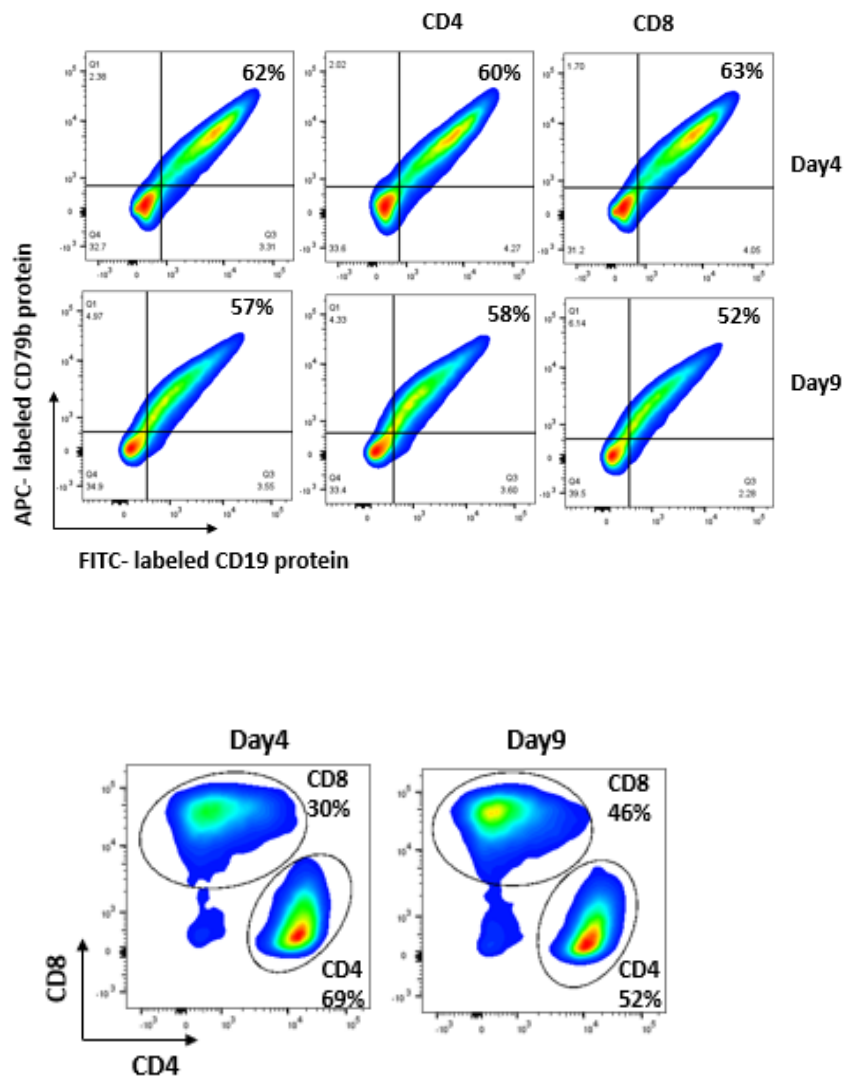


Figure 8: Generation of dual CD19-CD79b CAR T cells.

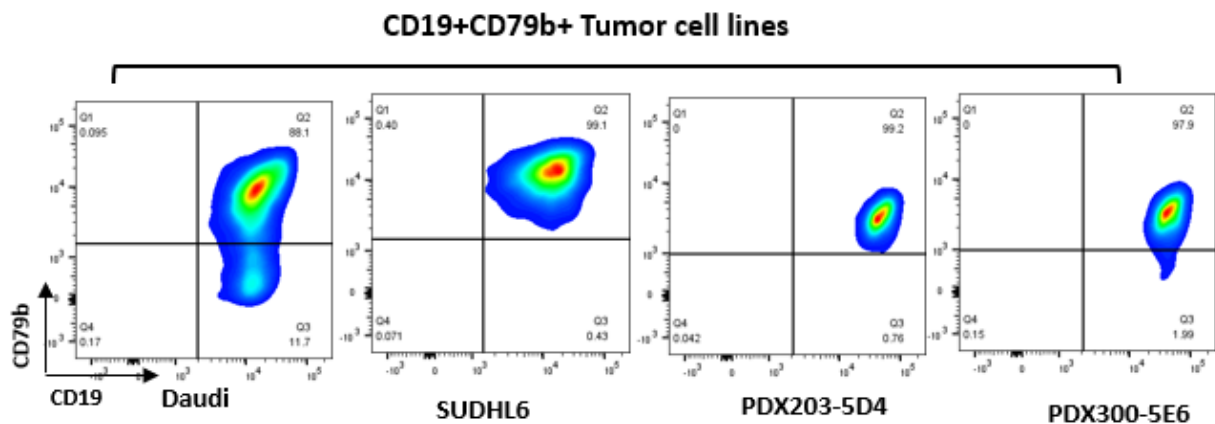
A) Dual CD19-CD79b CAR construct comprised of anti-CD19 CAR and anti-CD79b CAR were cloned into a third-generation lentiviral vector under the control of EF1 α promoter. Two CARs were linked by T2A self-cleaving peptide. **B)** The schematic figure shows that dual CD19-CD79b CAR T cells can target either CD19 or CD79b or simultaneously target two antigens on the surface of tumor cells. **C)** The expression of CD19 and CD79b on primary T cells

transduced with dual CD19-CD79b CAR construct were assessed on day 4 and day 9 in CD4+ and CD8+ subsets by FITC-conjugated CD19 protein and APC-conjugated CD79b protein stains. **D)** The flow cytometry plot showed that the ratio of CD4+ to CD8+ was 2:1 on day 4 and was about 1:1 on day 9 after transduction in dual CD19-CD79b CAR T cells.

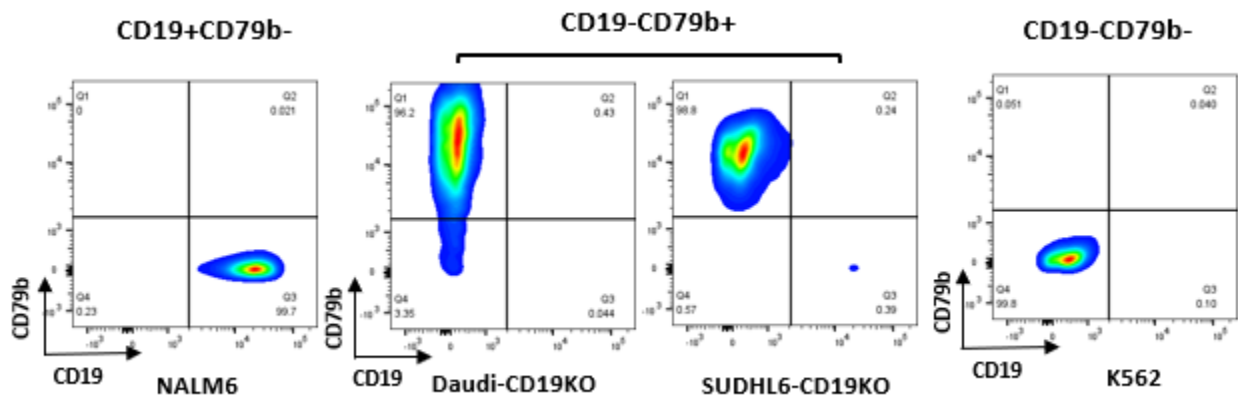
7. Dual CD19-CD79b CAR T cells degranulated in response to B-cell lymphoma and leukemia cell lines in a CD19 or CD79b dependent manner.

CD19+CD79b B cell lymphoma cell lines (Daudi, SUDHL6, PDX203 and PDX300), CD19+ CD79b- B-cell leukemia cell line (NALM6), CD19KO cell lines (Daudi-CD19KO and SUDHL6-CD19KO), and CD19-CD79b- cell lines (K562) were used for degranulation and cytotoxicity assays. The expression of CD19 antigen and CD79b antigen in the tumor cells was tested by flow cytometry (Figure 9A, 9B, 9C). Proliferation of tumor cells was measured by using CellTrace Violet via flow cytometry (Figure 9D). Dual CD19-CD79b CAR T cells degranulated in response to CD19 or CD79b when cultured with B-cell lymphoma and leukemia cell lines (Figure 9E, 9F, 9G, 9H)

A1.

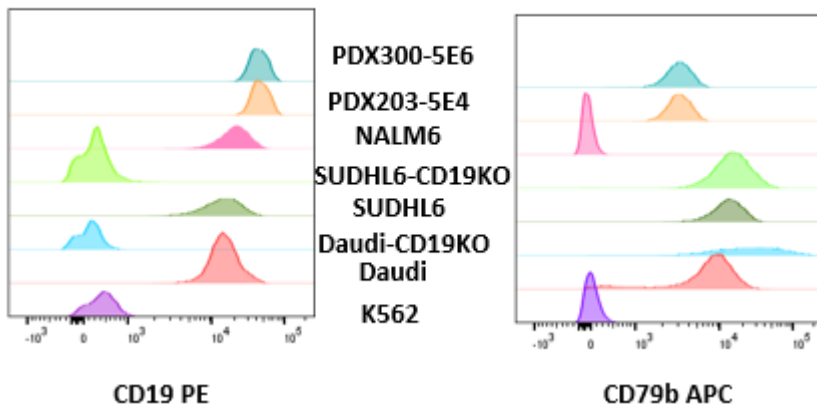


A2.

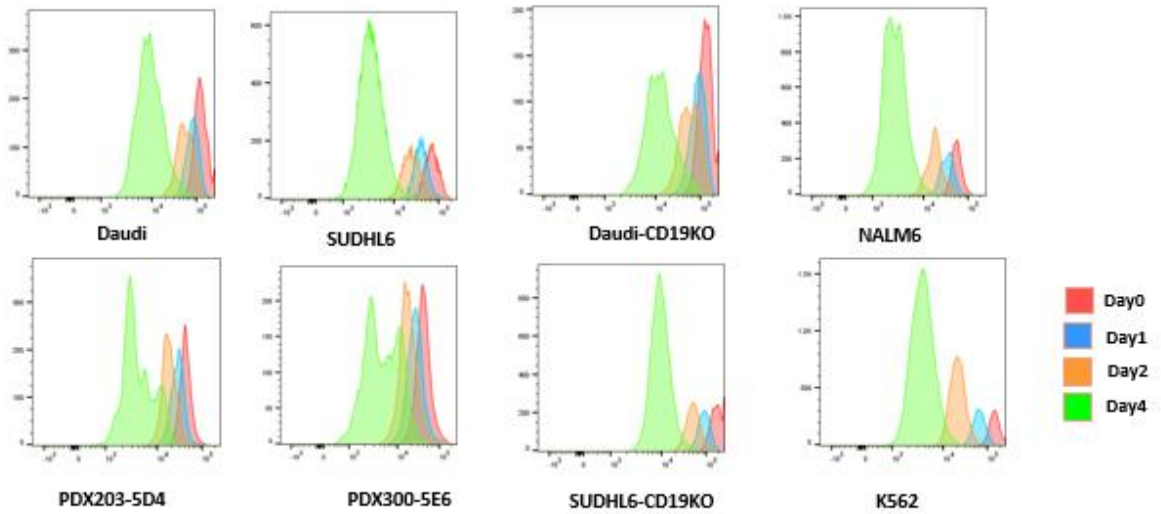


A3.

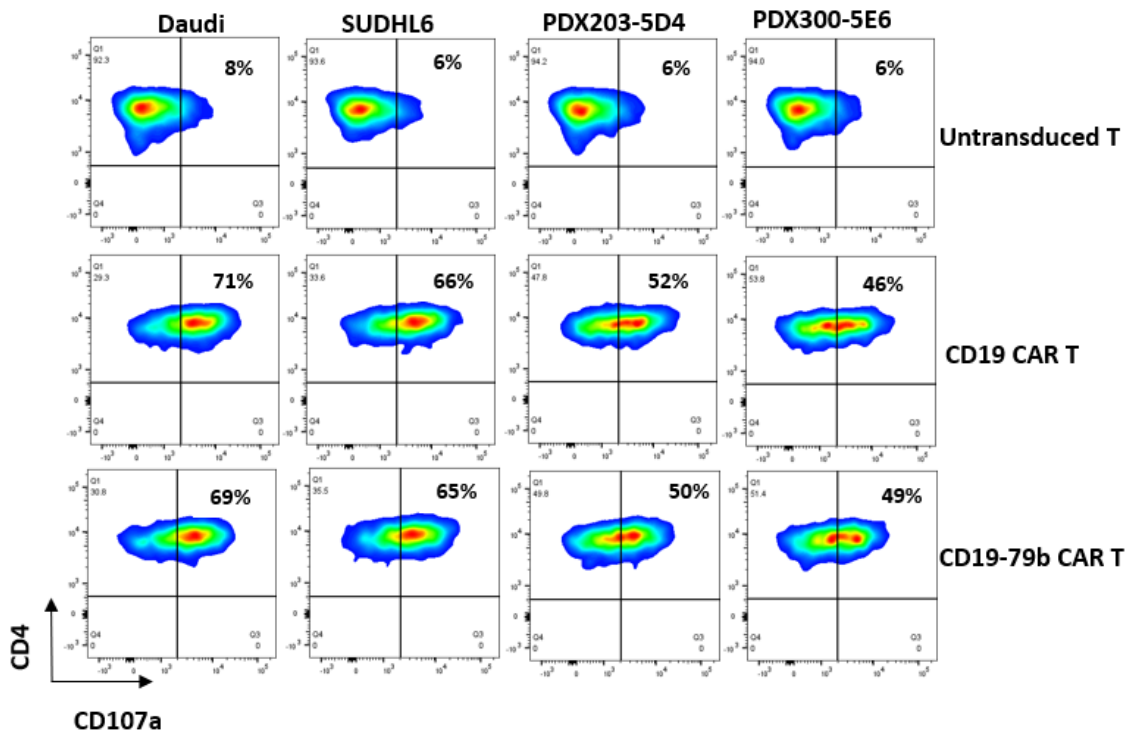
CD19 and CD79b expression in tumor cell lines



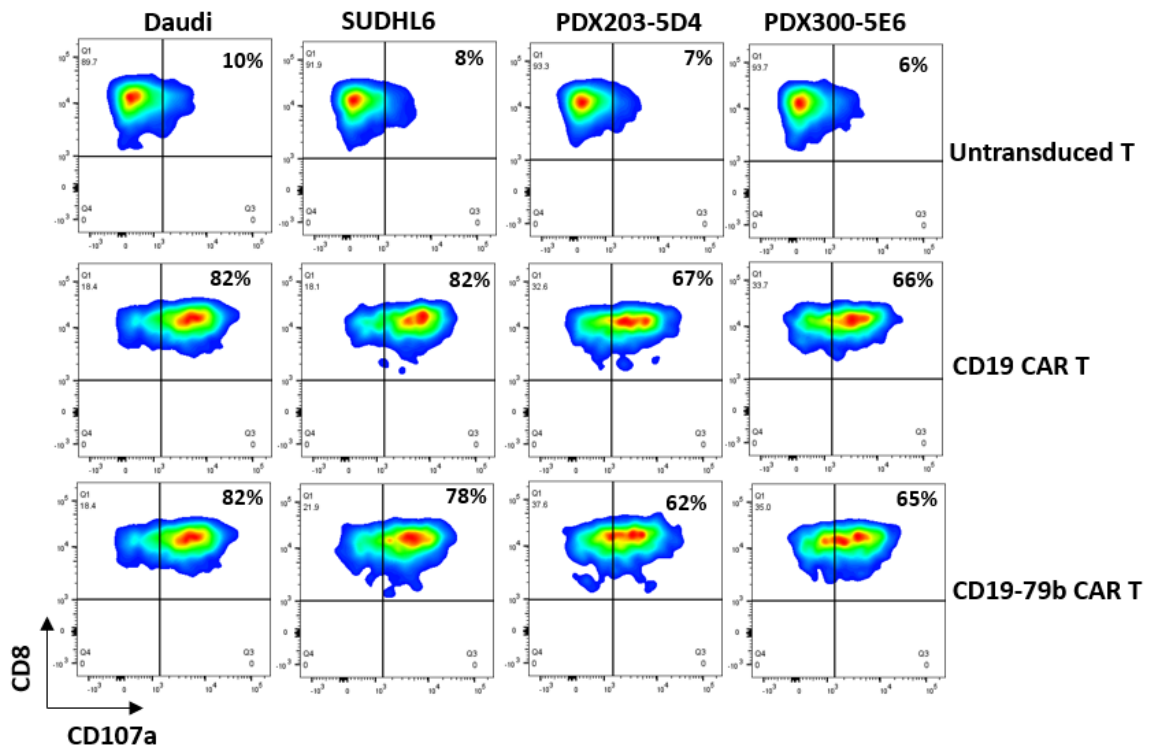
A4.



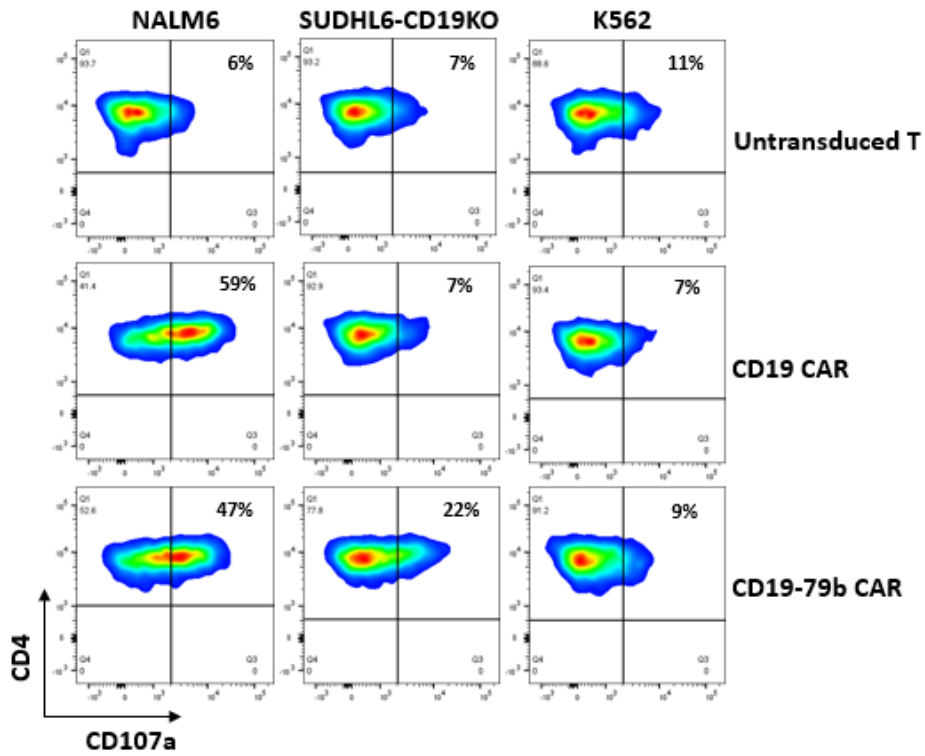
B1.



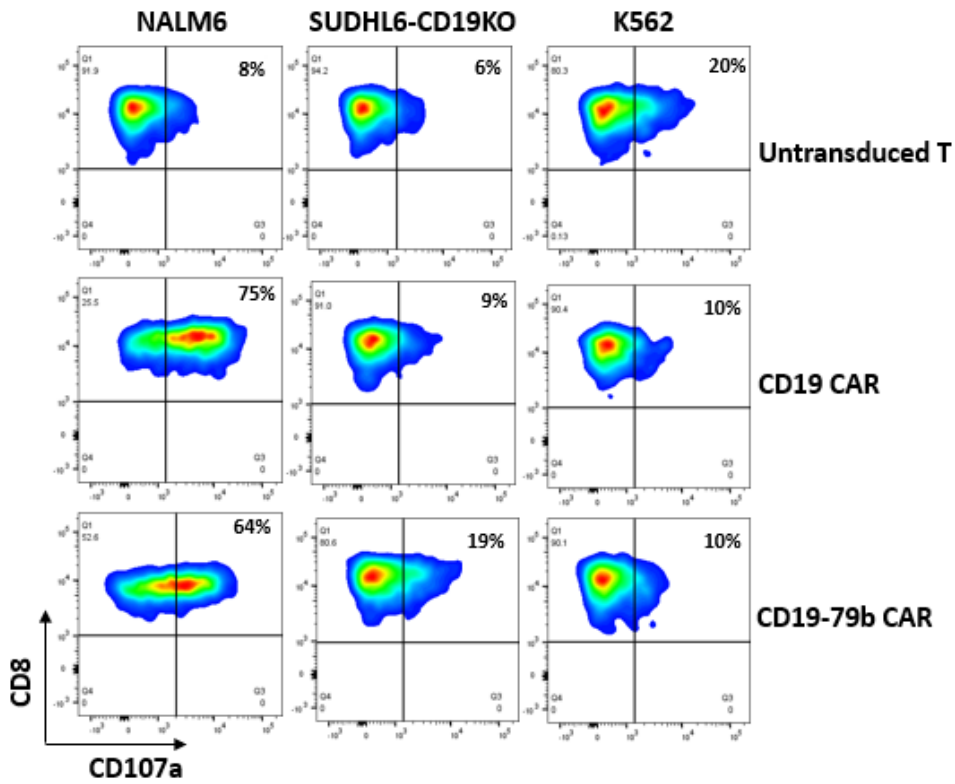
B2.



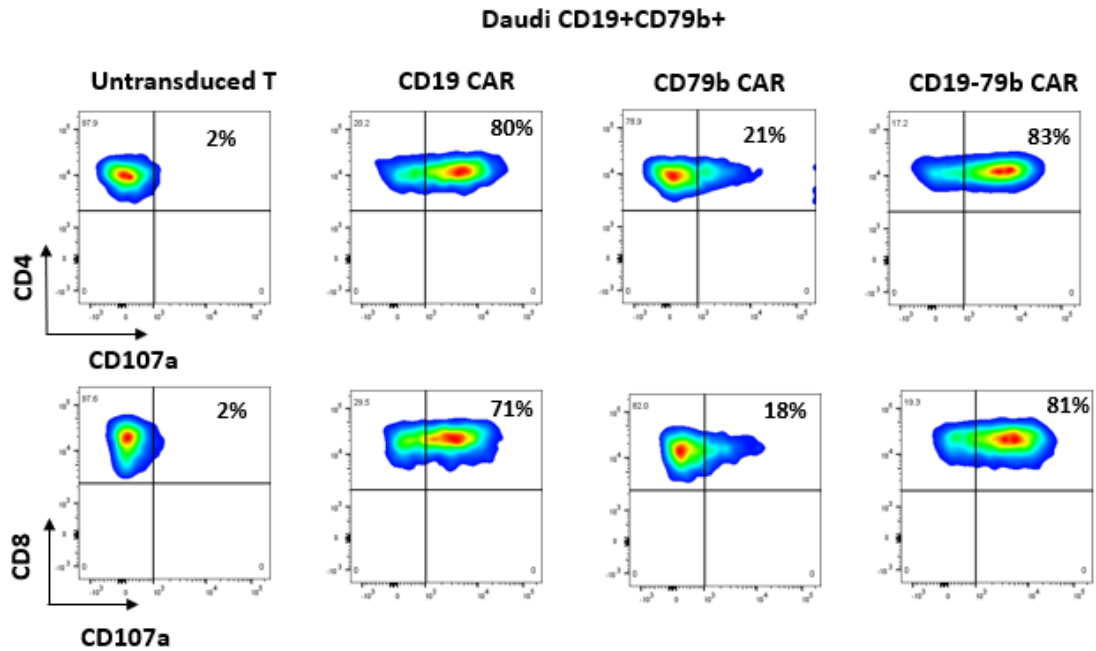
C1.



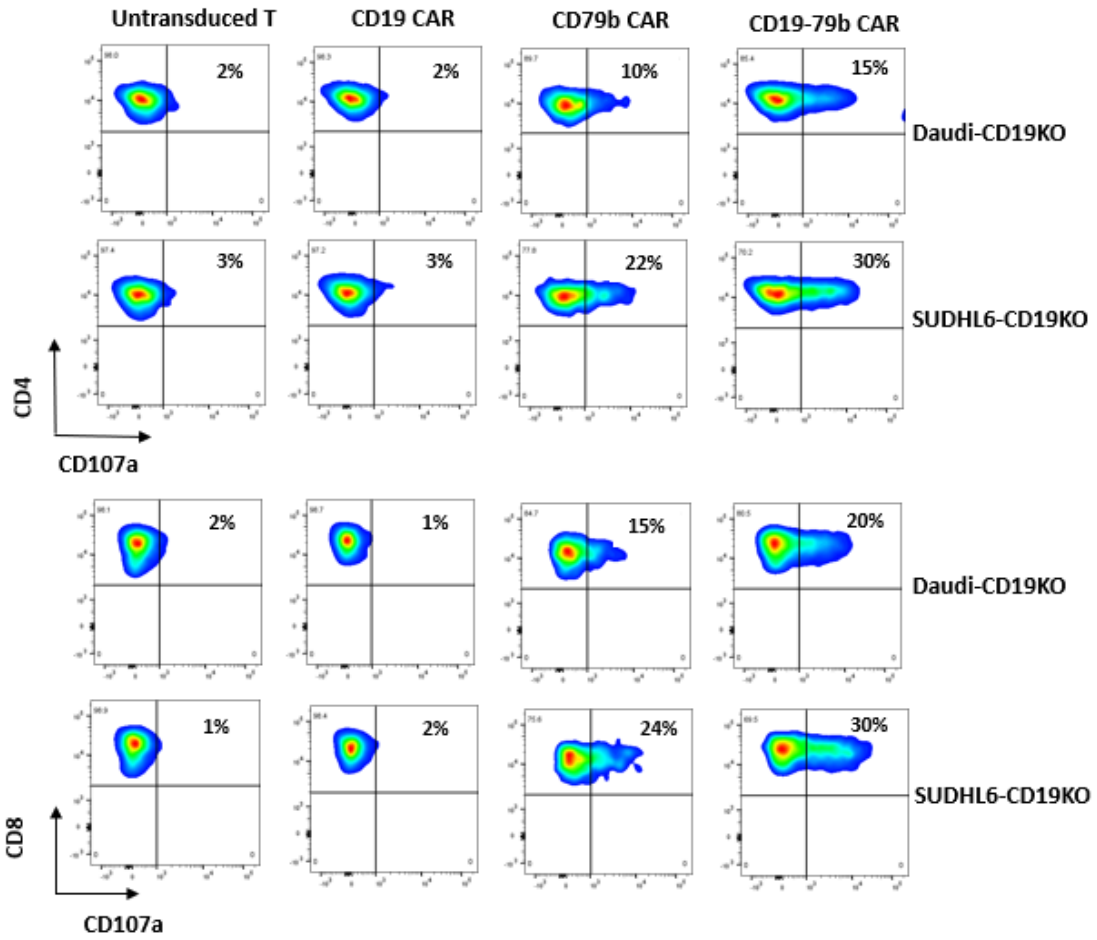
C2.



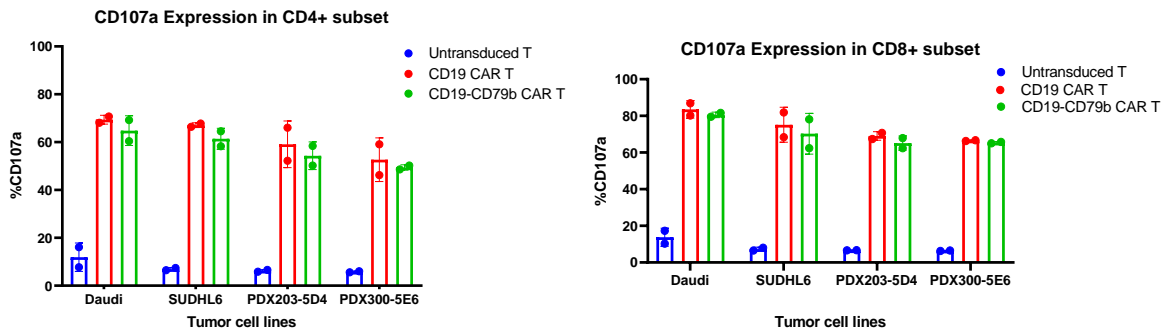
D



E.



F.



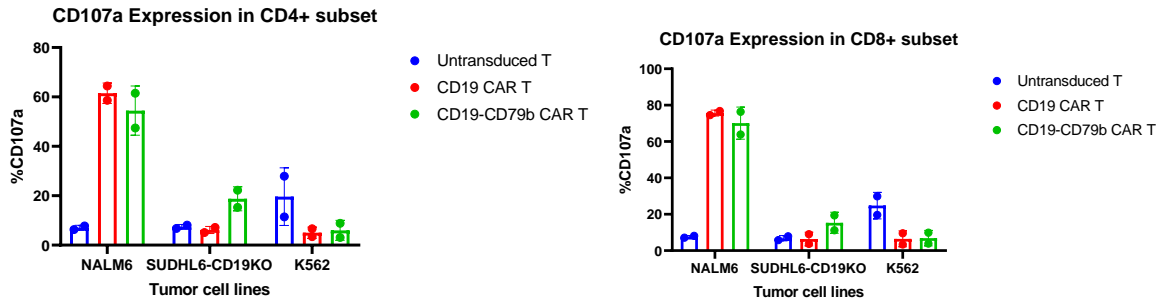


Figure 9. Tumor cell phenotypes and the degranulation of dual CD19-CD79b CAR T cells

A) A1:The expression of CD19 and CD79b antigen in CD19+CD79b+ B-cell lymphoma cell lines (Daudi, SUDHL6, PDX203 and PDX300), **A2:**CD19+ CD79b- B-cell leukemia cell line (NALM6), CD19KO cell lines (Daudi-CD19KO and SUDHL6-CD19KO), and CD19-CD79b- cell line (K562) were tested by flow cytometry using PE anti-CD19 and APC anti-CD79b stains. **A3:** The histogram plot showed the fluorescence intensity of CD19 and CD79b expression on tumor cells. **A4:** Tumor proliferation was tested by pre-labelling with CellTrace Violet on day0 and monitoring dye dilution on day1, day2 and day4 via flow cytometry.

B) Dual CD19-CD79b CAR T cells degranulated in response to CD19+CD79b+ tumor cells. Untransduced T cell, CD19 CAR T, and dual CD19-CD79b CAR T cells were co-cultured with B-cell lymphoma cell lines (Daudi, SUDHL6, PDX203-5D4 and PDX300-5E6) for 6 hours at 1:2 effector: target (E: T) ratio. The flow cytometry plots showed high CD107a expression in both CD4+ and CD8+ subset of CD19 CAR and dual CD19-CD79b CAR T cells.

C) Dual CD19-CD79b CAR T cells degranulated in a CD19/CD79b dependent manner and were not responsive to CD19-CD79b- tumor cells.

Untransduced T cell, CD19 CAR T and dual CD19-CD79b CAR T cells were co-cultured with B-cell leukemia cell lines (NALM6), SUDHL6-CD19KO, and K562 for 6 hours at 1:1 effector: target (E: T) ratio. The flow cytometry plots showed high CD107a expression in both CD4+ and CD8+ subset of CD19 CAR and dual CD19-CD79b CAR T cells when co-cultured with

NALM6. There was a slightly higher CD107a expression in both CD4+ and CD8+ subset of dual CD19-CD79b CAR T cells when co-cultured with SUDHL6-19KO. There was low CD107a expression in both CD4+ and CD8+ subset of CD19 CAR and dual CD19-CD79b CAR T cells when co-cultured with K562.

D) Cryopreserved and thawed dual CD19-CD79b CAR T cells degranulated in response to CD19+CD79b tumor cells.

Untransduced T-cell, CD19 CAR T, CD79b CAR and dual CD19-CD79b CAR T cells were co-cultured with Daudi for 6 hours at 1:1 effector: target (E: T) ratio. The high expression of CD107a was observed and determined by flow cytometry.

E) Cryopreserved and thawed dual CD19-CD79b CAR T cells degranulated in CD79b dependent manner.

Untransduced T-cell, CD19 CAR T, CD79b CAR, and dual CD19-CD79b CAR T cells were co-cultured with Daudi-CD19KO and SUDHL6-CD19KO for 6 hours at 2:1 effector: target (E: T) ratio. The expression of CD107a was determined by flow cytometry.

F) CD-19-CD79b CAR T cells generated with two different donor degranulated in response to tumor cells in CD19 or CD79b dependent manner.

The degranulation of untransduced T cell, CD19 CAR T, and dual CD19-CD79b CAR T were tested from two different normal donors. CD107a expression was determined by flow cytometry using an APC anti-CD107a stain. One dot presents cells generated from one donor.

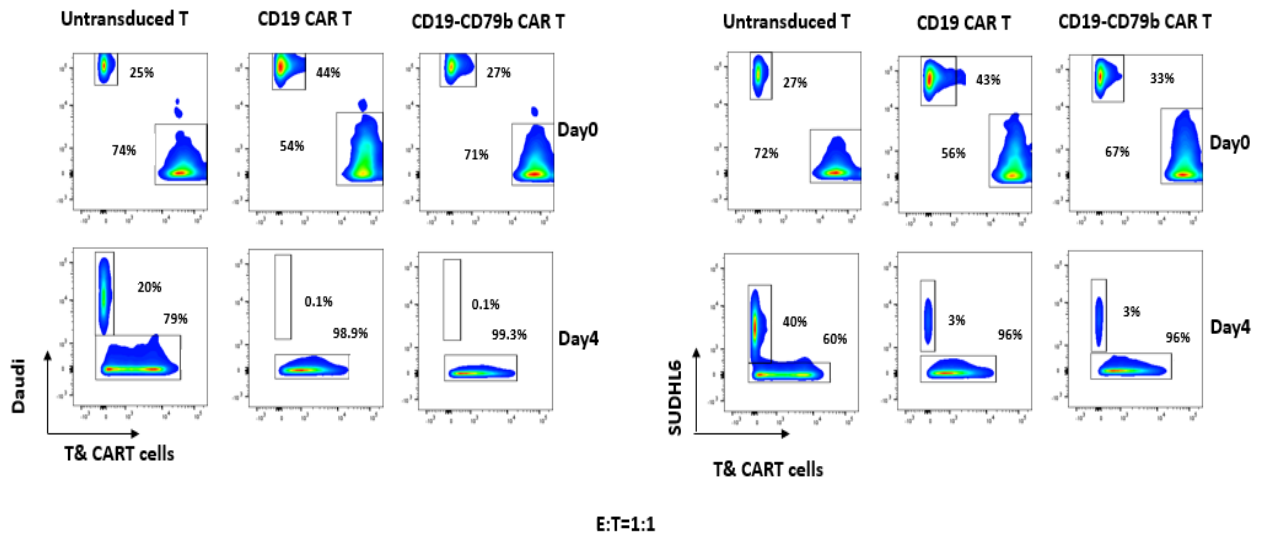
8. Dual CD19-CD79b CAR T cells were cytotoxic to B-cell lymphoma and leukemia cell lines in a CD19 or CD79b dependent manner.

Dual CD19-CD79b CAR T cells specifically recognized and induced lysis in B-cell lymphoma cells CD19+CD79b+ (Daudi, SUDHL6, PDX203-5D4, and PDX300-5E6) (Figure 10A1 and A2), B-cell leukemia CD19+CD79b- (NALM6) (Figure 10B), and CD19-CD79b+ tumor cell lines (Daudi-CD19KO and SUDHL6-CD19KO) (Figure 10C), but not CD19-CD79b-

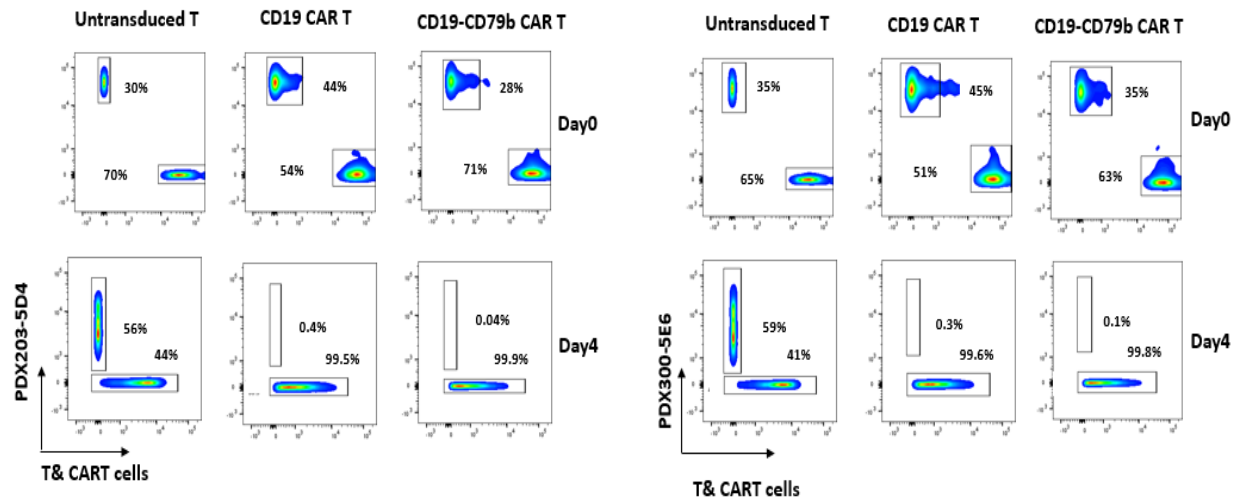
tumor cells (K562) (Figure 10D). The percentage of specific lysis by CAR T cells for each live tumor cell was calculated using the below formula and normalized to untransduced T-cells.

%Specific Lysis = 1- [live target cells with CAR T cells /live target cells with untransduced T cells] (Figure 10E)

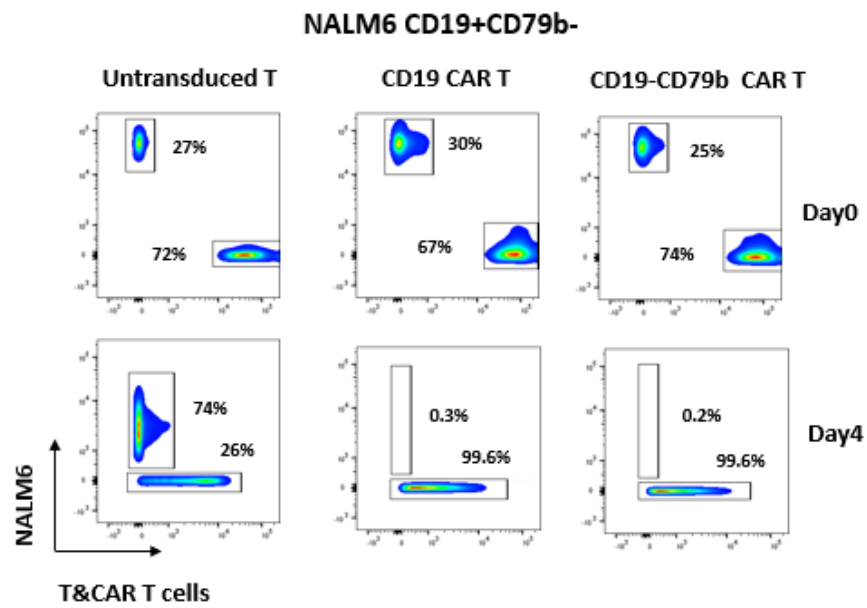
A1



A2

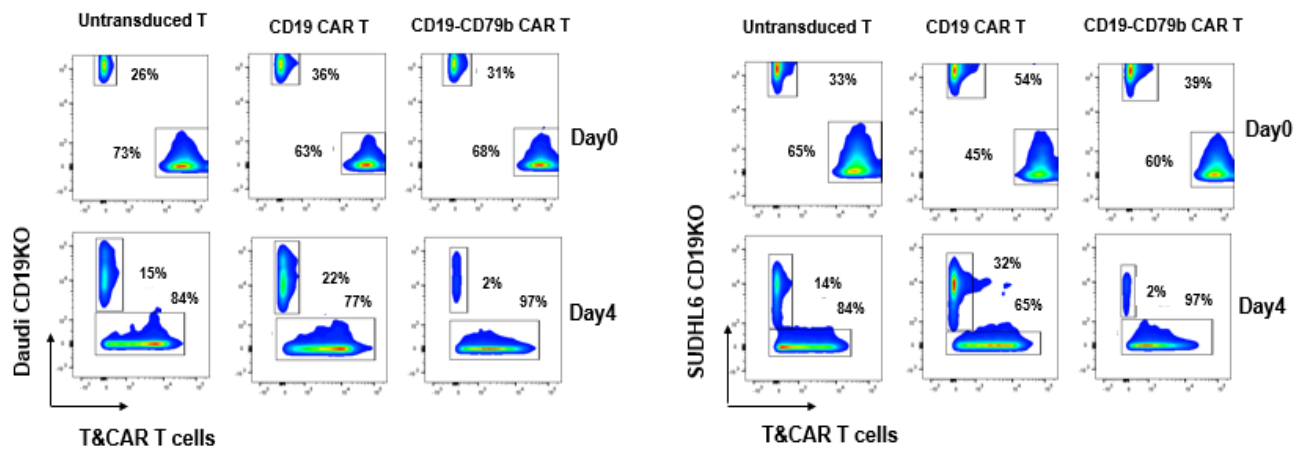


B.

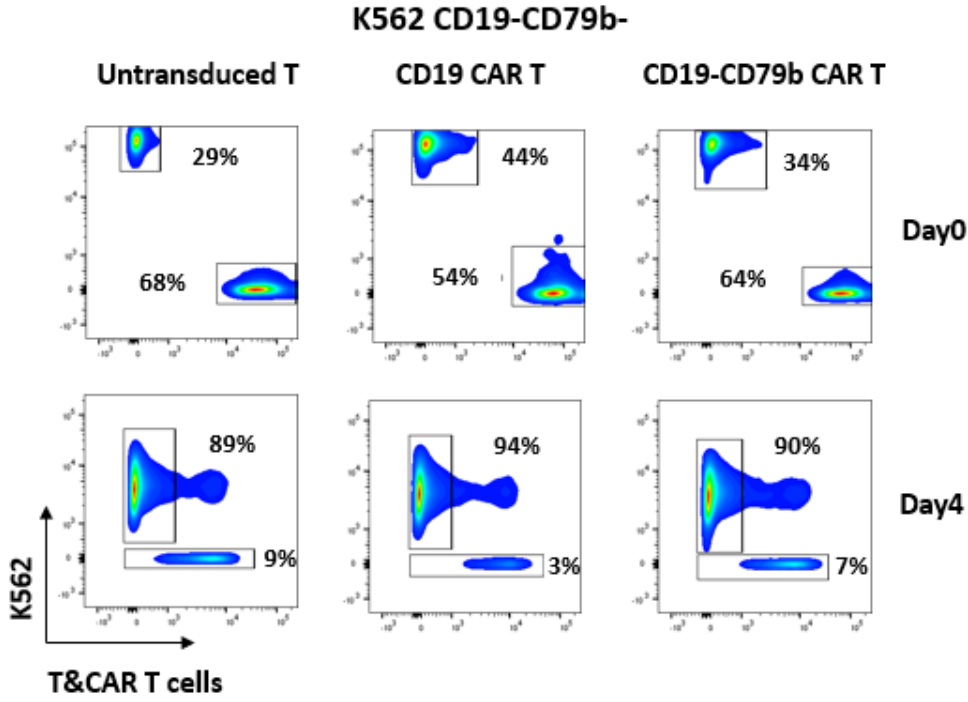


C.

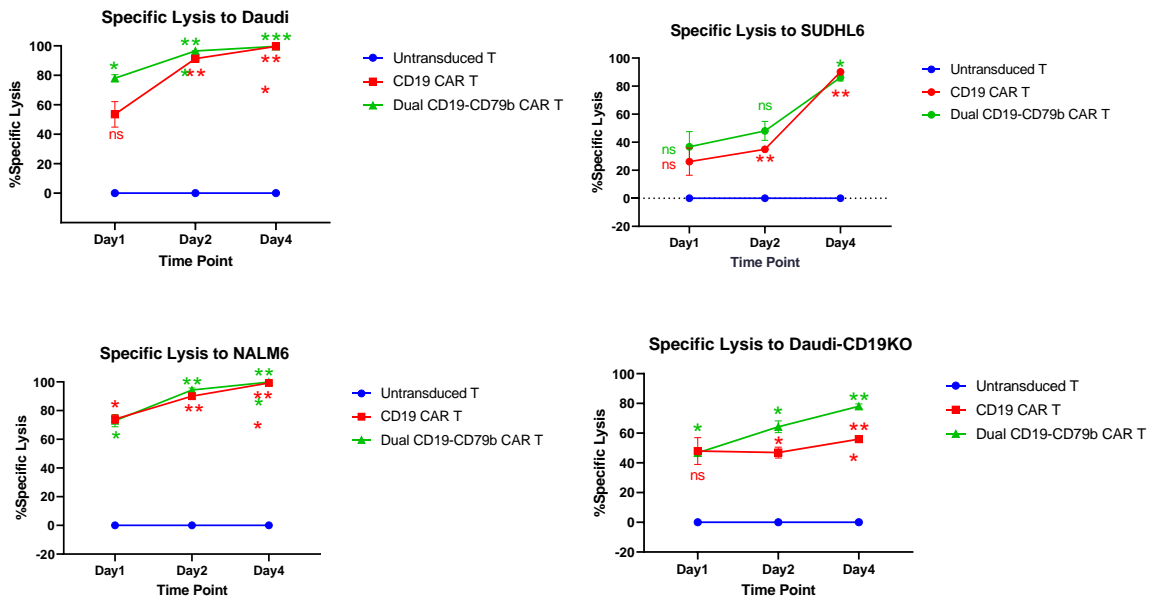
Figure 3C

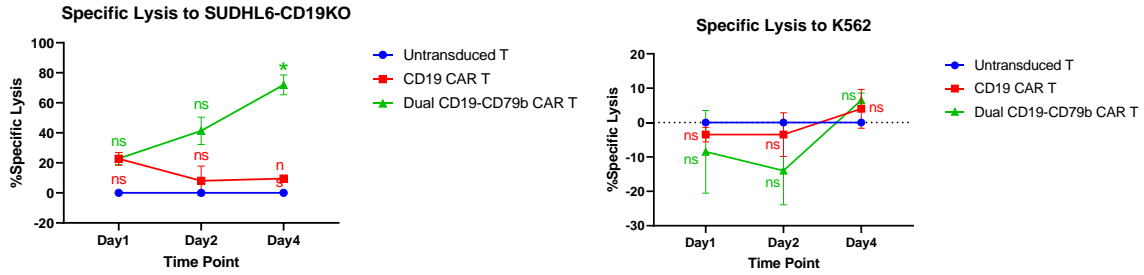


D.



E.





F.

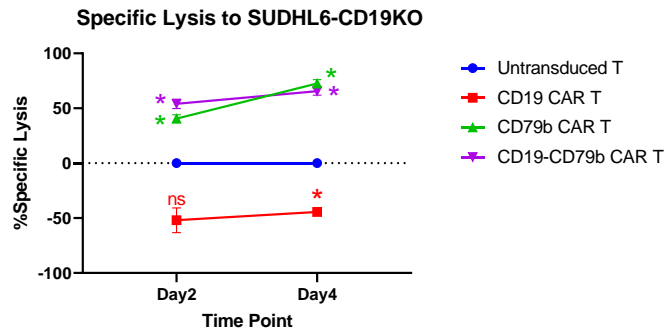


Figure 10. Dual CD19-CD79b CAR T cells were cytotoxic to CD19+CD79+, CD19+D79b-, and CD19-CD79b+ tumor cells.

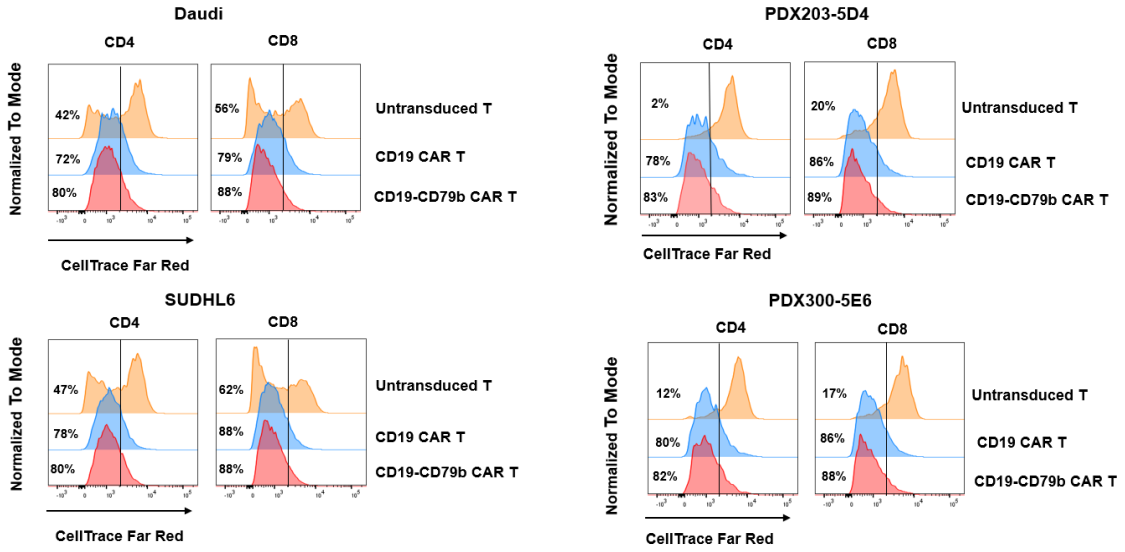
A1, A2) Dual CD19-CD79b CAR T cells induced lysis of CD19+CD79b+ tumor cells. Untransduced T cells, CD19 CAR T (CAR19 expression 78%), and dual CD19-CD79b CAR T cells (dual CAR expression 47%) were co-cultured with CD19+CD79b+ B-cell lymphoma cell lines (Daudi, SUDHL6, PDX203-5D4 and PDX300-5D6) for 96 hours at 1:1 effector: target (E:T) ratio. The flow cytometry plots show the percentages of live tumors on day 0 and day 4 for each co-culture condition. **B)** Untransduced T cells, CD19 CAR T and dual CD19-CD79b CAR cells were co-cultured with CD19+CD79b- B-cell leukemia cell lines (NALM6) for 96 hours at 1:1 effector: target (E: T) ratio. The flow cytometry plots show the percentages of live tumors on day 0 and day 4 for each co-culture condition. **C)** Untransduced T cells, CD19 CAR T and dual CD19-CD79b CAR cells were co-cultured with CD19KO B-cell lymphoma cell lines (Daudi-CD19KO and SUDHL6-CD19KO) for 96 hours at 1:1 effector: target (E: T) ratio. The

flow cytometry plots show the percentages of live tumors on day 0 and day 4 for each co-culture condition. **D)** Untransduced T cells, CD19 CAR T and dual CD19-CD79b CAR cells were co-cultured with CD19-CD79b+ tumor cell lines (K562) for 96 hours at 1:1 effector: target (E: T) ratio. The flow cytometry plots show the percentages of live tumors on day 0 and day 4 for each co-culture condition. **E)** Untransduced T cells, CD19 CAR T and dual CD19-CD79b CAR cells were co-cultured with tumor cells (Daudi, SUDHL6, PDX203-5D4, PDX300-5E6, NALM6, Daudi-CD19KO, SUDHL6-CD19KO and K562) for 24 hours, 48 hours, and 96 hours at 1:1 effector: target (E:T) ratio and percent specific lysis was calculated based on the absolute number of live tumor cells and normalized to untransduced T cells (%Specific Lysis = $1 - [\text{live target cells with CAR T cells} / \text{live target cells with untransduced T cells}]$). CD19 CAR and CD19-CD79b CAR T cells were compared to the untransduced T cell control using paired t test. ns: $P > 0.05$, *: $P \leq 0.05$; **: $P \leq 0.01$; ***: $P \leq 0.001$. **F)** Untransduced T, CD19 CAR T, CD79b CAR T, and dual CD19-CD79b CAR T cells were co-cultured with SUDHL6-CD19KO for 48 hours and 96 hours at 1:1 effector: target (E:T) ratio and percent specific lysis was calculated based on the absolute number of live tumor cells and normalized to untransduced T cells (%Specific Lysis = $1 - [\text{live target cells with CAR T cells} / \text{live target cells with untransduced T cells}]$). ns: $P > 0.05$, *: $P \leq 0.05$; **: $P \leq 0.01$; ***: $P \leq 0.001$

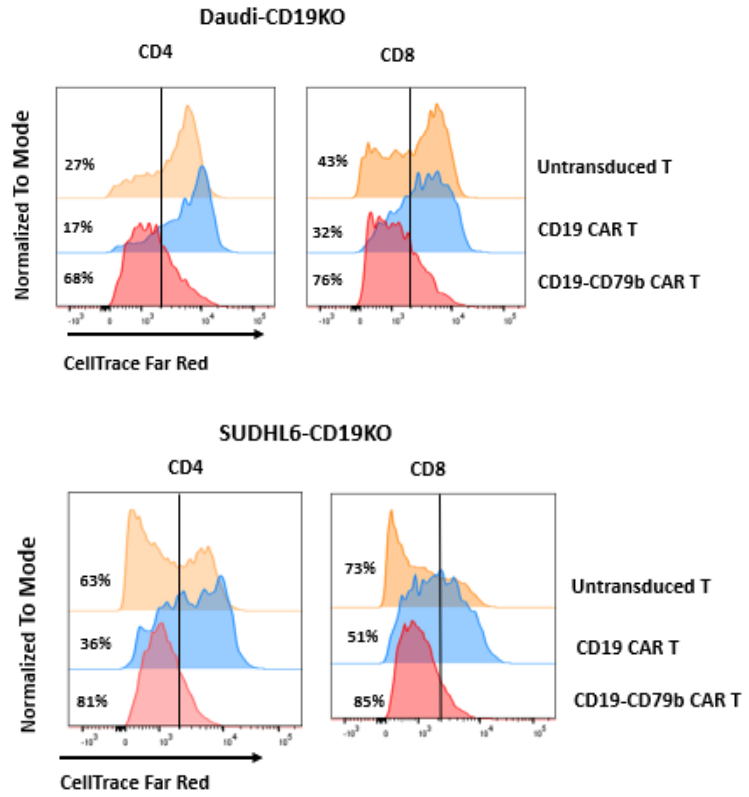
9. Dual CD19-CD79b CAR T cells proliferated in response to B-cell lymphoma and leukemia cell lines in a CD19 or CD79b dependent manner.

After co-culturing for 4 days, dual CD19-CD79b CAR T cells proliferated when co-cultured with B-cell lymphoma and leukemia tumor cell lines (Daudi, SUDHL6, PDX203-5D4, PDX300-5E6, NALM6, Daudi-CD19KO, SUDHL6-CD19KO and K562).

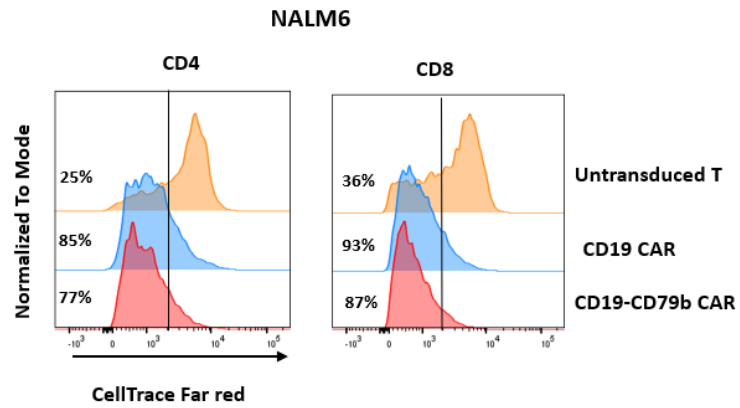
A.



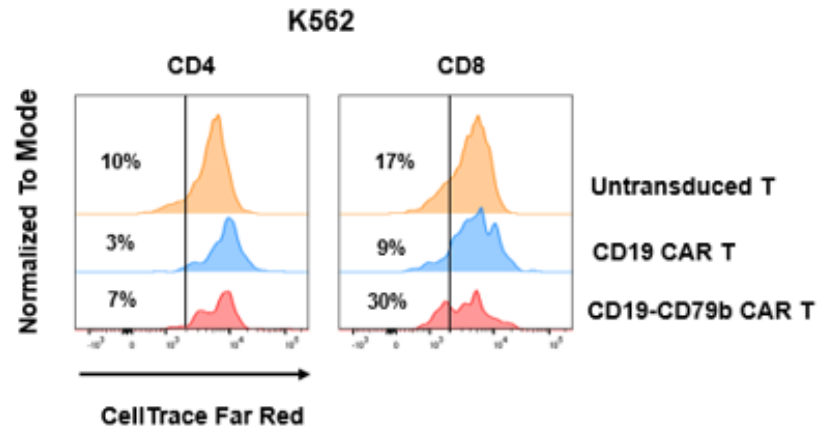
B.



C.



D



E.

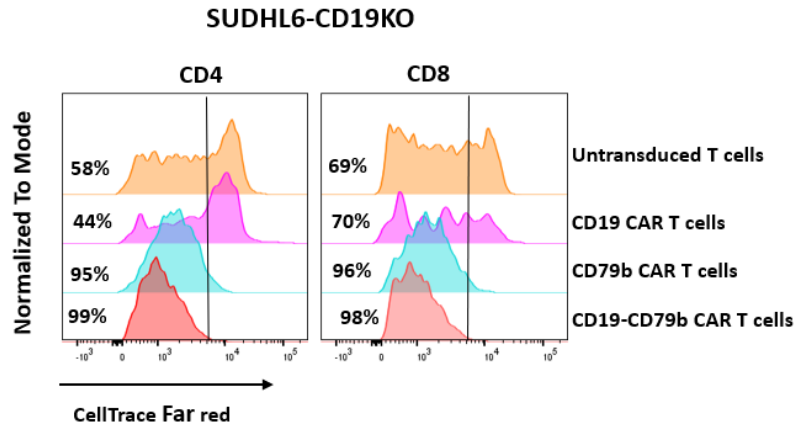


Figure 11. Dual CD19-CD79b CAR T cells proliferated in response to B-cell lymphoma and B-leukemia in CD19 or CD79b dependent manner.

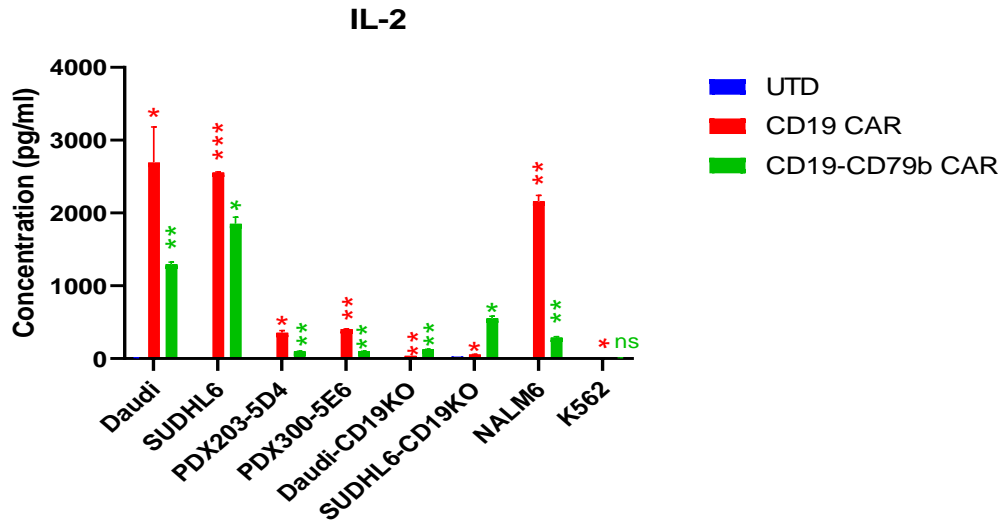
Untransduced T cells, CD19 CAR T, CD79b CAR T and dual CD19-CD79b CAR cells labelled with Cell Trace Far Red were co-cultured for 96 hours with tumor cells at 1:1 effector: target (E: T) ratio. The percentage of proliferating T cells were determined based on dye dilution on day 4 and indicated in each flow plot. **A:** Untransduced T cells, CD19 CAR T, and dual CD19-CD79b CAR cells were co-cultured with CD19+CD79b+ B-cell lymphoma cell lines (Daudi, SUDHL6, PDX203-5D4 and PDX300-5D6). **B:** Untransduced T cells, CD19 CAR T, and dual CD19-CD79b CAR cells were co-cultured with CD19KO B-cell lymphoma cell lines (Daudi-CD19KO and SUDHL6-CD19KO). **C.** Untransduced T cells, CD19 CAR T, and dual CD19-CD79b CAR cells were co-cultured with B-cell leukemia tumor cell lines CD19+CD79b- (NALM6). **D.** Untransduced T cells, CD19 CAR T, and dual CD19-CD79b CAR cells were co-cultured with CD19-CD79b- tumor cells lines K562. **E.** Untransduced T cells, CD19 CAR T, CD79b CAR T and dual CD19-CD79b CAR cells were co-cultured with CD19KO B-cell lymphoma cell lines SUDHL6-CD19KO.

10. CD19-CD79b CAR T cells produced effector cytokines in response to B-cell lymphoma and leukemia cell lines in CD19 or CD79b dependent manner.

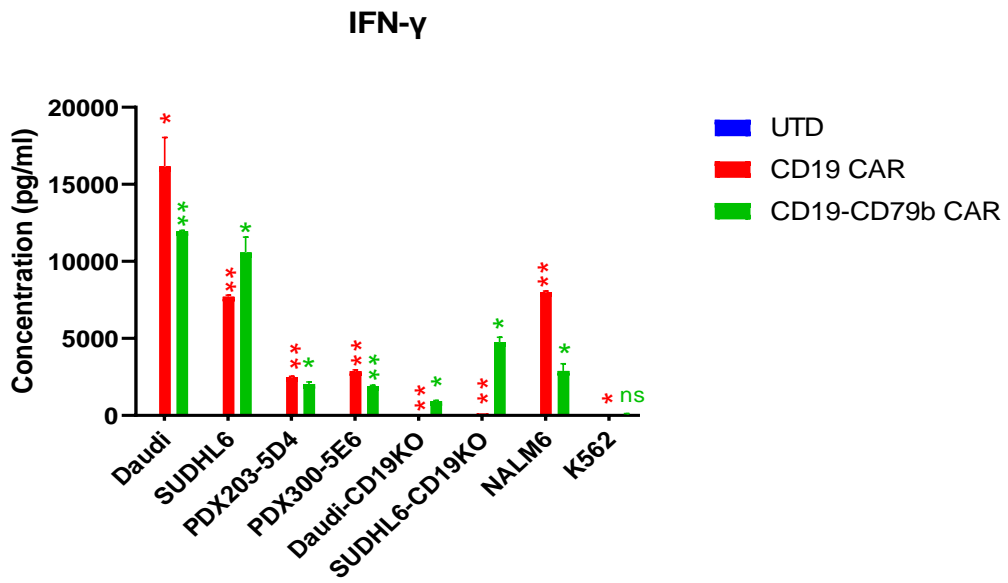
Dual CD19-CD79b CAR T cells specifically recognized and released IFN- γ (Figure 14A), IL-2 (Figure 14B), TNF- α (Figure 14C) and IL-13 (Figure 14D) in response to B-cell lymphoma cells CD19+CD79b+ (Daudi, SUDHL6, PDX203-5D4, and PDX300-5E6), B-cell leukemia CD19+CD79b- (NALM6) and CD19-CD79b+ tumor cell lines (Daudi-CD19KO and SUDHL6-CD19KO), but not CD19-CD79b-tumor cells (K562). Compared to CD19-CD79b CAR T cells,

CD19 CAR T cells released a slightly higher levels of cytokines when co-cultured with tumor expressing CD19+ or CD19+CD79b+.

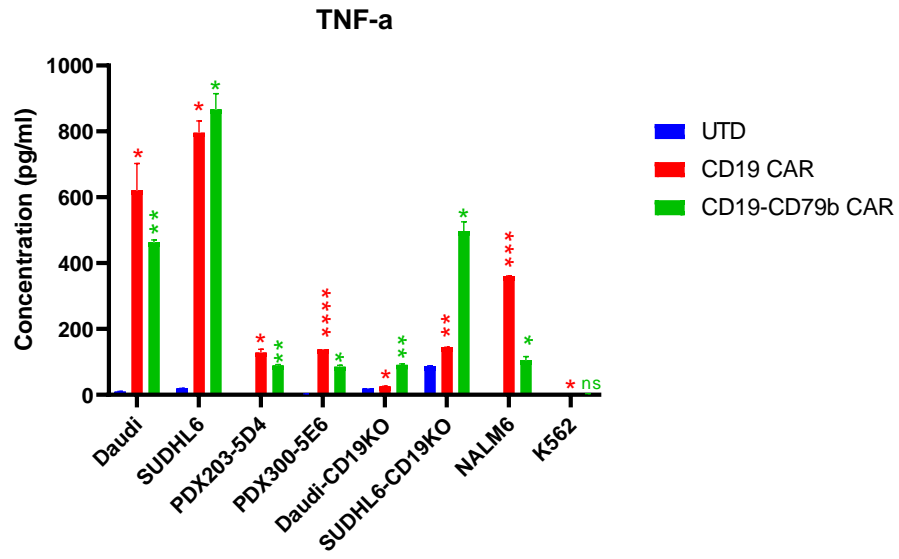
A.



B.



C.



D.

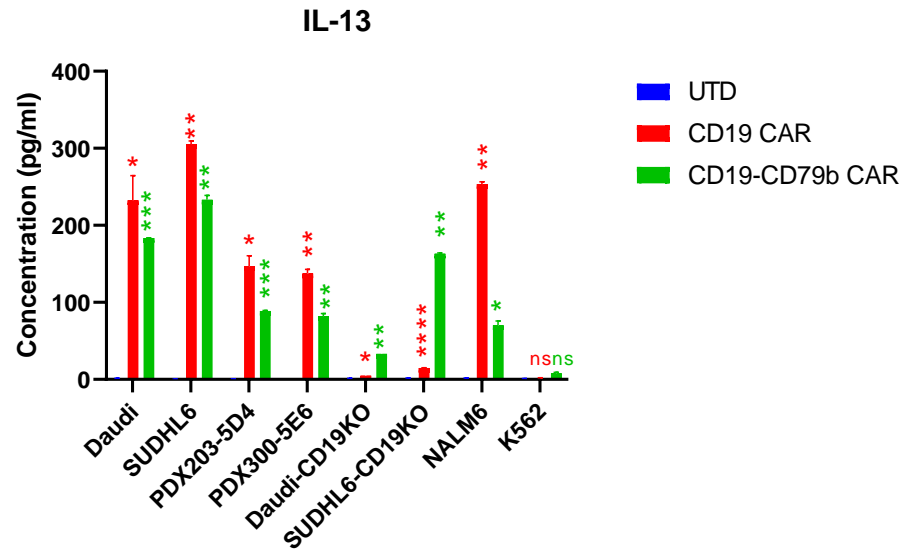


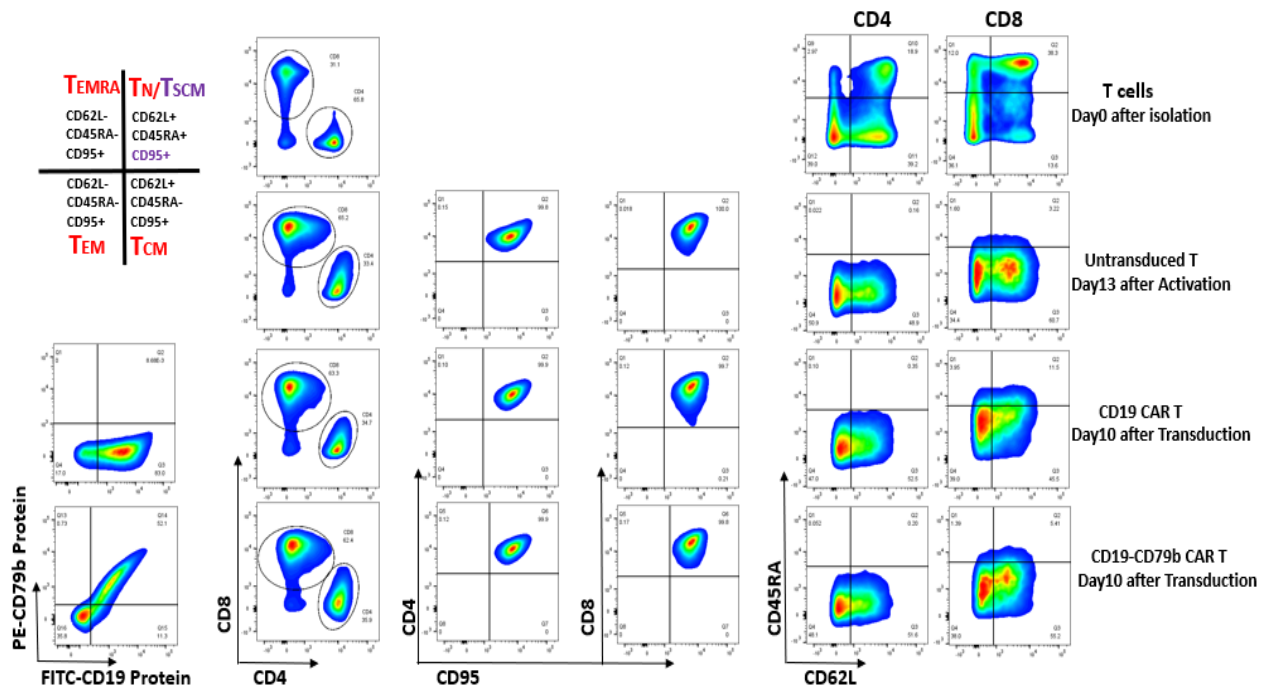
Figure 12. Dual CD19-CD79b CAR T cells released cytokines in response to tumor cells expressing either CD19 or CD79b and both.

The concentration of IL-2 (A), IFN- γ (B), TNF- α (C) and IL-13 (D) were measured by MSD multiplex cytokine assay. Untransduced T cells, CD19 CAR T, CD79b CAR T and dual CD19-CD79b CAR T cells were co-cultured overnight with tumor cells at 1:1 effector: target (E: T) ratio. The concentration of cytokine was determined by using MSD multiplex cytokine assays. CD19 CAR and CD19-CD79b CAR T cells were compared to the untransduced T cells control using paired t test. ns: P>0.05, *: P \leq 0.05; **: P \leq 0.01; ***: P \leq 0.001, ****: P \leq 0.0001.

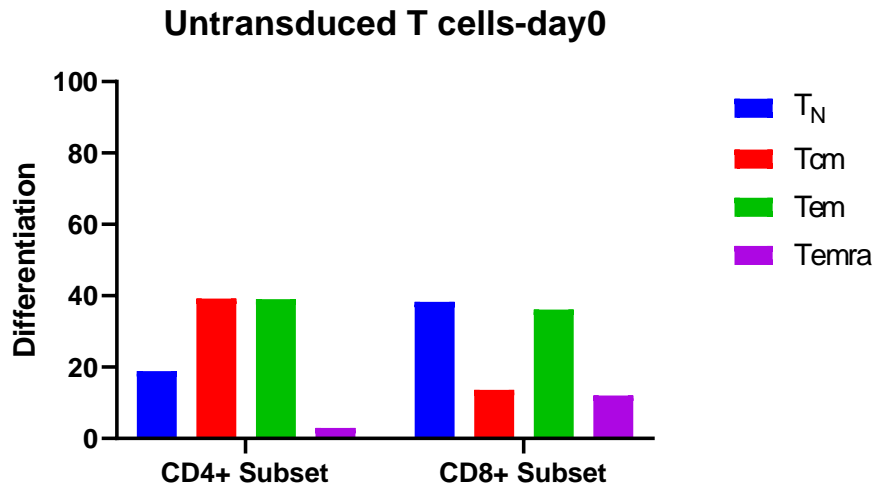
11. The subset and phenotype of CD19-CD79b CAR T cells were similar to untransduced T cells and CD19 CAR T cells.

In both CD4+ and CD8+ subsets, most of the untransduced T cells (Day13) and CAR T cells (transduced day10) were central memory and effector memory T cells (Figure 12A and C).

A.



B.



C.

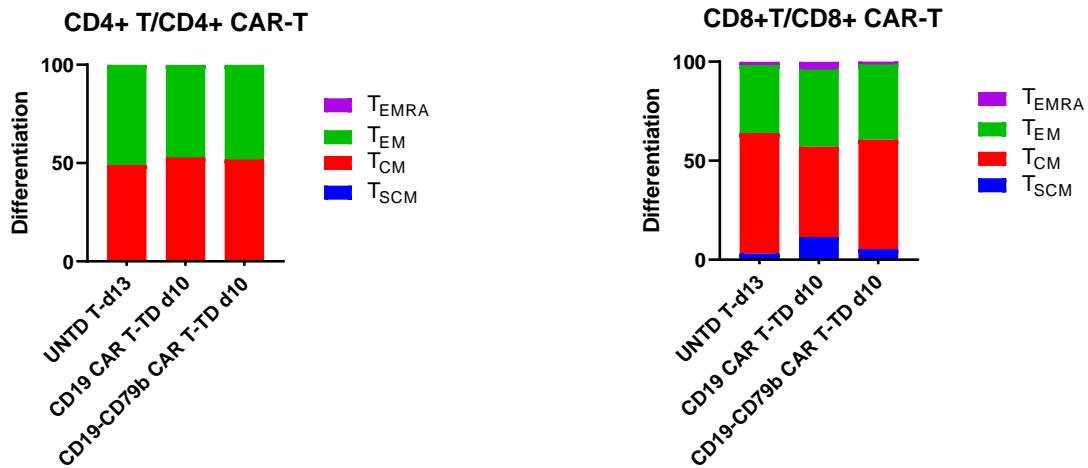


Figure 13. Similar subsets and phenotypes were observed in untransduced T cells, CD19 CAR T, and CD19-CD79b CAR T cells.

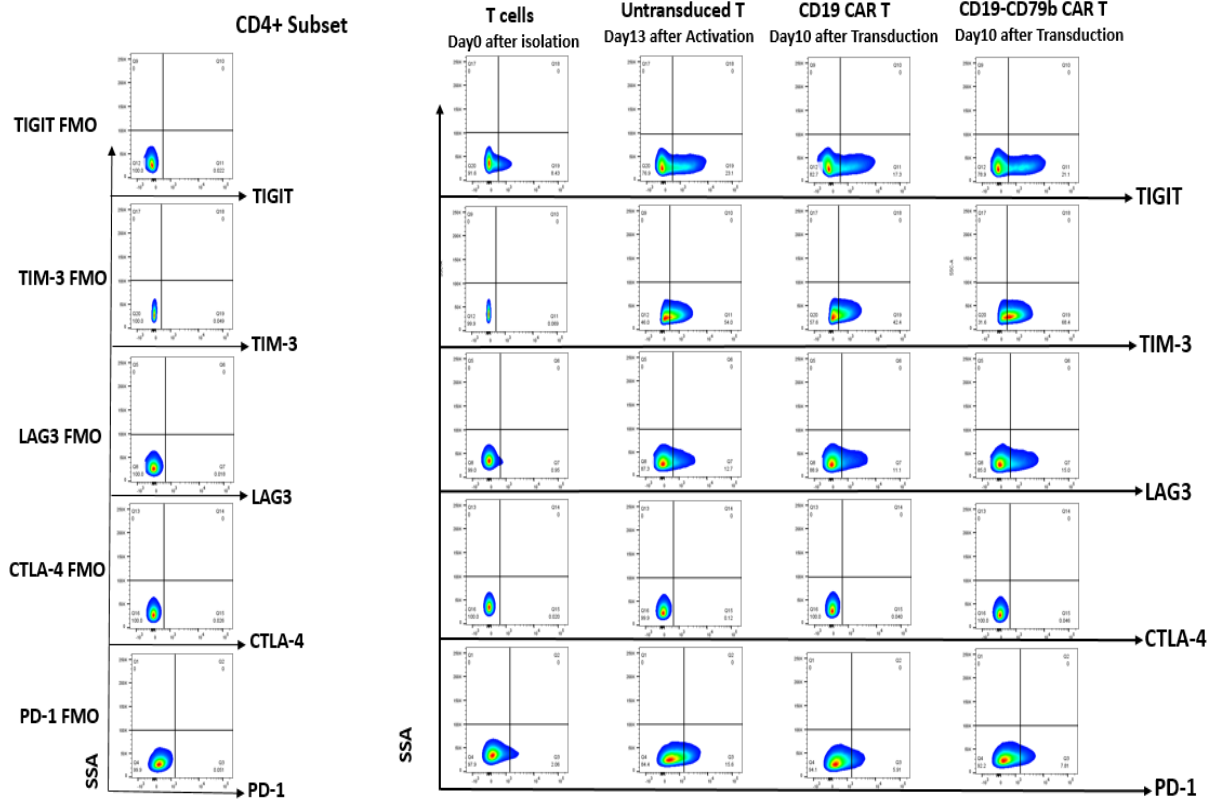
A) The subset and phenotype of untransduced T cells, CD19 CAR T, and CD19-CD79b CAR T were stained with AF700 anti-CD3, PerCP-Cy5.5 anti-CD4, BV605 anti-CD8, PE-CF594 anti-CD62L, PE-Cy7 anti-CD45RA, APC anti-CD95, and Amcyan Live-dead and were tested

by flow cytometry. Isolated T cells (day0) stained all the antibodies except for CD95. **B)** The phenotype of isolated T cells (day0) was determined by flow cytometry. **C)** Both of CD4+ and CD8+ subset of CD19-CD79b CAR T had a similar phenotype with untransduced T cells and CD19 CAR T cells with differentiation to central memory and effector memory cells.

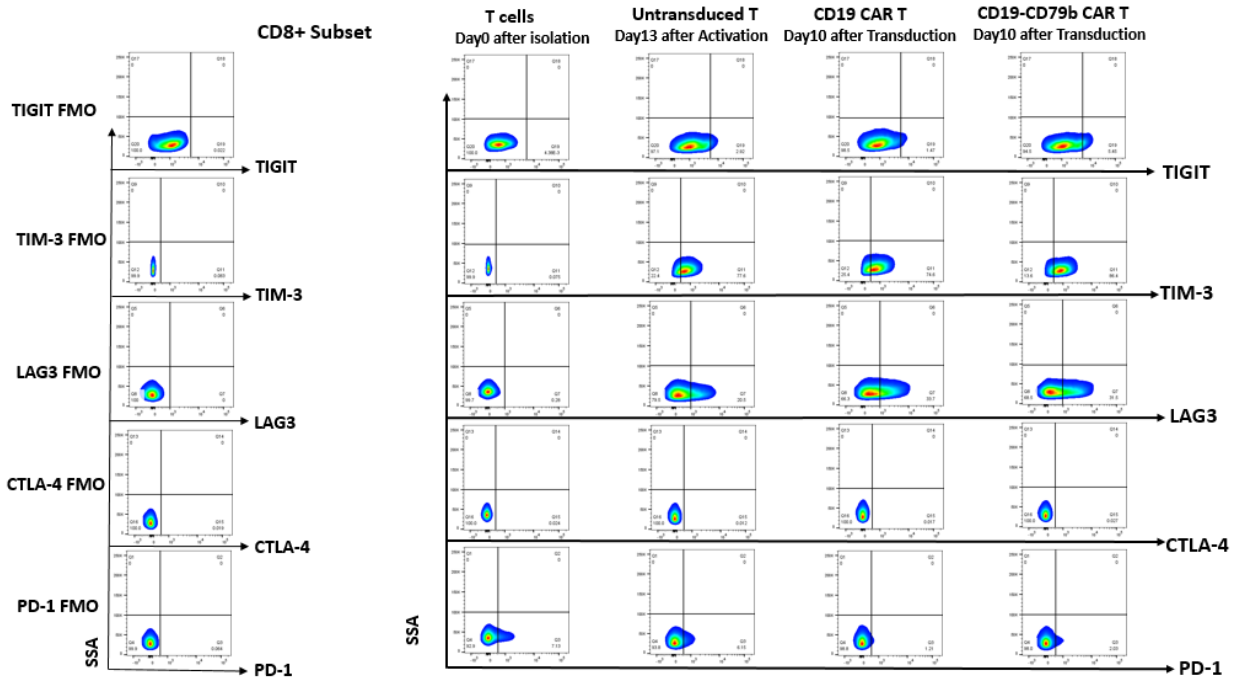
12. The expression of inhibitory receptors on CD19-CD79b CAR T cells was similar to untransduced T cells and CD19 CAR T cells.

The expression of CTLA-4 and PD-1 were low in both the CD4+ and CD8+ subset. High expression of TIM-3 was observed in both CD4+ and CD8+ subsets (**Figure 13A**). High expression of TIM3 and medium high expression of TIGIT were observed in the CD4+ subset. High expression of TIM3 and medium high expression of LAG3 were observed in the CD8+ subset (**Figure 13B**).

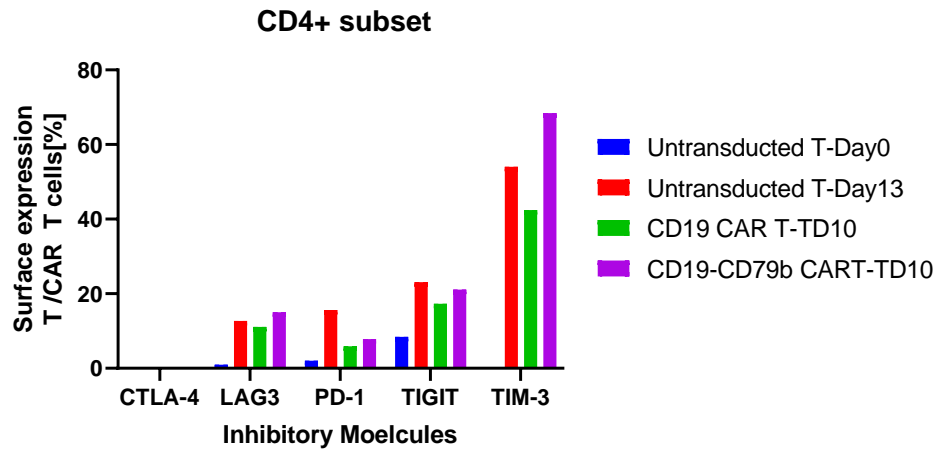
A1.



A2.



B.



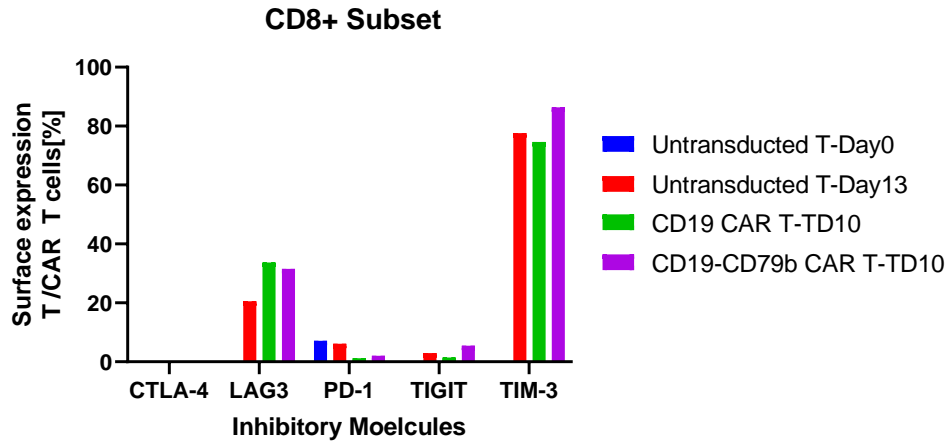


Figure 14. Low expression of PD-1 and CTLA-4 and high expression of TIM-3 were observed in both CD4+and CD8+ subsets.

A) The expression of inhibitory receptors in untransduced T cells, CD19 CAR and CD19-CD79b CAR were measured by flow cytometry. PD-1 FMO, CTLA-4 FMO, LAG3 FMO, TIM-3 FMO and TIGIT FMO were used for gating strategies. **B)** The plots show the expression of inhibitory receptors in both CD4+ and CD8+ subsets of untransduced T-cells, CD19 CAR and CD19-CD79b CAR T cells on day 0 isolation, day 13 after activation, day 10 after transduction.

Chapter 4: Discussions

CD19 CAR T therapy has demonstrated impressive efficacy in patients with relapsed or refractory B-cell leukemia and B-cell non-Hodgkin lymphoma (13, 15, 16, 42-45). However, about 30-60% patients eventually relapse following CD19 CAR T therapy (46-53). Relapsed patients fall into two categories: CD19 positive relapse and CD19 negative relapse. CD19 positive relapses are due to poor CD19 CAR T persistence, dysfunctional T cells or due to tumor intrinsic resistance mechanisms. CD19 negative relapse is due to CD19 loss. About 30-95% relapsed patients experience disease progression related to CD19 antigen loss (37). Low antigen expression or loss of antigen is also a main cause for resistance to CD19 CAR T therapy for B-cell malignancies (40, 49, 54, 55). CD22 loss has also been observed in relapsed patients following CD22 CAR-T therapy (56). But, other pan-B antigens such as CD20, CD22, CD79a and CD79b are not altered in patients relapsing after CD19 CAR T therapy (57, 58). Multiple antigen targeting is a potential strategy to overcome antigen escape for CAR-T therapy. CD79b is a pan-B marker and broadly expressed in >90% of B-cell non-Hodgkin lymphomas and chronic lymphocytic leukemias (59-61). Dual targeting of CD19 and CD79b may decrease antigen escape and increase efficacy of CAR-T therapy for patients with B-cell non-Hodgkin lymphoma or chronic lymphocytic leukemia.

Currently, several strategies have been used for targeting two antigens to decrease immune escape including coadministration (62), co-transduction, tandem CAR T cells and bicistronic CAR T cells (37). Both tandem and bicistronic CAR T cells products are homogeneous and may enhance the strength of the immune synapse by engaging the interaction between tumor cells and CAR T cells via simultaneously targeting two antigens (63). Tandem CAR construct can achieve higher transduction efficiency compared to bicistronic CAR due to transgene size. However, the orientation of two CARs in tandem CAR is not optimal due to steric hindrance, which may have an important impact on the function of tandem CARs. The result from a study of CD19-CD20 tandem CAR demonstrated that anti-

CD20 scFv should be placed in the distal position of the CAR construct because CD20 epitope is membrane proximal (64). In the study of dual targeting BCMA and GPRC5D in multiple myeloma, bicistronic CAR and two mono-specific CARs demonstrated superior efficacy in BCMA-relapsed model compared with tandem CARs, and bicistronic CAR showed better antitumor activity than two mono-specific CARs in a tumor model expressing both BCMA and GPRC5D (65). Considering the challenge of designing tandem CARs in the scFv order, flexible linkers, and hinge length, bicistronic construct was used in this study because it could be more feasible way for targeting two antigens to minimize antigen escape.

Importantly, dual CAR construct must enable two distinct CARs to express on the same cells. This study found that CD19 CAR and CD79b CAR could not be equally expressed on the surface of 293 T cells using dual CAR construct when incorporating CD28 H/TM in CD19 CAR. It was also observed that a CD8 α hinge/transmembrane domain (H/TM) in a dual CD19-CD79b CAR construct achieved high CAR expression on the surface of 293T cells compared to CD28 H/TM. CD19 CAR expression did not improve even when it was placed after promoter (Figure3, Figure4, Figure5). The expression of CD19 CAR engineering with CD28 T/TM was about 25%-47% compared to the CD79b CAR expression with 66%-72%. Previous studies have shown that CAR expression level is dependent on scFv structure when CARs have the same hinge and transmembrane domain, and endodomain (co-stimulatory domain and CD3 zeta) (66, 67). It was further proved that the CAR surface expression efficiency was influenced by scFv structural stability (28). Hinge and transmembrane domain also play a critical role in the control of CAR surface expression level. In particular, the CAR expression level is positively associated with the number of amino acids in the hinge, which further imply that the scFv' s folding efficiency relies on the hinge length. The CAR surface expression levels and stability were also affected by different transmembrane domain structures. In other words, it suggests that the regulation of CAR expression stability on cell surface is associated with its transmembrane cellular localization (28). Thus, the length and

structure of CD8 α H/TM (CD8 α H:45AA >CD28H:42AA) may contribute to improved CD19 CAR expression in a dual CD19-CD79b CAR construct.

It is known that transduction efficiency is associated with CAR construct, packaging system, envelope protein, and T cells. In this study, the low transduction efficiency (5%) and high cytotoxicity to the producer cells were observed when using the third generation packing system and VSV-G envelope protein. VSV-G cytotoxicity could affect 293 T cells to generate lentivirus particles. Third generation packing system improved the safety by splitting one packaging plasmid into two packaging plasmids (68). However, it also increased the difficulty in producing functional lentiviral particles, since it involved transfecting four plasmids into 293 T cells – including two packaging plasmids, one transfer plasmid encoding transgene, and one envelope plasmid. Although VSV-G (the vesicular stomatitis virus) is commonly used for pseudotyped protein due to broad tropism and particle stability, the high concentration of VSV-G could pose risk of cytotoxicity to both the packaging cell lines and the transduced cells (69). RD114 (the endogenous feline virus) not only could provide particle stability, but also is a non-toxic protein (70). Additionally, RD114 can bind a T-cell receptor, neutral amino acid transporter, that is widely expressed on activated primary T cells, which provides a favorable and feasible way to use for producing CD19-CD79b CAR lentivirus.

By using the second-generation packaging system and RD114, the transduction efficiency was slightly improved (12%; Figure 6). It is known that cloning capacity of lentiviral vector is about 8.5kb between the LTRs, however the package efficiency will be influenced by the inserts if bigger than 3kb. For pX10 dual CAR, the inserts between the LTRs was 7.78kb, which could decrease packaging efficiency and generate less functional lentivirus particles. In order to decrease the transgene size, we removed tEGFR suicide gene. Some studies showed that the poor persistence of CD19 CAR T cells accounts for CD19 positive relapse and resistance against CD19 CAR therapy (36, 38, 47). Long-lasting CAR T cells could continue to perform surveillance and clear CD19+ tumor cells. Considering the limited

persistence and the expected safety of CD19 and CD79b-targeting CAR T products, incorporation of a safety switch such as tEGFR is not essential. By removing tEGFR, the transduction efficiency of dual CD19-CD79b CAR increased from 12% to up to 50% (Figure 6)

Despite the improvement in transduction efficiency of dual CD19-CD79b CAR after removal of tEGFR, the sharp decrease of dual CAR expression was observed on day 8 after transduction, especially for CD79b CAR expression. To confirm this result, two other normal T cells were tested for four dual CAR constructs (pX2A, pX2B, pX2C and pX2D), the dual CAR expression on day 8 decreased more than 50% compared with dual CAR expression on day 3 after transduction. It was also observed that the order of CD79b CAR did not contribute to declined CD79 CAR expression. Considering dual CAR's gene size and the decrease of CD79b CAR expression, it can be posited that the promoter could play an important role in CAR expression and stability. The promoter is critical for producing a functional protein and impacting the expression level of CAR in T-cells. Dual CAR encodes CD19 CAR and CD79b CAR, which needs a strong and efficient promoter to transcribe the longer mRNA within CAR T cells. One study found that the EF-1 α promoter was the best promoter for efficiently driving long and complex RNA in CAR T cells compared to promoters such as CMV, hPGK and RPBSA. The EF1 α promoter provided the best transduction efficiency in primary T-cells as well as resistance to silencing in cells (71). To this end, replacing the promoter MSCV with EF1 α led to stable expression of dual CAR in dual CD19-CD79b CAR constructs X2E and X2F. However, a decrease in CD19 CAR expression was observed (Figure 7).

One study showed that protein expression was dramatically decreased in the second gene position in a bicistronic vector compared to the first gene. They found that the highest level of protein expression could be achieved by both T2A and tandem P2A-T2A for the second gene position in bicistronic construct compared to P2A and tandem P2A-T2A-E2A (71). In the polycistronic vector, 2A self-cleavable peptide was used for co-expression of

multiple transgenes such as E2A, T2A and P2A. P2A and T2A are known as the highest 2A self-cleavable peptide. Due to decreased CD19 CAR expression, dual construct X2K and X2L were generated with CD19 CAR in the first place and CD79b in the second place after T2A. Stable CD19 CAR expression was observed on day 7 and day 10 after transduction, and the expression of CD79b CAR placed after T2A was not affected (Figure 7).

Engineering the optimal CD19-CD79b CAR involves many factors including the affinity of scFv, the distribution of target antigen, the length of hinge, the transmembrane domain, and co-stimulatory domain. Co-stimulatory domains play an important role in CAR T cell function. Both pX2K and pX2L dual CAR construct achieved the stable expression of dual CARs, however, incorporating 4-1BB or OX40 to CD19 CAR could affect dual CAR T cells' efficacy and persistence. The current FDA-approved CD19 CAR T products are the second-generation CARs with either CD28 or 4-1BB co-stimulatory domain. Preclinical and clinical studies have shown that CD28 co-stimulation induced rapid CAR T cell activation and potent antitumor activity but limited persistence. In contrast, 4-1BB co-stimulation displayed slow tumor killing and similar antitumor potency, but greater CAR T cells persistence with long-term memory phenotype (72, 73). In addition, longer persisting CD4+ CAR T cells with 4-1BB co-stimulation were detected in two patients with chronic lymphocytic leukemia after complete remission for 12 years. CD4+ CAR T cells still retained anti-tumor capacity and the function of activation and proliferation (74). Furthermore, in other preclinical studies where co-stimulation OX40, CD27 and ICOS were used, anti-tumor activity and CAR T cell persistence were exhibited (75-77). Considering transduction efficiency and potential persistence of 4-1BB co-stimulation, pX2K was selected for further testing, which contains CD19 CAR with 4-1BB co-stimulatory domain and CD79b CAR with OX40 co-stimulatory domain.

To evaluate dual CD19-CD79b CAR T cell function, degranulation, cytotoxicity and proliferation assays were conducted. Dual CD19-CD79b CAR degranulated in response to B-cell lymphoma cell lines (CD19+CD79b+: Daudi, SUDHL6, PDX203-5D4, and PDX300-5E6;

Figure 7B), B-cell leukemia cells lines (CD19+CD79b-: NALM6; Figure C1), and CD19KO B-cell lymphoma cell lines (CD19-CD79b+-Daudi-CD19KO and SUDHHL6-CD19KO; Figure D) in a CD19 or CD79b dependent manner. The similar result was confirmed from the two degranulation assays tested by using two different normal donor T cells (Figure 9F). The data also demonstrated the potency of CD19-CD79b CAR in killing tumor cells in B-cell lymphoma cell lines (the percentage of specific lysis to Daudi and SUDHL6 on day4 was 99.6% and 86%, respectively), B-cell leukemia cell lines (the percentage of specific lysis to NALM6 on day4 was 99.9%), and CD19KO cell lines (the percentage of specific lysis to Daudi-CD19KO and SUDHL6-CD19KO on day4 was 78% and 72%, respectively). The best killing was achieved on day 4 after the coculture (Figure 10). Upon binding the targeted tumor cells, rapid proliferation of dual CAR T cells was observed, which is dependent in a CD19 or CD79b manner. However, CD79b CAR showed slow activity in degranulation and tumor cell killing compared to CD19 CAR. This could be due to scFv construct, antigen distribution, hinge and transmembrane domain, or co-stimulatory domain. The CD79b CAR could be further optimized to improve the efficacy of dual CD19-CD79b CARs.

Based on clinical studies, the ratio of CD4+:CD8+ and memory phenotype could influence antitumor activity and persistence of CAR T cells. It has been agreed that the optimal CAR T product is composed of a CD4+:CD8+ ratio of 1:1 (47). The optimal ratio of CD4+:CD8+ (1:1) was observed on day 9 after transduction in dual CD19-CD79b CAR T cells. Recently, one pre-clinical trial of bi-specific CD19-CD22 showed that the final CAR T product was dominated by CD4+ cells after pre-selective enrichment for T_{CM} and T_{SCM} with low T_{EMRA}. Additionally, CD4+ cells expressed higher levels of CD39 and PD-1, which can lead to T cell exhaustion and poor persistence (40). During the process of producing dual CD19-CD79b CAR T cells, untouched human T-cells isolated from normal donors were activated by anti-CD3/CD28/CD2 with IL-2 (200IU/mL). The ratio of CD4+:CD8+ (1:1) on day4 and day9 after transduction was 2:1 and 1:1, respectively. Furthermore, both CD4 and CD8 subsets of dual

CAR T cells mainly contained T_{CM} and T_{EM}. In addition, like untransduced T-cells, dual CD19-CD79b CAR exhibited low expression of PD-1 and CTLA-4 that are associated with T-cell exhaustion.

Chapter 5. Conclusions and Future Directions

Within this thesis work, I successfully generated dual CD19-CD79b CAR construct targeting either CD19 or CD79b, or both simultaneously in B-cell lymphoma and leukemia cell lines. The dual CD19-CD79b CAR was engineered with 2nd generation anti-CD19 CAR (murine anti-CD19 FMC63) and anti-CD79b (murine anti-CD79b 28B clone) linked by a T2A self-cleaving peptide. In the dual CAR construct, CD19 CAR was incorporated with a 4-BB co-stimulatory domain followed by CD79b CAR containing an OX40 co-stimulatory domain under the control of human EF1 α promoter.

With optimized process of lentivirus production and transduction, high transduction efficiency of dual CD19-CD79b CAR was achieved. The dual CAR stably expressed on T cells and equally distributed in CD4+ and CD8+ T cell subsets. The method of generation of dual CAR T cells attained the optimal CD4:CD8 ratio of 1:1 on day9 after transduction.

Dual CD19-CD79b CAR T cells degranulated, proliferated, and exhibited robust cytotoxic activity against B-cell lymphoma and leukemia cell lines expressing either CD19 or CD79b or both, suggesting that both CD19 CAR and CD79b CAR in the dual CAR construct are functional. Also, CD19-CD79b CAR T produced distinct effector cytokines in response to tumor cells expressing either CD19 or CD79 or both. Furthermore, the phenotype and expression of various inhibitory receptors were similar between CD19 CAR and CD19-CD79b dual CAR T cells, suggesting that the expression of two distinct CAR molecules in the same cell did not adversely affect T cell differentiation during CAR T generation.

To decrease CD19 negative relapse rate and resistance to CD19 CAR therapeutics, several studies investigated the efficacy of CARs by simultaneously targeting multiple antigens (41, 64, 78). Two phase 1 trials of bispecific (CD19-22.BB.z) and bicistronic (Auto-3) CD19-CD22 CAR have demonstrated a favorable safety profile and no dose-limiting toxicity. A high complete molecular response rate was observed in Auto-3 clinical trial and a high six-month PFS was found after CD19-22.BB.z CAR therapy in LBCL. Both were similar to tisagenlecleucel (40, 41). However, two clinical studies also found that several factors

influence the efficacy of CAR therapy such as unbalanced CD4:CD8 ratio and weak CD22 CAR in CD19-22.BB.z CAR therapy and poor persistence of CAR T in Auto-3 clinical trial.

Considering the moderate efficacy of CD79b CAR in dual CD19-CD79b CARs, future work is needed to optimize CD79b CAR for improved efficacy of dual CAR and to evaluate the efficacy and persistence of dual CD19-CD79b CAR in CD19+CD79b+, CD19+CD79b- and CD19-CD79b+ tumor xenograft models. Dual CD19-CD79b CAR T therapy has great potential to minimize CD19 antigen escape and improve antitumor potency for patients with B-cell non-Hodgkin lymphoma, chronic lymphocytic leukemia and hairy cell leukemia.

Chapter 6. Bibliography

1. Teras LR, DeSantis CE, Cerhan JR, Morton LM, Jemal A, Flowers CR. 2016. 2016 US lymphoid malignancy statistics by World Health Organization subtypes. *CA Cancer J Clin* 66: 443-59
2. Rebecca L. Siegel KDM, Hannah E. Fuchs, Ahmedin Jemal, DVM, . 2021. Cancer Statistics, 2021. *CA: A Cancer Journal for Clinicians* 71:7–33
3. Patel KK, Isufi I, Kothari S, Davidoff AJ, Gross CP, Huntington SF. 2020. Cost-effectiveness of first-line vs third-line ibrutinib in patients with untreated chronic lymphocytic leukemia. *Blood* 136: 1946-55
4. Cyster JG, Allen CDC. 2019. B Cell Responses: Cell Interaction Dynamics and Decisions. *Cell* 177: 524-40
5. Küppers R. 2005. Mechanisms of B-cell lymphoma pathogenesis. *Nat Rev Cancer* 5: 251-62
6. Hauke RJ, Armitage JO. 2000. Treatment of non-Hodgkin lymphoma. *Curr Opin Oncol* 12: 412-8
7. Abramson JS, Ghosh N, Smith SM. 2020. ADCs, BiTEs, CARs, and Small Molecules: A New Era of Targeted Therapy in Non-Hodgkin Lymphoma. *Am Soc Clin Oncol Educ Book* 40: 302-13
8. Zahid U, Akbar F, Amaraneni A, Husnain M, Chan O, Riaz IB, McBride A, Iftikhar A, Anwer F. 2017. A Review of Autologous Stem Cell Transplantation in Lymphoma. *Curr Hematol Malig Rep* 12: 217-26
9. Yang Y. 2015. Cancer immunotherapy: harnessing the immune system to battle cancer. *J Clin Invest* 125: 3335-7
10. Kimiz-Gebologlu I, Gulce-Iz S, Biray-Avci C. 2018. Monoclonal antibodies in cancer immunotherapy. *Mol Biol Rep* 45: 2935-40
11. Nair R, Westin J. 2020. CAR T-Cells. *Adv Exp Med Biol* 1244: 215-33

12. Finney HM, Lawson AD, Bebbington CR, Weir AN. 1998. Chimeric receptors providing both primary and costimulatory signaling in T cells from a single gene product. *J Immunol* 161: 2791-7
13. Maude SL, Frey N, Shaw PA, Aplenc R, Barrett DM, Bunin NJ, Chew A, Gonzalez VE, Zheng Z, Lacey SF, Mahnke YD, Melenhorst JJ, Rheingold SR, Shen A, Teachey DT, Levine BL, June CH, Porter DL, Grupp SA. 2014. Chimeric antigen receptor T cells for sustained remissions in leukemia. *N Engl J Med* 371: 1507-17
14. Maude SL, Teachey DT, Porter DL, Grupp SA. 2015. CD19-targeted chimeric antigen receptor T-cell therapy for acute lymphoblastic leukemia. *Blood* 125: 4017-23
15. Lee DW, Kochenderfer JN, Stetler-Stevenson M, Cui YK, Delbrook C, Feldman SA, Fry TJ, Orentas R, Sabatino M, Shah NN, Steinberg SM, Stroncek D, Tschernia N, Yuan C, Zhang H, Zhang L, Rosenberg SA, Wayne AS, Mackall CL. 2015. T cells expressing CD19 chimeric antigen receptors for acute lymphoblastic leukaemia in children and young adults: a phase 1 dose-escalation trial. *Lancet* 385: 517-28
16. Davila ML, Riviere I, Wang X, Bartido S, Park J, Curran K, Chung SS, Stefanski J, Borquez-Ojeda O, Olszewska M, Qu J, Wasielewska T, He Q, Fink M, Shinglot H, Youssif M, Satter M, Wang Y, Hosey J, Quintanilla H, Halton E, Bernal Y, Bouhassira DC, Arcila ME, Gonen M, Roboz GJ, Maslak P, Douer D, Frattini MG, Giralto S, Sadelain M, Brentjens R. 2014. Efficacy and toxicity management of 19-28z CAR T cell therapy in B cell acute lymphoblastic leukemia. *Sci Transl Med* 6: 224ra25
17. Administration USFD. 2017, September 7. FDA approves tisagenlecleucel for B-cell ALL and tocilizumab for cytokine release syndrome.
18. Administration USFD. 2018, May 3. FDA approves tisagenlecleucel for adults with relapsed or refractory large B-cell lymphoma.
19. Administration USFD. 2017, October 25. FDA approves axicabtagene ciloleucel for large B-cell lymphoma.

20. Administration USFD. 2021, March 8. FDA grants accelerated approval to axicabtagene ciloleucel for relapsed or refractory follicular lymphoma.
21. Administration USFD. 2021, October 1. FDA approves brexucabtagene autoleucel for relapsed or refractory B-cell precursor acute lymphoblastic leukemia.
22. Administration USFD. 2021, March 4. FDA D.I.S.C.O. Burst Edition: Breyanzi (lisocabtagene maraleucel).
23. Administration USFD. 2021, April 7. FDA D.I.S.C.O. Burst Edition: FDA approval of ABECMA (idecabtagene vicleucel) the first FDA approved cell-based gene therapy for the treatment of adult patients with relapsed or refractory multiple myeloma.
24. Administration USFD. 2022, March 7. FDA approves ciltacabtagene autoleucel for relapsed or refractory multiple myeloma.
25. Srivastava S, Riddell SR. 2015. Engineering CAR-T cells: Design concepts. *Trends Immunol* 36: 494-502
26. Sadelain M, Brentjens R, Rivière I. 2013. The basic principles of chimeric antigen receptor design. *Cancer Discov* 3: 388-98
27. Mumtaz YB. August 2, 2019. Components and design of chimeric antigen receptors. In *Basics of chimeric antigen receptor (CAR) immunotherapy*, pp. 13-21: Academic Press
28. Fujiwara K, Tsunei A, Kusabuka H, Ogaki E, Tachibana M, Okada N. 2020. Hinge and Transmembrane Domains of Chimeric Antigen Receptor Regulate Receptor Expression and Signaling Threshold. *Cells* 9
29. Hong M, Clubb JD, Chen YY. 2020. Engineering CAR-T Cells for Next-Generation Cancer Therapy. *Cancer Cell* 38: 473-88
30. Chmielewski M, Abken H. 2020. TRUCKS, the fourth-generation CAR T cells: Current developments and clinical translation. *ADVANCES IN CELL AND GENE THERAPY* 3: e84

31. Larson RC, Maus MV. 2021. Recent advances and discoveries in the mechanisms and functions of CAR T cells. *Nat Rev Cancer* 21: 145-61
32. Mumtaz YB. 2019. scFv cloning, vectors, and CAR-T production in laboratory for preclinical applications. In *Basics of chimeric antigen receptor (CAR) immunotherapy*, pp. 25-44
33. Skorka K, Ostapinska K, Malesa A, Giannopoulos K. 2020. The Application of CAR-T Cells in Haematological Malignancies. *Arch Immunol Ther Exp (Warsz)* 68: 34
34. Albinger N, Hartmann J, Ullrich E. 2021. Current status and perspective of CAR-T and CAR-NK cell therapy trials in Germany. *Gene Ther* 28: 513-27
35. Adami A, Maher J. 2021. An overview of CAR T-cell clinical trial activity to 2021. *Immunother Adv* 1: Itab004
36. Nie Y, Lu W, Chen D, Tu H, Guo Z, Zhou X, Li M, Tu S, Li Y. 2020. Mechanisms underlying CD19-positive ALL relapse after anti-CD19 CAR T cell therapy and associated strategies. *Biomark Res* 8: 18
37. Majzner RG, Mackall CL. 2018. Tumor Antigen Escape from CAR T-cell Therapy. *Cancer Discov* 8: 1219-26
38. Xu X, Sun Q, Liang X, Chen Z, Zhang X, Zhou X, Li M, Tu H, Liu Y, Tu S, Li Y. 2019. Mechanisms of Relapse After CD19 CAR T-Cell Therapy for Acute Lymphoblastic Leukemia and Its Prevention and Treatment Strategies. *Front Immunol* 10: 2664
39. Han X, Wang Y, Wei J, Han W. 2019. Multi-antigen-targeted chimeric antigen receptor T cells for cancer therapy. *J Hematol Oncol* 12: 128
40. Spiegel JY, Patel S, Muffly L, Hossain NM, Oak J, Baird JH, Frank MJ, Shiraz P, Sahaf B, Craig J, Iglesias M, Younes S, Natkunam Y, Ozawa MG, Yang E, Tamaresis J, Chinnasamy H, Ehlinger Z, Reynolds W, Lynn R, Rotiroti MC, Gkitsas N, Arai S, Johnston L, Lowsky R, Majzner RG, Meyer E, Negrin RS, Rezvani AR, Sidana S, Shizuru J, Weng WK, Mullins C, Jacob A, Kirsch I, Bazzano M, Zhou J, Mackay S,

- Bornheimer SJ, Schultz L, Ramakrishna S, Davis KL, Kong KA, Shah NN, Qin H, Fry T, Feldman S, Mackall CL, Miklos DB. 2021. CAR T cells with dual targeting of CD19 and CD22 in adult patients with recurrent or refractory B cell malignancies: a phase 1 trial. *Nat Med* 27: 1419-31
41. Cordoba S, Onuoha S, Thomas S, Pignataro DS, Hough R, Ghorashian S, Vora A, Bonney D, Veys P, Rao K, Lucchini G, Chiesa R, Chu J, Clark L, Fung MM, Smith K, Peticone C, Al-Hajj M, Baldan V, Ferrari M, Srivastava S, Jha R, Arce Vargas F, Duffy K, Day W, Virgo P, Wheeler L, Hancock J, Farzaneh F, Domning S, Zhang Y, Khokhar NZ, Peddareddigari VGR, Wynn R, Pule M, Amrolia PJ. 2021. CAR T cells with dual targeting of CD19 and CD22 in pediatric and young adult patients with relapsed or refractory B cell acute lymphoblastic leukemia: a phase 1 trial. *Nat Med* 27: 1797-805
42. Kochenderfer JN, Dudley ME, Kassim SH, Somerville RP, Carpenter RO, Stetler-Stevenson M, Yang JC, Phan GQ, Hughes MS, Sherry RM, Raffeld M, Feldman S, Lu L, Li YF, Ngo LT, Goy A, Feldman T, Spaner DE, Wang ML, Chen CC, Kranick SM, Nath A, Nathan DA, Morton KE, Toomey MA, Rosenberg SA. 2015. Chemotherapy-refractory diffuse large B-cell lymphoma and indolent B-cell malignancies can be effectively treated with autologous T cells expressing an anti-CD19 chimeric antigen receptor. *J Clin Oncol* 33: 540-9
43. Porter DL, Levine BL, Kalos M, Bagg A, June CH. 2011. Chimeric antigen receptor-modified T cells in chronic lymphoid leukemia. *N Engl J Med* 365: 725-33
44. Neelapu SS, Locke FL, Bartlett NL, Lekakis LJ, Miklos DB, Jacobson CA, Braunschweig I, Oluwole OO, Siddiqi T, Lin Y, Timmerman JM, Stiff PJ, Friedberg JW, Flinn IW, Goy A, Hill BT, Smith MR, Deol A, Farooq U, McSweeney P, Munoz J, Avivi I, Castro JE, Westin JR, Chavez JC, Ghobadi A, Komanduri KV, Levy R, Jacobsen ED, Witzig TE, Reagan P, Bot A, Rossi J, Navale L, Jiang Y, Aycock J, Elias M, Chang

- D, Wiezorek J, Go WY. 2017. Axicabtagene Ciloleucel CAR T-Cell Therapy in Refractory Large B-Cell Lymphoma. *N Engl J Med* 377: 2531-44
45. Kochenderfer JN, Wilson WH, Janik JE, Dudley ME, Stetler-Stevenson M, Feldman SA, Maric I, Raffeld M, Nathan DA, Lanier BJ, Morgan RA, Rosenberg SA. 2010. Eradication of B-lineage cells and regression of lymphoma in a patient treated with autologous T cells genetically engineered to recognize CD19. *Blood* 116: 4099-102
46. Park JH, Rivière I, Gonen M, Wang X, Sénéchal B, Curran KJ, Sauter C, Wang Y, Santomasso B, Mead E, Roshal M, Maslak P, Davila M, Brentjens RJ, Sadelain M. 2018. Long-Term Follow-up of CD19 CAR Therapy in Acute Lymphoblastic Leukemia. *N Engl J Med* 378: 449-59
47. Turtle CJ, Hanafi LA, Berger C, Gooley TA, Cherian S, Hudecek M, Sommermeyer D, Melville K, Pender B, Budiarto TM, Robinson E, Steevens NN, Chaney C, Soma L, Chen X, Yeung C, Wood B, Li D, Cao J, Heimfeld S, Jensen MC, Riddell SR, Maloney DG. 2016. CD19 CAR-T cells of defined CD4+:CD8+ composition in adult B cell ALL patients. *J Clin Invest* 126: 2123-38
48. Gardner RA, Finney O, Annesley C, Brakke H, Summers C, Leger K, Bleakley M, Brown C, Mgebroff S, Kelly-Spratt KS, Hoglund V, Lindgren C, Oron AP, Li D, Riddell SR, Park JR, Jensen MC. 2017. Intent-to-treat leukemia remission by CD19 CAR T cells of defined formulation and dose in children and young adults. *Blood* 129: 3322-31
49. Plaks V, Rossi JM, Chou J, Wang L, Poddar S, Han G, Wang Z, Kuang SQ, Chu F, Davis RE, Vega F, Bashir Z, Jacobson CA, Locke FL, Reagan PM, Rodig SJ, Lekakis LJ, Flinn IW, Miklos DB, Bot A, Neelapu SS. 2021. CD19 target evasion as a mechanism of relapse in large B-cell lymphoma treated with axicabtagene ciloleucel. *Blood* 138: 1081-5

50. Schuster SJ, Svoboda J, Chong EA, Nasta SD, Mato AR, Anak Ö, Brogdon JL, Pruteanu-Malinici I, Bhoj V, Landsburg D, Wasik M, Levine BL, Lacey SF, Melenhorst JJ, Porter DL, June CH. 2017. Chimeric Antigen Receptor T Cells in Refractory B-Cell Lymphomas. *N Engl J Med* 377: 2545-54
51. Yu H, Sotillo E, Harrington C, Wertheim G, Paessler M, Maude SL, Rheingold SR, Grupp SA, Thomas-Tikhonenko A, Pillai V. 2017. Repeated loss of target surface antigen after immunotherapy in primary mediastinal large B cell lymphoma. *Am J Hematol* 92: E11-e3
52. Shalabi H, Kraft IL, Wang HW, Yuan CM, Yates B, Delbrook C, Zimelman JD, Giller R, Stetler-Stevenson M, Jaffe ES, Lee DW, Shern JF, Fry TJ, Shah NN. 2018. Sequential loss of tumor surface antigens following chimeric antigen receptor T-cell therapies in diffuse large B-cell lymphoma. *Haematologica* 103: e215-e8
53. Brudno JN, Shi V, Stroncek D, Pittaluga S, Kanakry JA, Curtis LM, Gea-Banacloche JC, Pavletic S, Bagheri M-H, Rose JJ, Patel R, Hansen B, Gress RE, Kochenderfer JN. 2016. T Cells Expressing a Novel Fully-Human Anti-CD19 Chimeric Antigen Receptor Induce Remissions of Advanced Lymphoma in a First-in-Humans Clinical Trial. *Blood* 128: 999-
54. Sotillo E, Barrett DM, Black KL, Bagashev A, Oldridge D, Wu G, Sussman R, Lanauze C, Ruella M, Gazzara MR, Martinez NM, Harrington CT, Chung EY, Perazzelli J, Hofmann TJ, Maude SL, Raman P, Barrera A, Gill S, Lacey SF, Melenhorst JJ, Allman D, Jacoby E, Fry T, Mackall C, Barash Y, Lynch KW, Maris JM, Grupp SA, Thomas-Tikhonenko A. 2015. Convergence of Acquired Mutations and Alternative Splicing of CD19 Enables Resistance to CART-19 Immunotherapy. *Cancer Discov* 5: 1282-95
55. Orlando EJ, Han X, Tribouley C, Wood PA, Leary RJ, Riester M, Levine JE, Qayed M, Grupp SA, Boyer M, De Moerloose B, Nemecek ER, Bittencourt H, Hiramatsu H, Buechner J, Davies SM, Verneris MR, Nguyen K, Brogdon JL, Bitter H, Morrissey M,

- Pierog P, Pantano S, Engelman JA, Winckler W. 2018. Genetic mechanisms of target antigen loss in CAR19 therapy of acute lymphoblastic leukemia. *Nat Med* 24: 1504-6
56. Fry TJ, Shah NN, Orentas RJ, Stetler-Stevenson M, Yuan CM, Ramakrishna S, Wolters P, Martin S, Delbrook C, Yates B, Shalabi H, Fountaine TJ, Shern JF, Majzner RG, Stroncek DF, Sabatino M, Feng Y, Dimitrov DS, Zhang L, Nguyen S, Qin H, Dropulic B, Lee DW, Mackall CL. 2018. CD22-targeted CAR T cells induce remission in B-ALL that is naive or resistant to CD19-targeted CAR immunotherapy. *Nat Med* 24: 20-8
57. Neelapu SS, Rossi JM, Jacobson CA, Locke FL, Miklos DB, Reagan PM, Rodig SJ, Lekakis LJ, Flinn IW, Zheng L, Milletti F, Chang E, Xue A, Plaks V, Kim JJ, Bot A. 2019. CD19-Loss with Preservation of Other B Cell Lineage Features in Patients with Large B Cell Lymphoma Who Relapsed Post-Axi-Cel. *Blood* 134: 203-
58. Ormhøj M, Scarfò I, Cabral ML, Bailey SR, Lorrey SJ, Bouffard AA, Castano AP, Larson RC, Riley LS, Schmidts A, Choi BD, Andersen RS, Cédile O, Nyvold CG, Christensen JH, Gjerstorff MF, Ditzel HJ, Weinstock DM, Barington T, Frigault MJ, Maus MV. 2019. Chimeric Antigen Receptor T Cells Targeting CD79b Show Efficacy in Lymphoma with or without Cotargeting CD19. *Clin Cancer Res* 25: 7046-57
59. Maloney DG, Ogura M, Fukuhara N, Davis J, Lasher J, Izquierdo M, Banerjee H, Tobinai K. 2020. A phase 3 randomized study (HOMER) of ofatumumab vs rituximab in iNHL relapsed after rituximab-containing therapy. *Blood advances* 4: 3886-93
60. D'Arena G, Musto P, Cascavilla N, Dell'Olio M, Di Renzo N, Carotenuto M. 2000. Quantitative flow cytometry for the differential diagnosis of leukemic B-cell chronic lymphoproliferative disorders. *Am J Hematol* 64: 275-81
61. Pfeifer M, Zheng B, Erdmann T, Koeppen H, McCord R, Grau M, Staiger A, Chai A, Sandmann T, Madle H, Dörken B, Chu YW, Chen AI, Lebovic D, Salles GA, Czuczman MS, Palanca-Wessels MC, Press OW, Advani R, Morschhauser F, Cheson BD, Lenz

- P, Ott G, Polson AG, Mundt KE, Lenz G. 2015. Anti-CD22 and anti-CD79B antibody drug conjugates are active in different molecular diffuse large B-cell lymphoma subtypes. *Leukemia* 29: 1578-86
62. Huang L, Wang N, Li C, Cao Y, Xiao Y, Xiao M, Zhang Y, Zhang T, Zhou J. 2017. Sequential Infusion of Anti-CD22 and Anti-CD19 Chimeric Antigen Receptor T Cells for Adult Patients with Refractory/Relapsed B-Cell Acute Lymphoblastic Leukemia. *Blood* 130: 846-
63. Simon S, Riddell SR. 2020. Dual Targeting with CAR T Cells to Limit Antigen Escape in Multiple Myeloma. *Blood Cancer Discov* 1: 130-3
64. Zah E, Lin MY, Silva-Benedict A, Jensen MC, Chen YY. 2016. T Cells Expressing CD19/CD20 Bispecific Chimeric Antigen Receptors Prevent Antigen Escape by Malignant B Cells. *Cancer Immunol Res* 4: 498-508
65. Fernández de Larrea C, Staehr M, Lopez AV, Ng KY, Chen Y, Godfrey WD, Purdon TJ, Ponomarev V, Wendel HG, Brentjens RJ, Smith EL. 2020. Defining an Optimal Dual-Targeted CAR T-cell Therapy Approach Simultaneously Targeting BCMA and GPRC5D to Prevent BCMA Escape-Driven Relapse in Multiple Myeloma. *Blood Cancer Discov* 1: 146-54
66. Jensen MC, Riddell SR. 2014. Design and implementation of adoptive therapy with chimeric antigen receptor-modified T cells. *Immunol Rev* 257: 127-44
67. Inoo K, Inagaki R, Fujiwara K, Sasawatari S, Kamigaki T, Nakagawa S, Okada N. 2016. Immunological quality and performance of tumor vessel-targeting CAR-T cells prepared by mRNA-EP for clinical research. *Mol Ther Oncolytics* 3: 16024
68. Dull T, Zufferey R, Kelly M, Mandel RJ, Nguyen M, Trono D, Naldini L. 1998. A third-generation lentivirus vector with a conditional packaging system. *J Virol* 72: 8463-71
69. Joglekar AV, Sandoval S. 2017. Pseudotyped Lentiviral Vectors: One Vector, Many Guises. *Hum Gene Ther Methods* 28: 291-301

70. Bell AJ, Jr., Fegen D, Ward M, Bank A. 2010. RD114 envelope proteins provide an effective and versatile approach to pseudotype lentiviral vectors. *Exp Biol Med (Maywood)* 235: 1269-76
71. Liu Z, Chen O, Wall JBJ, Zheng M, Zhou Y, Wang L, Vaseghi HR, Qian L, Liu J. 2017. Systematic comparison of 2A peptides for cloning multi-genes in a polycistronic vector. *Sci Rep* 7: 2193
72. Zhao Z, Condomines M, van der Stegen SJC, Perna F, Kloss CC, Gunset G, Plotkin J, Sadelain M. 2015. Structural Design of Engineered Costimulation Determines Tumor Rejection Kinetics and Persistence of CAR T Cells. *Cancer Cell* 28: 415-28
73. Stoiber S, Cadilha BL, Benmebarek MR, Lesch S, Endres S, Kobold S. 2019. Limitations in the Design of Chimeric Antigen Receptors for Cancer Therapy. *Cells* 8
74. Melenhorst JJ, Chen GM, Wang M, Porter DL, Chen C, Collins MA, Gao P, Bandyopadhyay S, Sun H, Zhao Z, Lundh S, Pruteanu-Malinici I, Nobles CL, Maji S, Frey NV, Gill SI, Tian L, Kulikovskaya I, Gupta M, Ambrose DE, Davis MM, Fraietta JA, Brogdon JL, Young RM, Chew A, Levine BL, Siegel DL, Alanio C, Wherry EJ, Bushman FD, Lacey SF, Tan K, June CH. 2022. Decade-long leukaemia remissions with persistence of CD4(+) CAR T cells. *Nature* 602: 503-9
75. Guedan S, Posey AD, Jr., Shaw C, Wing A, Da T, Patel PR, McGettigan SE, Casado-Medrano V, Kawalekar OU, Uribe-Herranz M, Song D, Melenhorst JJ, Lacey SF, Scholler J, Keith B, Young RM, June CH. 2018. Enhancing CAR T cell persistence through ICOS and 4-1BB costimulation. *JCI Insight* 3
76. Song DG, Ye Q, Poussin M, Harms GM, Figini M, Powell DJ, Jr. 2012. CD27 costimulation augments the survival and antitumor activity of redirected human T cells in vivo. *Blood* 119: 696-706

77. Hombach AA, Heiders J, Foppe M, Chmielewski M, Abken H. 2012. OX40 costimulation by a chimeric antigen receptor abrogates CD28 and IL-2 induced IL-10 secretion by redirected CD4(+) T cells. *Oncoimmunology* 1: 458-66
78. Hegde M, Mukherjee M, Grada Z, Pignata A, Landi D, Navai SA, Wakefield A, Fousek K, Bielamowicz K, Chow KK, Brawley VS, Byrd TT, Krebs S, Gottschalk S, Wels WS, Baker ML, Dotti G, Mamonkin M, Brenner MK, Orange JS, Ahmed N. 2016. Tandem CAR T cells targeting HER2 and IL13R α 2 mitigate tumor antigen escape. *J Clin Invest* 126: 3036-52

VITA

Xiaoyun Cheng was born in Henan, the People's Republic of China. She was the daughter of Xiuzhen Li and Cunshuan Cheng. She received her Bachelor of Medicine degree from Department of Clinical Medicine of Health Science Center in Peking University, P.R. China in June 1999. In August of 2019, she entered The University of Texas MD Anderson Cancer Center UTHealth Graduate School of Biomedical Science.

Permanent Address:

2907 Green Fields Drive

Sugar Land, Texas, 77479